THE ROLES OF ESTRADIOL-17β AND PROLACTIN IN UTERINE GLAND DEVELOPMENT IN THE NEONATAL EWE

A Dissertation

by

KAREN DENISE CARPENTER

Submitted to the Office of Graduate Studies of
Texas A&M University
in partial fulfillment of the requirements for the degree of

DOCTOR OF PHILOSOPHY

August 2005

Major Subject: Animal Science

THE ROLES OF ESTRADIOL-17β AND PROLACTIN IN UTERINE GLAND DEVELOPMENT IN THE NEONATAL EWE

A Dissertation

by

KAREN DENISE CARPENTER

Submitted to the Office of Graduate Studies of
Texas A&M University
in partial fulfillment of the requirements for the degree of

DOCTOR OF PHILOSOPHY

Approved by:

Co-Chairs of Committee,	Thomas E. Spencer
	Fuller W. Bazer
Committee Members,	Robert Burgardt
	Thomas Welsh, Jr.
	David Adelson
Head of Department,	Gary Acuff

August 2005

Major Subject: Animal Science

ABSTRACT

The Roles of Estradiol-17β and Prolactin in Uterine Gland Development in the Neonatal Ewe (August 2005)

Karen Denise Carpenter, B.S., Texas A&M University

Co-Chairs of Advisory Committee: Dr. Thomas E. Spencer
Dr. Fuller W. Bazer

Endometrial glands are required for adult uterine function and develop post-natally in mammalian species. Therefore, studies were conducted using neonatal ewes as a model to determine: 1) the roles of estradiol-17β and estrogen receptor-alpha (ERα) in endometrial gland development; 2) the role of ovaries in endometrial gland development; 3) the role of prolactin in endometrial gland development; and 4) factors regulating prolactin receptor expression in endometrial glands.

Study one determined the effects of neonatal exposure of ewes to estradiol-17β valerate (EV); EM-800, an ERα antagonist; or CGS-20267, an aromatase inhibitor on endometrial gland development. Results indicate E2-17β does not regulate endometrial gland differentiation or development. Additionally, ERα does not regulate primary differentiation of glandular epithelium, but does influence coiling and branching morphogenesis of endometrial glands.

Study two determined the effects of ovariectomy on endometrial gland morphogenesis. Results suggest that the ovary and, thus, an ovarian-derived factor(s) regulate, in part, the coiling and branching of endometrial glands. Expression of subunits of activin, follistatin, and inhibin in the neonatal ovine ovary in addition to

modulation of the components of the activin/follistatin system in the uterus of ovariectomized ewes supports the hypothesis that the ovarian factors that influence endometrial adenogenesis in the neonatal ewe may be activin, follistatin, and/or inhibin.

Studies three and four determined the role of prolactin in endometrial adenogenesis in the neonatal ewe. Studies in which either hypoprolactinemia or hyperprolactinemia were induced indicate that prolactin regulates ovine endometrial adenogenesis in the neonatal ewe. The aim of study five was to determine transcription factors that regulate the glandular epithelium specific expression of prolactin receptor. Prolactin receptor exon 2 was cloned and sequenced, but no identifiable exon 1 or promoter was found. Additionally, many bovine contigs containing portions of the prolactin receptor gene were identified suggesting the bovine genome will be a useful tool as it becomes more complete.

These results indicate ERα, prolactin and prolactin receptor, along with an unidentified ovarian factor(s), influence endometrial gland development in the neonatal ewe; however, exposure of the neonatal ewe to exogenous estradiol-17β prevents differentiation and development of endometrial glands.

DEDICATION

I would like to dedicate this dissertation to all of my family for believing in me and supporting me all these years. Their love and faith in my ability to succeed could be felt over the great distances that separate us. My undergraduate education was made possible by my grandparents, Dolph and Mildred Harrod, and to them I am eternally grateful. To my parents, John and Penny Harrod, who taught me I could do anything I wanted if I worked hard enough and that the world did not end at the county line. To my husband's family for taking me in and supporting me as one of their own. I am especially grateful to my sister, Rheadon Harrod, who has never been further than a phone call away with whatever I needed. Finally, I can never express the sincere gratitude I feel towards my husband, Todd, for the love, encouragement, and understanding he has given me. Thank you all for everything. I would not be the person I am today without all of you.

ACKNOWLEDGEMENTS

The studies presented in this dissertation would not have been possible without the help and support of many people. I would like to thank the co-chairs of my committee, Dr. Thomas Spencer and Dr. Fuller Bazer, who gave me the opportunity to work with and learn from them. Their continued patience, guidance and support are very much appreciated. The members of my committee, Dr. Robert Burghardt, Dr. David Adelson, and Dr. Thomas Welsh, Jr. have given unselfishly of their time and expertise over the years. I would like to thank all of the past and present members of the laboratory that I have worked with over the years. Carrying out the neonatal lamb studies would have been impossible without their help. Mr. Kendrick Leblanc and various undergraduate students performed the daily care of the sheep and provided their assistance with surgeries and the studies. I would like to give special thanks to Dr. Allison Gray and Dr. Jo-Ann Fleming who taught me many of the techniques I used in these studies, and Dr. Kanako Hayashi who worked very closely with me the last few years. I also appreciate the help I received from Tina Lane and Dr. Marcel Amstalden in performing radioimmunoassays. Finally, this research would not have been possible without the generous monetary support of the National Institutes of Health, grant number NIH HD38274.

TABLE OF CONTENTS

CHAPTER Page

LIST OF FIGURES

FIGURE Page

FIGURE Page

LIST OF TABLES

CHAPTER I

INTRODUCTION

All mammalian uteri contain endometrial glands that synthesize, secrete and transport molecules collectively termed histotroph. Evidence accumulated from primate and subprimate species during the last century supports an unequivocal role for histotroph as primary regulators of conceptus (embryo/fetus and associated extra-embryonic placental membranes) survival, development, and implantation/placentation [1-4]. Histotroph contains a variety of binding and transport proteins, mitogens, cytokines, lymphokines, enzymes, hormones, growth factors, protease inhibitors, and many other substances [5-9]. Exposure of neonatal ewes to a progestin from birth epigenetically ablates endometrial gland differentiation and produces a uterine gland knockout (UGKO) phenotype in the adult [10, 11]. UGKO ewes are subfertile and exhibit early pregnancy loss during the peri-implantation stage of conceptus elongation, thus demonstrating that endometrial glands and, therefore, their secretions are required for conceptus survival and development prior to the establishment of hematotrophic nutrition [12]. Additionally, Burton et al. [9] recently provided evidence that histotrophic nutrition is required throughout the first trimester of pregnancy in humans.

Although a functional role for endometrial glands has been established in many mammals, the developmental mechanisms regulating endometrial gland morphogenesis, or adenogenesis, are not well understood. Uterine gland development begins after birth

---

This dissertation follows the style of Biology of Reproduction.

in sheep as in most mammals and involves differentiation of the endometrial glandular epithelium (GE) from the lumenal epithelium (LE), specification of intercaruncular stroma, development of endometrial folds and, to a lesser extent, growth of endometrial caruncular areas and the myometrium [3, 11, 13-15]. By postnatal day (PND) 56, uterine gland morphogenesis is essentially complete, as the histoarchitecture of the endometrium is similar to that found in a cyclic adult [14]. Further maturation and growth of the ovine uterus occurs after puberty [16] and during the first pregnancy [17, 18].

In the neonatal ewe, estradiol-17β (E2-17β), pituitary prolactin (PRL), and stromal growth factors (*i.e.* fibroblast growth factors-7 (FGF-7) and FGF-10, hepatocyte growth factor (HGF), and insulin-like growth factors one (IGF-I) and IGF-II, with their respective epithelial receptors have been implicated as endocrine and paracrine regulatory molecules controlling postnatal ovine endometrial adenogenesis [11, 14, 15]. Postnatal uterine development is accompanied by expression of estrogen receptor-alpha (ERα) in both the nascent and developing GE and endometrial stroma in rodents, pigs and sheep. Studies with rodents indicate that endometrial adenogenesis is not dependent on the ovary, adrenal gland, estrogen or uterine ERα expression [14, 19-23]. In the neonatal pig, endometrial adenogenesis is also not dependent on the ovary [23]; however, it is regulated by expression and activation of a functional ERα system [24]. Interestingly in Fall born ewes, circulating concentrations of E2-17β are high from birth through PND 56 [14]. The emerging, proliferating and developing endometrial glands express abundant levels of ERα as well as progesterone receptor (PR), which is an

estrogen-responsive gene [14]. During this period, the stroma is also ERα-positive and expresses both IGF-I and IGF-II [15]. The developing GE expresses the IGF-I receptor [15], and IGF-I can activate ERα in a ligand-independent manner in other model systems [25]. The precise roles of circulating E2-17β and uterine ERα in endometrial gland morphogenesis in the neonatal ovine uterus have not been evaluated.

Studies of several species revealed that uterine development and endometrial adenogenesis can proceed normally in the absence of the ovary and, by default, ovarian steroids for varying periods of time during early postnatal life. At birth the ovine ovary contains numerous growing and vesicular follicles, which decrease in number until PND 14 and then increase to peak in number on PND 28. The number of ovarian follicles remains high from PND 42 to PND 56, and declines thereafter [26, 27]. These changes in ovarian follicles correlate with the ontogeny of endometrial gland development in the ewe lamb [14]. Interestingly, ovariectomy of the ewe at birth does not affect uterine wet weight [27] or the initial stages of endometrial gland tubulogenesis on PND 14 [28]. However, ovariectomy does affect uterine growth after PND 14 [29]. Postnatal uterine growth and endometrial adenogenesis are ovary- and steroid-independent in rodents [30-32] and pigs [23]. While the ovary does influence postnatal uterine growth, its specific role in ovine endometrial gland development after PND 14 has not been investigated.

Prolactin regulates the growth and differentiation of a number of epitheliomesenchymal organs, including the pigeon crop-sac, mammary gland, prostate, and uterus [33]. In the mammary gland, PRL and PRLR are required for development and differentiation of the lobuloalveolar portion of the GE [34-36]. In neonatal ewes,

circulating levels of PRL are relatively high on PND 1, reach a maximum on PND 14, and then decline slightly to PND 56 [15, 37]. Expression of mRNAs for the short and long forms of the PRL receptor (PRLR) is exclusive to the nascent uterine GE buds on PND 7 and the proliferating and differentiating GE from PNDs 14 to 56 [14]. In the adult ovine uterus, PRLR expression is also restricted to the endometrial glands [18]. Hyperprolactinemia causes uterine glandular hyperplasia in the adult mouse, rabbit and pig [38-40]. The precise role of PRL in neonatal ovine uterine adenogenesis has not been elucidated. Given the central role ascribed to PRLR in mammary gland morphogenesis and function, PRLR in the nascent GE of the developing uterus may play a similar, albeit undiscovered, regulatory role in endometrial gland morphogenesis in the neonatal ewe.

Mechanisms regulating endometrial gland differentiation and development in the neonate determine, in part, the functional capacity and embryotrophic potential of the mature uterus [3, 12, 41]. Therefore, it is important to understand the molecular aspects of endometrial adenogenesis. Previous results indicate that E2-17β, ERα, the ovary, ovarian factors, PRL, and PRLR may play roles in regulating endometrial gland differentiation and development in the neonatal ewe. The present studies were designed to determine: 1) the roles of estradiol-17β and ERα in endometrial gland development; 2) the role of ovaries in endometrial gland development; 3) the role of prolactin in endometrial gland development; and 4) factors regulating prolactin receptor expression in endometrial glands.

CHAPTER II

LITERATURE REVIEW

Endometrial Glands

The female reproductive tract (FRT) includes the oviduct, uterus, cervix and vagina. The uterus is an essential organ for reproduction in mammals. Essential functions of the uterus include: (1) production of prostaglandin F2α, which is the luteolysin required for ovarian cyclicity in domestic animals; (2) transport, storage and maturation of spermatozoa; (3) provision of an embryotrophic environment for conceptus (embryo/fetus and associated extraembryonic membranes) growth and development; and (4) delivery of the conceptus at parturition [42, 43]. In the adult, the uterine wall is comprised of two functional compartments, the endometrium and myometrium (Fig. 2.1). The endometrium is the inner mucosal lining of the uterus, derived from the innermost layer of ductal mesenchyme. Histologically, the endometrium consists of two epithelial cell types, LE, GE, two stratified stromal compartments including a densely organized stromal zone (stratum compactum), and a more loosely organized stromal zone (stratum spongiosum), blood vessels and immune cells. The myometrium is the smooth muscle component of the uterine wall that includes an inner circular layer, derived from the intermediate layer of ductal mesenchymal cells, and an outer longitudinal layer, derived from subperimetrial mesenchyme.

Uterine endometrial glands are present in all mammalian uteri. The uterine glands selectively transport or synthesize and secrete substances, termed histotroph, into

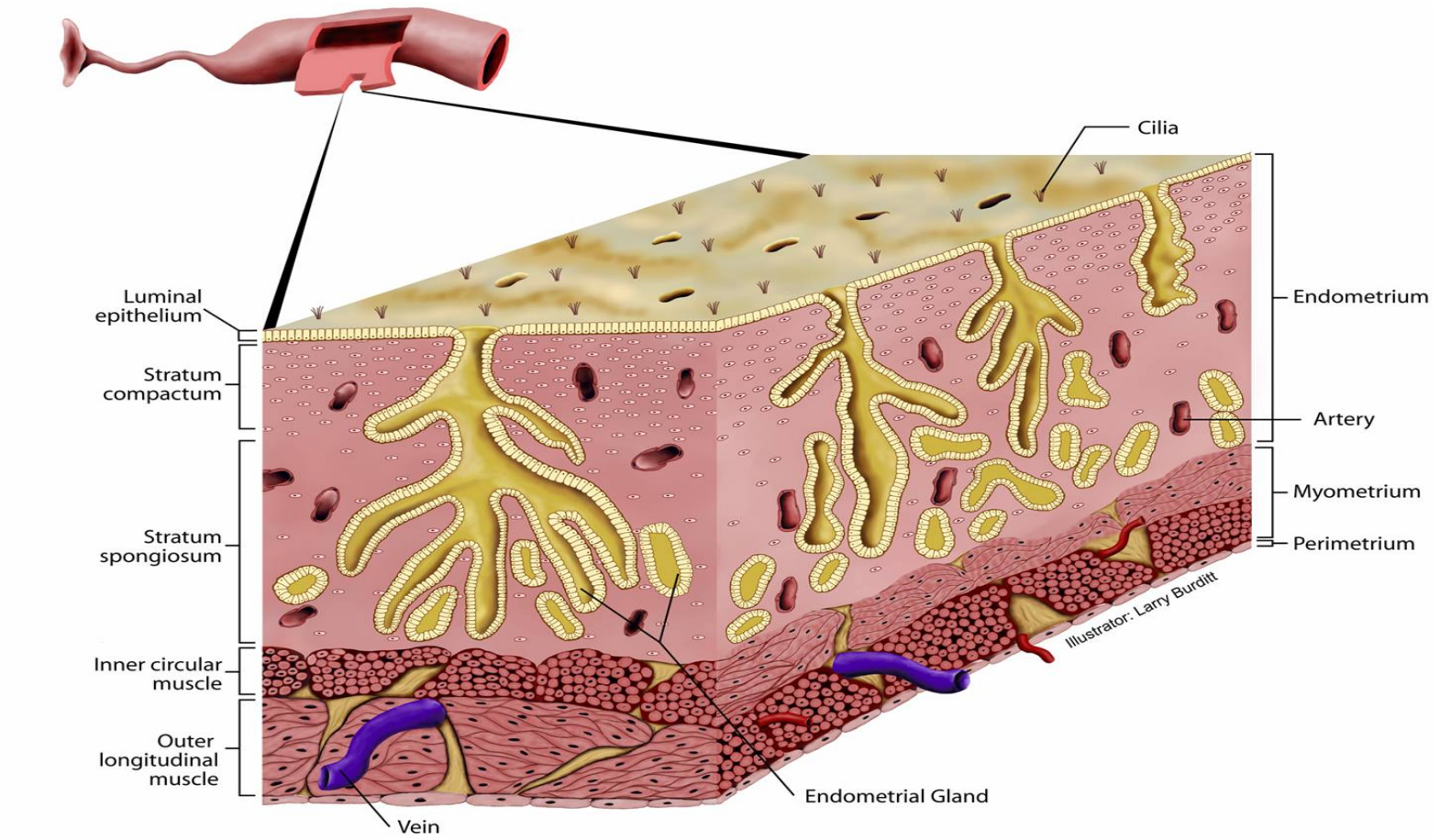

FIG 2.1. Morphology of the mammalian uterine wall. The mammalian uterine wall contains two functional layers, a mucosal endometrium and muscular myometrium. The uterine lumen is lined by a single cell layer of luminal epithelium. The mesenchymal stroma is divided into a dense stratum compactum layer and an underlying stratum spongiosum layer that is more loosely organized. The stroma is perforated by many blood vessels and endometrial glands which are lined with glandular epithelium and open into the lumen. The myometrium is made up of inner circular and outer longitudinal muscle layers. The uterus is surrounded by a layer of connective tissue, the perimetrium (Graphic courtesy of Rodney Geisert and Larry Burditt, Oklahoma State University, Stillwater, USA).

the uterine lumen [1-4]. All components of histotroph are not known in any animal, but it is a complex material containing transport proteins, mitogens, cytokines, lymphokines, enzymes, hormones, growth factors, protease inhibitors, and many other substances [5-9]. The idea that uterine secretions nourish the developing conceptus was discussed first by Aristotle in the third century BC and then by William Harvey in the 17th century. In 1882, Bonnett stated that secretions of uterine glands were important for fetal well being in ruminants.

Evidence accumulated from primate and subprimate species during the last century overwhelmingly supports a role for uterine gland secretions in establishment of endometrial receptivity to the embryo and subsequent conceptus survival, growth and development [1-4]. In rodents, two genes, calcitonin and leukemia inhibitory factor (LIF), are produced by uterine glands and are essential for the establishment of uterine receptivity and embryo implantation [2, 44]. LIF is a pleitrophic cytokine produced exclusively by the LE and GE preceding blastocyst implantation on day 4 of gestation in mice[45, 46]. The endometrium of LIF-null females fails to undergo decidualization, thus preventing implantation [47]. Calcitonin, a peptide hormone, is another factor produced by the rat uterus exclusively during the peri-implantation period [48, 49]. Administration of anti-sense oligonucleotides for calicitonin severely reduced litter size by 50-80 percent [50]. Both LIF and calcitonin are also expressed by the human LE and GE during the secretory phase which coincides with the peri-implantation period indicating they may play similar roles in human blastocyst implantation [51-53]. Evaluation of placental tissues by Burton and colleagues [9] revealed that in the human

histotrophic nutrition during early gestation is necessary, because the formation of the discrete channels from the maternal blood supply into the intervillous space of the placenta, which allow direct communication and exchange of nutrients, occurs only at the end of the first trimester. These findings support the conclusion that hematotrophic nutrition in humans is not well established until the second trimester of gestation [9].

Histotroph appears to be particularly important for conceptus survival and development in domestic animals as well, especially given the prolonged nature of implantation and placentation. In sheep [17, 18], cattle [54], pigs [55, 56], and horses [57-59], endometrial glands undergo extensive hyperplasia and hypertrophy during pregnancy, presumably in response to increasing demands of the developing conceptus for histotroph [1, 17, 59]. Indeed, the epitheliochorial placentae of domestic animals develop unique placental structures, termed areolae, over the mouth of each uterine gland. Areolae are specialized areas for absorption and transport of uterine histotroph by fluid-phase pinocytosis [60]. Several components of ruminant histotroph have been identified and include osteopontin (OPN), glycosylated cell adhesion molecule one (GlyCAM-1), and uterine milk proteins (UTMP). Osteopontin (OPN) is a member of the Small Integrin-Binding, N-Linked Glycoprotein (SIBLING) family of related extracellular matrix proteins which is a major component of histotroph in primate, pigs, sheep, and mice (for review, see [61]). OPN is an extracellular matrix-adhesion molecule and is hypothesized to serve as a bridging ligand that mediates adhesion between LE and trophoblast essential for implantation and placentation [61-63]. The high levels of expression of GlyCAM-1, a member of the mucin family of glycoproteins

[64], in the pregnant ovine endometrium during the peri-implantation period suggests of this adhesion molecule may also be a potent regulator of implantation [65]. UTMP belong to the serpin family of serine protease inhibitors [66] and, along with OPN, are excellent markers of endometrial gland differentiation and overall uterine secretory capacity during pregnancy in ewes [18, 67].

Treatment of neonatal ewes with a non-metabolizable progestin from birth to at least PND56 epigenetically ablates endometrial gland development and creates an UGKO phenotype in the adult [10, 11]. Other reproductive tract tissues, including the anterior vagina, cervix and oviduct, are not significantly affected by postnatal exposure to progesterone [10, 11]. The mechanism of progestin action to inhibit endometrial gland development is not known, but it is not due to inhibition of epithelial cell proliferation as no difference in expression of proliferating cell nuclear antigen (PCNA) is detected in the LE of progestin-treated versus control ewes [11]; however, an increase in PCNA was seen in the stratum compactum stroma of progestin treated ewes [11]. This increase in stromal cell proliferation may alter epithelial-mesenchymal interactions that have been shown to be critical to uterine development or the extracellular matrix thereby altering normal uterine development [11, 68, 69]. Evidence suggests that progestin may ablate glandular development by suppressing ERα expression in the LE and stroma or by altering expression of growth factors in the stroma and/or their receptors in the LE [11].

In addition to insights into endometrial gland development, the UGKO ewe provides an excellent model to study the role of endometrial glands and their secretions

in pregnancy. Embryos recovered from UGKO ewes on Days 6 and 9 after breeding were developmentally normal, which confirmed that UGKO ewes are capable of ovulating viable oocytes and have a normal rate of fertilization [12]. However, embryos recovered from untreated ewes on Day 7 were unable to establish pregnancy when transferred into uteri of UGKO recipient ewes [12]. Additionally, UGKO ewes examined on Day 14 of pregnancy were found to possess either growth-retarded conceptuses or no conceptuses. These studies indicate that endometrial glands and, by extension, their secretions are required for maintenance of pregnancy [12]. Therefore, it is important to understand the mechanisms that regulate uterine adenogenesis as development and function of endometrial glands is critical for mammalian reproduction.

Uterine Morphogenesis

Despite the importance of the uterus for the fertility and health of women and their offspring, relatively little is known about the hormonal, cellular and molecular mechanisms that regulate its development in either the fetus [70] or neonate [3, 41]. Factors that regulate events during critical developmental periods ultimately determine the functional capacity and embryotrophic potential of the adult uterus in both humans and domestic animals.

Prenatal Organogenesis

Development of the uterus begins prenatally with formation, patterning, and then fusion of the Müllerian ducts. During vertebrate embryogenesis, the FRT is initially formed as part of the urogenital system, which is derived from the intermediate mesoderm formed during gastrulation of the embryo [70-72]. The urogenital system

encompasses the kidneys and gonads as well as the accompanying urinary and reproductive tracts. After differentiation, the embryonic intermediate mesoderm subsequently proliferates and some cells transition from a mesenchymal to an epithelial cell type in order to generate the tubules that compose the male and female reproductive tracts, as well as the kidneys and gonads. Before sexual differentiation, embryos are bipotential and have both male and female reproductive tract primordia regardless of their genetic sex. The FRT system develops primarily from the Müllerian (paramesonephric) ducts, whereas the male reproductive tract forms from the Wolffian (mesonephric) ducts. The Wolffian duct is first formed from the intermediate mesoderm. Subsequently, the Müllerian duct is formed by invagination of the surface epithelium of the anterior mesonephros in the developing urogenital ridge. This epithelial invagination extends caudally along the Wolffian duct laterally and then medially towards the urogenital sinus to form the primordium of the FRT. The Wolffian duct can differentiate into the epididymis, vas deferens, and seminal vesicle of the male reproductive tract. The Müllerian duct can differentiate into the oviducts, uterus, cervix and anterior vagina of the FRT [71].

Mammalian sex determination and subsequent development of either the Wolffian or Müllerian ducts depends on the genetic sex of the gonads [73, 74]. Given the absence of any genetic anomilies, XY embryos become males, and XX embryos become females. In XX females, the absence of the Y chromosome permits the bipotential gonad to differentiate into an ovary leading to the female phenotype [75]. After gonadal sex is determined, the differentiating gonads secrete hormones that promote sexual

differentiation. In males, the fetal testis secretes several important hormones, including Müllerian Inhibiting Substance (MIS; also termed Anti-Müllerian Hormone), testosterone, and insulin-like 3 (Insl3) [76]. The Müllerian duct regression is stimulated by MIS, and testosterone promotes the differentiation and development of the Wolffian duct. All three hormones are involved in testicular descent. In females, the differentiating ovaries do not produce MIS, testosterone, or Insl3. Thus, the Müllerian duct differentiates and develops into the FRT, while the Wolffian duct degenerates.

The morphology of the FRT organs can differ markedly among mammalian species [70, 77]. Regardless of the eutherian species, the point at which the gubernacula cross the Müllerian duct marks the uterotubal junction. The portion of the female duct lateral and cephalic to the crossing becomes the oviduct, whereas the medial and caudal portion becomes the uterus, cervix and anterior vagina [71]. Müllerian duct formation is similar between species, and differences in morphology mainly results from differences in the extent of anterior fusion of the two Müllerian ducts [77]. The degree of Müllerian duct fusion, which can be complete, partial or incomplete, is species-specific and defines gross (i.e. simplex, bicornuate, or duplex) morphological characteristics of adult uteri. In rodents, Müllerian fusion is absent or limited, which leads to the formation of two or 'duplex' uteri. In domestic animals, the Müllerian ducts fuse more at the posterior ends, which results in a long (pig) to medium-length (sheep and cow) bicornuate uterus with a small common corpus, single cervix, and vagina. In contrast, fusion of the Müllerian ducts of higher primates (including humans) is primarily anterior, which results in

formation of a single ('simplex') uterus with a single cervix and vagina. Anatomical variations of the FRT can even be observed within a species [77].

Postnatal Morphogenesis

Unlike most FRT organs, the uterus is not fully developed or differentiated at birth. Establishment of tissue-specific histoarchitecture is completed postnatally in laboratory rodents, domestic animals, and humans [3, 41, 78, 79]. The process of postnatal radial patterning morphogenesis establishes the three classic histological elements of the uterine wall, including the: (1) endometrium; (2) myometrium, which consists of an inner circular layer and an outer longitudinal layer of oriented smooth muscle; and (3) perimetrium (Fig. 2.2). Morphogenetic events common to postnatal development of uteri include: (1) organization and stratification of endometrial stroma; (2) differentiation and growth of the myometrium; and (3) coordinated development of the endometrial glands [3, 41, 79]. The timing of these developmental events differs among species and is subject to differences in uterine maturity at birth. Importantly, endometrial gland morphogenesis is a uniquely or primarily postnatal event in all studied mammals. Available evidence strongly supports the hypothesis that the functional capacity of the adult uterus is defined, to a significant extent, by developmental events associated with ‘programming’ of uterine tissues during prenatal and postnatal life [41, 70, 80, 81]. Postnatal uterine morphogenesis depends on maturity of the uterus at birth, e.g. gestation length, and perhaps the interval between birth and puberty [3]. For instance, postnatal development of the rodent uterus after birth begins with differentiation of the mesenchyme into endometrial stroma and myometrium, whereas

the uterine mesenchyme in domestic animals and humans is already differentiated into endometrial stroma and myometrium at birth.

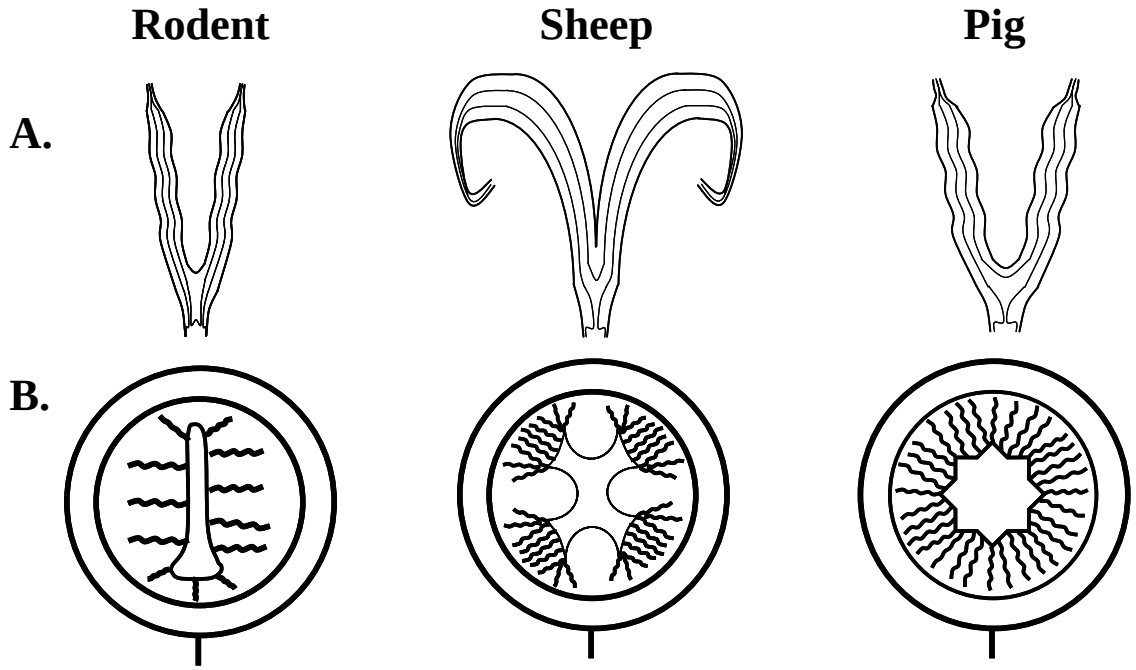

FIG 2.2. Uterine morphology and radial patterning in rodents, sheep, and pigs. A. Diagrams of ideal frontal sections of uterine types. The drawings cut off the oviducts near the uterotubal junctions, and the vaginae just caudal to the cervices. Rodents (rats and mice) have a long duplex type of uterus with dual cervices. Pigs have a long bicornuate type of uterus with a short uterine body and a single cervix. Sheep have a medium–length bicornuate type of uterus, a short uterine body and a single cervix. B. Diagrams of ideal radial patterns of the uterine wall. The curved lines in the endometrium denote the tubular, coiled and branched glands that extend from the uterine lumen to the inner layer of myometrium. The rodent uterus contains only a few endometrial glands. The sheep uterus contains large number of glands in the intercaruncular areas of the endometrium, whereas the caruncles are glandless. The pig uterus contains large numbers of glands throughout the endometrium.

Comparative Morphogenesis

Laboratory Animals

The histological organization of the adult rodent uterus consists of a simple columnar LE surrounded by mesenchymal (i.e., stromal) cells that contain endometrial glands lined by simple columnar epithelial cells (Fig 2.2). The endometrium typically contains

only 10 to 20 glands in a cross-section of the mature uterine wall. The rodent uterus does not contain the tightly coiled and slightly branched glands that are characteristic of endometrium in humans and domestic animals. However, the rodent endometrium is surrounded by circular and longitudinal layers of smooth muscle (i.e., myometrium) that define the outer boundary of the uterus, similar to other mammals [79, 82, 83].

Postnatal development of the uterus is very similar in rats and mice [83]. At birth, the uteri of mice and rats lack endometrial glands and consist of a simple epithelium supported by undifferentiated mesenchyme. Between birth and PND 5 in mice, epithelial invaginations appear representing formation of GE buds, and the three layers of mesenchyme are distinctly segregated into radially oriented endometrial stroma and inner-circular and outer-longitudinal myometrial layers [83]. Genesis of endometrial glands is not observed until PND 7 and PND 9 in mice and rats, respectively [84]. By PND 10 in mice, uterine glands extend from the LE into the surrounding endometrial stroma, and the outer-longitudinal layer of the myometrium becomes organized into bundles [83]. The basic adult configuration of the uterus in mice is established by PND 15 [85]. In the rat uterus, endometrial gland morphogenesis proceeds from PND 9 through PND 15 [84] and results in development of simple, tubular glands that, unlike ungulate or human endometrial glands, are neither tightly coiled nor extensively branched [85].

Domestic Animals

Pig

The mature uterine wall in the adult gilt or sow has a similar architecture to that of humans and other domestic animals, because the endometrium contains hundreds of glands in a single uterine cross-section (Fig 2.2). Transformation of the porcine uterine wall from histoarchitectural infancy to maturity occurs within 120 days of birth [23, 78, 86, 87]. Uterine development in the neonatal pig includes appearance and proliferation of endometrial glands, organization of the stroma, development of endometrial folds, and growth of the myometrium. At birth or PND 0, the porcine uterus consists of a simple, slightly corrugated, columnar epithelium supported by unorganized stromal mesenchyme, encircled by a rudimentary myometrium [41, 86]. Shallow, epithelial depressions can be observed on PND 0, and are the presumed precursors for the coiled and slightly branched uterine glands characteristic of the adult porcine uterus. Endometrial adenogenesis is initiated when GE develops into simple epithelial tubes that extend radially from the LE into the stroma. By PND 7, stromal zones, including a shallow stratum compactum and a deep stratum spongiosum, are evident and accompanied by the presence of distinct, simple tubular glands present throughout the shallow stroma. Eventually, tubular glands undergo coiling and some branching within the stroma until they reach the adluminal border of the myometrium. By PND 14, many coiled tubular glands are apparent, and they extend approximately one-third of the distance from the LE to the myometrium, which has clearly differentiated into inner-circular and outer-longitudinal layers. On PND 28, many of the coiled glands have

obvious branches, and GE is present throughout the endometrial stroma. Well developed endometrial folds are apparent by PND 28 and serve to increase the uterine lumenal surface area. By PND 56, the endometrial gland population is dense and extensive. The porcine uterus is capable of supporting pregnancy by PND 120, indicating that it is functionally mature [41].

Sheep

Ruminants (cattle, goats, and sheep) have a bicornuate uterus with a small common corpus and single cervix. The uterine wall is lined by the endometrium and surrounded by the myometrium. The myometrium has two layers of smooth muscle including the inner-circular and outer-longitudinal layers. The endometrium in adult sheep and cattle consists of a large number of raised aglandular caruncles, which are dense stromal protuberances covered by a simple LE, and glandular intercaruncular areas (Fig 2.2) [17, 88]. As in humans and pigs, the intercaruncular areas of the endometrium contain many hundreds of glands in a cross-section of the uterine wall. However, it is the caruncular areas that are the sites of superficial implantation and placentation [17, 77]. In synepitheliochorial placentation found in ruminants, fusion of placental cotyledons with endometrial caruncles forms placentomes, which serve a primary role in fetal-maternal gas exchange and derivation of micronutrients by the placenta [4, 17, 89]. The dichotomous nature of the adult ruminant endometrium, consisting of both aglandular caruncular areas and glandular intercaruncular areas, makes it an excellent model for the study of mechanisms underlying establishment of divergent structural and functional areas within a single, mesodermally derived organ [13].

The ovine vagina, cervix, and oviduct appear to be histologically completely developed at birth [11, 90]. This is in contrast to the uterus, which is not fully developed at birth. Postnatal uterine morphogenesis involves the emergence and proliferation of endometrial glands, development of endometrial folds and, to a lesser extent, growth of endometrial caruncular areas and myometrium [10, 13, 14, 28]. Development of the endometrial GE, progressing from the LE to the inner-circular layer of myometrium, is a coordinated morphological event involving bud formation, tubulogenesis, coiling, and branching prior to completion. In sheep, endometrial gland genesis is initiated between PND 0 and PND 7, when shallow epithelial invaginations appear along the LE in presumptive intercaruncular areas [10, 14]. Between PND 7 and PND 14, nascent GE buds proliferate and invaginate into the stroma, forming tubular structures that coil and slightly branch by PND 21. After PND 21, the majority of glandular morphogenetic activity involves coiling and branching morphogenesis of tubular endometrial glands as they extend into the deeper stratum spongiosum stroma adjacent to the inner-circular layer of myometrium. By PND 56, the caruncular and intercaruncular endometrial areas are histoarchitecturally similar to those of the adult uterus.

Humans

Humans have a simplex uterus that consists of a single uterine corpus that is lacking uterine horns, which are characteristic of the bicornuate uterus found in domestic animals. The endometrium is lined by LE and contains tubular glands that radiate from the surface to the endometrial-myometrial interface. The adult human and primate endometria are divided into two functional layers, the upper stratum functionalis, which

contains glands surrounded loosely by stroma, and the lower stratum basalis, consisting of branching glands and dense stroma [91-93]. The endometrial functionalis is shed during menses. The endometrial basalis is a dynamic, but structurally stable, compartment of the uterus that is not eroded during menstruation or at the end of gestation. This tissue functions as the germinal compartment of the endometrium in these species, and provides stem cells from which the functionalis regenerates with each cycle, or after gestation [92, 94, 95].

Our knowledge of human prenatal and postnatal FRT organogenesis and morphogenesis is very limited [96]. As seen in neonatal rodents and ungulates, the simple columnar epithelium of the undifferentiated uterine body gives rise to numerous invaginations that represent primordial GE buds; however, this occurs during gestation in humans. By 20 to 22 weeks of gestation, the myometrium is well-defined and endometrial gland development is present but remains very superficial [97].

Uterine histoarchitecture at birth resembles that of the adult, but is less developed. Neonatal endometrial LE is low columnar or cuboidal and the GE is sparse and limited to the adluminal stroma [98]. From birth to the onset of puberty, endometrial glands develop slowly. By six years of age, endometrial glands extend from one-third to one-half of the distance to the myometrium. Mature uterine histoarchitecture is observed at puberty, with endometrial glands extending to the inner- circular layer of the myometrium [98]. Although initiated during fetal life, endometrial gland proliferation in the human uterus is completed postnatally, in a manner similar to that observed for domestic ungulates. Thus, genesis of endometrial glands in the human fetus and neonate

involves differentiation of GE from LE, followed by radial development of the tubular glands through endometrial stroma to the myometrium. This initial pattern of endometrial development is opposite to the process of endometrial gland genesis associated with the menstrual cycle in uteri of adult women and primates, where endometrial glands develop adluminally from the basalis during the proliferative phase after menses [91].

Factors That Influence Endometrial Adenogenesis

Postnatal uterine morphogenesis is governed by a variety of hormonal, cellular and molecular mechanisms, for which details remain relatively undefined as compared to other epitheliomesenchymal organs [3, 41]. Morphogenetic events common to postnatal development of uteri include: (1) organization and stratification of endometrial stroma; (2) differentiation and growth of the myometrium; and (3) coordinated development of the endometrial glands [3, 41, 99]. The timing of these developmental events differs among species, but development of the endometrial glands is a uniquely or primarily postnatal event in all studied mammals. Development of the uterine glands is a particularly pivotal and critical event, because alteration or ablation of endometrial glands and/or their secretory products compromises survival and growth of the conceptus in the mouse, rat, pig, cow, sheep and humans [2, 9, 41, 100]. Postnatal uterine development is regulated by many factors including the ovaries, steroids and their receptors, growth factors, and epithelial-stromal interactions.

Ovaries, Steroids, and Steroid Receptors

Jost established the concept that prenatal urogenital tract development in female mammals is an ovary-independent process [101]. In the neonatal pig, ovariectomy at birth does not affect genesis of uterine glands or related endometrial morphogenetic events prior to PND 120, but does inhibit uterine weight after PND 60 [23]. Early postnatal events in rodent uterine development and endometrial adenogenesis are also both ovary-independent [102] and adrenal-independent [30, 32]. From PND 10 to PND 14 in rodents, uterine growth is dependent on the presence of the ovaries and, to a lesser extent, the adrenal glands [32], which is thought to be mediated by the appearance of systemic estrogens beginning at this age [103]. Estrogen is formed from testosterone by the aromatase enzyme, and female aromatase null mice (ArKO) have underdeveloped external genitalia and uteri at 9 weeks of age [104]. Thus, estrogen from the ovary appears to regulate peri-pubertal uterine growth in mice and pigs, but not endometrial adenogenesis.

Ovaries of Spring-born ewes contain significant numbers of growing and antral ovarian follicles at birth (~455 and 935 per ovary, respectively) that increase in number by PND 28 (~683 and 1100 per ovary) and then decline in number by PND 84 (~100 and 287 per ovary) [16]. However, there is no evidence that these ovarian follicles secrete appreciable amounts of estrogens between birth and puberty [16]. Ovariectomy of ewe lambs at birth reduces uterine weight after PND 28 [16]; however, the effects of ovariectomy on endometrial adenogenesis is unknown. In neonatal and prepubertal girls, uterine development and adenogenesis is also likely to be an ovary- and steroid-

independent process [105]. However, functional differentiation of the uterus after puberty requires ovarian steroids [93, 106-109].

Endometrial adenogenesis involves coordinated changes in epithelial phenotype that are marked by ERα expression in nascent and proliferating endometrial GE as well as in stroma and myometrium in neonatal porcine [23, 24], rodent [19-21], and ovine [14] uteri. Homozygous ERα null mice (αERKO) have hypoplastic uteri that contain all characteristic cell types in reduced proportions [110]. Thus, ERα expression is not essential for organogenetic development and differentiation of the fetal uterus nor postnatal uterine histogenesis, but is essential for normal peripubertal uterine growth and development in the mouse [110]. However, homozygous ERβ null mice have no defects in FRT differentiation or fertility [111]. The requirement of ERα for uterine growth and development in the mouse is related to the uterotrophic actions of estrogen [32, 112].

In contrast to rodents, ERα has a particularly important regulatory role in uterine development in the neonatal pig. In the neonatal gilt, administration of the anti-estrogen ICI 182,780, a potent ERα antagonist, to neonatal pigs from birth inhibited endometrial adenogenesis and overall uterine growth at PND 14 without effects on ERα protein expression [24]. The precise roles of E2-17β and ERα in endometrial adenogenesis have not been studied in the neonatal ewe; however, circulating concentrations of E2-17β are high at birth, increase from PND 7 to a peak on PND 28, and then decline to PND 56 in Fall born ewes [14]. During this time, the developing endometrial glands express abundant levels of ERα as well as PR, an estrogen-responsive gene [14].

Collectively, these results are generally consistent with the idea that uterine ERα expression and activation, which may be species-specific, are important elements of the organizational program that determines patterns of uterine growth and endometrial morphogenesis. In this regard, elegant tissue recombination studies involving mouse uterine stroma and epithelium indicate that epithelial ERα is neither necessary nor sufficient to mediate the mitogenic actions of estrogen [113, 114]. In addition to direct ligand-dependent activation of epithelial ERα, proliferative effects of estrogen on epithelium appear to be mediated primarily by stromal ERα via production of paracrine-acting, stromal-derived growth factors such as epidermal growth factor (EGF), IGF-I and IGF-II [113, 115].

ERα can be activated by estrogens, in a ligand-dependent manner, or by growth factor-coupled pathways, in a ligand-independent manner [116, 117]. Transient transfection experiments indicate that ligand-independent ERα activation can be induced by many factors including dopamine, EGF, transforming growth factor α (TGFα), heregulin, and IGF-I [25, 118]. The precise roles and significance of ligand-dependent and ligand-independent actions of ERα in endometrial gland morphogenesis remain to be determined, but the neonatal sheep uterus expresses both IGF-I and IGF-II in the periglandular stroma of the developing endometrium [15]. In the human and primate uterus, organogenetic and perhaps functional differentiation of the endometrium during the proliferative phase is regulated by ovarian estrogen acting through ERα present in the stroma and epithelium [93]. Therefore, the regulatory role of ERα in uterine development and endometrial adenogenesis is species- and developmental stage-specific.

Growth Factors

Stromal-derived growth factors play important roles in epithelial proliferation, differentiation and branching morphogenesis in many developing epitheliomesenchymal organs, including the uterus [68, 69, 119]. Interactions between growth factors and their receptors can involve elements of the ECM, which not only affect patterns of growth factor presentation to target cells, but may also participate as elements of cell surface receptor complexes. Although many studies have promoted the concept that local growth factors regulate organ morphogenesis and differentiated function, recent evidence indicates that systemic growth factors, such as IGF-I, are also important [120]. Thus, uterine development is likely regulated by a carefully orchestrated network of growth factors and hormones from local as well as systemic origins.

Fibroblast growth factors and hepatocyte growth factor

FGF-7 is an established paracrine growth factor that stimulates epithelial cell proliferation and differentiation [121] and FGF-10, isolated originally from rat lung mesenchyme, is essential for patterning of early events in branching morphogenesis [122]. HGF functions as a paracrine mediator of mesenchymal-epithelial interactions that govern mitogenic, motogenic and morphogenic behaviors of epithelia in developing liver, lung and mammary tissues [123]. In the developing neonatal ovine uterus, FGF-7, FGF-10, HGF and their epithelial receptors ($FGFR2_{IIIb}$ and *c-met*) were identified as growth factor systems associated with endometrial morphogenesis [11, 15]. Although FGF-7 mRNA was constitutively expressed in uteri from PND 1 to PND 56, FGF-10 and HGF mRNA levels increased markedly after PND 21, a period characterized by coiling

and branching morphogenesis of endometrial glands in the neonatal ovine uterus. Studies have shown that postnatal progestin exposure suppresses HGF mRNA expression in the stroma and $FGFR2_{IIIb}$ and *c-met* mRNA expression in the LE suggesting these systems may play a role in the epigenetic ablation of endometrial glands in the UGKO [11]. In the human uterus, profiles of HGF and FGF-7 expression are consistent with roles in epithelial proliferation and morphogenesis during the proliferative phase of the menstrual cycle [124, 125].

Insulin-like growth factors

IGF-I and IGF-II regulate cell proliferation, differentiation, and functions acting through autocrine and/or paracrine mechanisms in many organ systems including the uterus [126, 127]. Null mutation of the IGF-I gene in mice demonstrated the critical role of this growth factor in normal development of the female reproductive tract [128], as well as estrogen-induced uterine growth. In the human endometrium, IGFs mediate proliferative growth responses to ovarian estradiol [126, 129]. IGF-II may also be important in growth of the fetal human uterus. IGF-II and variant IGF-II mRNA are expressed in the uterus at 10 to 22 weeks of gestation [130], and the endometrium contains immunoreactive insulin, insulin receptors, IGF-I and IGF-1R in the epithelium of uteri from 19 to 22 weeks of gestation [131].

In neonatal rodent and ovine uteri, the IGF system is involved in postnatal uterine morphogenesis and growth [15, 128, 132]. IGF-I mRNA expression in the neonatal rat uterus is confined to the stroma and myometrium and increases during endometrial adenogenesis [132]. In the neonatal ovine uterus, IGF-I and IGF-II are expressed

predominantly in the stroma surrounding the developing endometrial glands that express the IGF-I receptor [15]; however, their roles in ovine endometrial gland development have not been elucidated.

Epithelial-Mesenchymal Interactions

Development of the uterus depends upon epithelial-mesenchymal interactions for local control and coordination of morphogenetically important cell behaviors including movement, adhesion, differentiation and proliferation [69, 79, 133]. Tissue recombination studies in rodents clearly indicate that uterine mesenchyme directs and specifies patterns of epithelial development, whereas epithelium is required to support organization of endometrial stroma and myometrial differentiation [68, 69, 134, 135]. In rodents, distinct cytodifferentiation of the uterine mesenchyme occurs during postnatal development, and differentiation is complete two weeks after birth. Experiments in which neonatal epithelium from any part of the FRT is recombined with presumptive uterine or vaginal mesenchyme revealed that the epithelium is developmentally plastic and adopts either a uterine (simple columnar) or vaginal (squamous/stratified) epithelial fate dependent upon the origin of the mesenchyme [69, 135].

Studies of neonatal ovine and porcine uterine development, as well as the regenerating primate endometrium during the menstrual cycle, also support the hypothesis that endometrial gland morphogenesis or adenogenesis is supported and regulated through interactions between epithelium and stroma [11, 15, 86, 91, 136, 137]. It is through such interactions that developmentally critical tissue microenvironments, necessary to support and maintain spatially focused changes in cell behaviors associated

with gland genesis, are thought to evolve [41]. The initial differentiation and budding of endometrial GE from LE does not appear to require cell proliferation in the pig and sheep [11, 14, 86]. Rather, the initial growth of the GE buds into the stroma is hypothesized to involve alterations in the basal lamina that permit and direct GE cell migration into the underlying stroma [13, 28].

Epithelial-mesenchymal interactions are mediated by intrinsic growth factor systems as well as by changes in the composition and distribution of extracellular matrix (ECM) components. Glycosaminoglycans (GAGs), oligosaccharide components of the ECM, can affect cell function directly and indirectly, by mediating access of growth factors and other molecules to their receptors or target cells. During adenogenesis in many tissues, including salivary glands, prostate, and uterus, sulfated GAGs, such as chondroitins and heparans, become localized to morphogenetically inactive sites, such as the necks of glands, while non-sulfated GAGs, such as hyaluronic acid, accumulate in morphogenetically active sites, such as the tips of proliferating glands [28, 86, 119].

Matrix metalloproteinases (MMPs) and other factors that alter the biochemical nature of the basal lamina, affect both physical and chemical interactions between epithelium and underlying stroma in human and menstruating primate uteri during the menstrual cycle [138]. Mice lacking tissue inhibitor of metalloproteinase one (TIMP-1) gene have an increased number of endometrial glands in the uterus [139]. Microarray analysis of the developing postnatal uterus in mice found that a number of MMPs and TIMPs were present [85, 140]. MMP-2 mRNA was detected only in the uterine stroma, whereas MMP-10 mRNA was present only in the uterine epithelium from PND 3 to

PND 9. Other MMPs (MMP-11, MMP-14, and MMP-23) and TIMPs 1-3 were detected in both epithelial and stromal cells of the endometrium, but not in the myometrium. Immunoreactive MMP-9 protein was detected only in the endometrial stroma, whereas immunoreactive MMP-2 was detected in both stroma and epithelium of the uterus. These results support the hypothesis that MMPs and TIMPs regulate postnatal development of the mouse uterus.

Prolactin and Prolactin Receptor

PRL, a member of the somatolactogenic superfamily [34], regulates growth and differentiation in many epitheliomesenchymal organs including the pigeon crop sac, mammary glands, and prostate [141]. Available results support the hypothesis that PRL plays a similar role in uterine adenogenesis. In fact, hyperprolactinemia causes uterine glandular hyperplasia in the adult mouse, rabbit and pig [38-40]. In the neonatal ewe, circulating levels of PRL are relatively high on PND 1, reach a maximum on PND 14, and then decline slightly to PND 56 [14, 37]. These temporal changes in circulating levels of PRL in the neonatal ewe parallel the ontogeny of endometrial glands in the developing intercaruncular endometrium of the uterine wall [14]. Additionally, budding, nascent and proliferating endometrial glands express mRNAs for both the long and short PRLR forms on PNDs 7 and 14 [14]. After the budded glands elongate to a more tubular form and begin coiling and branching morphogenesis by PND 21, the ductal GE loses PRLR expression [14]. Only the GE in the stratum spongiosum expresses PRLR on PNDs 28 to 56 [14]. In the adult ovine uterus, PRLR expression is also restricted to GE [18]. Moreover, intrauterine administration of ovine placental lactogen, a PRL-like

hormone that signals through the PRLR [142], stimulates proliferation of endometrial glands in the adult ewe and, in particular, the coiled and branched glands in the stratum spongiosum of adult ewes [67]. Given the central role ascribed to PRLR in other epitheliomesenchymal organs [141], PRLR in the nascent GE of the developing neonatal ovine uterus may play a similar albeit undiscovered regulatory role in endometrial gland morphogenesis; however, the precise role of PRL in neonatal ovine uterine adenogenesis has not been elucidated. Additionally, the GE specific expression of PRLR suggests that its expression is an integral component of GE differentiation. Therefore, the factor(s) responsible for controlling PRLR expression also possesses some level of control over GE differentiation.

PRLR Gene Structure

The complete gene structure for PRLR has been determined in the human, rat, and mouse. While there is variation among these species, many similarities exist including the location of the start codon in exon 3. Both the human [143] and the rat [144] PRLR genes are comprised of eleven exons, while the mouse PRLR gene contains thirteen exons [145]. In these species, the transcriptional start site is located in exon 3; therefore, exons 1 and 2 as well as part of exon 3 comprise the 5'-untranslated region of the gene. Most mammals, including rats, express both long and short forms of the PRLR protein due to alternative splicing of exons 10 and 11, respectively [144]. Alternative splicing of exons 10 and 11 also occurs in humans resulting in one long and two short isoforms [143, 146]. The mouse expresses four isoforms, one long and three short, also arising from alternative splicing of the 3' exons [145, 147]. The variant forms within a species

are identical in their extracellular and transmembrane domain, but differ in the length of their cytoplasmic domains as well as the mechanisms through which they signal [143, 148]. Additionally, the PRLR gene contains a complex 5' genomic structure made up of multiple promoters and non-coding first exons. These alternative first exons are differentially expressed depending on tissue type and developmental stage [149-153].

Rat

The rat PRLR gene spans a 145kb region on chromosome 2 (2q16) [154] and contains four known first exons ($E1_1$, $E1_2$, $E1_3$, and $E1_4$) [150, 151]. The expression of each E1 is controlled by a separate, proximal promoter (PI, PII, PIII, and PIV) [151, 155]. Interestingly, canonical TATAA elements, found in most promoters, are absent from the PRLR promoters; however, they do contain TATA-like sequences [151]. In rats, the long PRLR is encoded for by a 9.7kb mRNA, while the short PRLR is the product of two shorter (2.1kb and 1.8kb) mRNA species [156]. The variability in length of the first exon does determine in part the species of mRNA expressed (2.1kb or 1.8kb) but does not influence the length of the protein product which is most likely determined by post-transcriptional processing [151]. $E1_1$ is 442 nucleotides (nt) long and spans from -557 to -116 (ATG +1) [151]. Expression of $E1_1$ is primarily controlled by a steroidogenic factor-1 (SF1) binding domain in PI [154]. SF1 is an orphan nuclear receptor that is involved in the regulation of sexual differentiation, steroidogenesis and reproduction. Thus, $E1_1$ is highly expressed in ovaries and has a low level of expression in the testis [151, 154]. Expressed only in the liver, $E1_2$ is 233 nt long and spans from -348 to -116 [151]. The expression of this exon is controlled by hepatic nuclear factor-4,

a transcription factor required for the expression of several liver specific genes [153]. The more ubiquitous expression pattern of $E1_3$ can be attributed to the presence of binding sites for the transcription factors C/EBPβ, a member of the CCAAT-enhancer binding protein family (C/EBP), and Sp1, a transcription factor that binds to GC-rich sequence, within PIII [152]. Hu et al. [151] detected high levels of $E1_3$ expression in testis where it was the predominant form with low levels being detected in ovaries and liver. A brain specific PRLR first exon, $E1_4$, was first described by Tanaka et al. [150]. Interestingly, the splicing of this E1 onto PRLR mRNA prohibits the inclusion of exon 2 and is also controlled by a Sp1 binding site [150].

Mouse

The mouse prolactin gene (Prlr) resides on chromosome 15 [157] and encodes four species of mRNA (9.5kb, 4.2kb, 2.4kb, and 1.4kb) [154]. A total of five first exons and promoters span more than 60kb of the 5' region of Prlr [145]. Exons homologous to rat $E1_1$, $E1_2$, and $E1_3$ have been described as well as two novel first exons [145, 154]. The expression patterns of murine $E1_1$, $E1_2$ and $E1_3$ are similar to that seen in the rat. The two novel first exons were isolated by 5'-rapid amplification of cDNA ends (5'-RACE) using liver cDNA [145]. They and their respective promoters have yet to be characterized.

Human

The PRLR gene spans 167kb on human chromosome 5 (5p13) [158]. Six first exons ($hE1_3$, $hE1_{N1}$, $hE1_{N2}$, $hE1N_3$, $hE1_{N4}$, and $hE1_{N5}$) and promoters (hPIII, hP_{N1}, hP_{N2}, hP_{N3}, hP_{N4}, and hP_{N5} respectively) have been isolated (Fig 2.3) [158, 159]. Divergence in the

human PRLR mRNA is seen 5' of nucleotide -106. Only one of the human first exons, $hE1_3$, is homologous to an E1 found in rats and mice [159]. Spanning from -357 to -106, $hE1_3$ is comprised of 253 nt, and, like rodents, its expression is controlled by C/EBP and Sp1 [158]. hE_{N1} is 147 nucleotides long from -252 to -106 [159]. The hP_{N1} promoter contains putative binding sites for the transcription factors ETS-1, Sp1, and AP2, as well as a cyclic-AMP responsive element (CRE) [159]. The ETS element has been proven to be functional; however, Sp1 was not able to bind to this region [158]. The AP2 and CRE sites have not yet been examined. The remaining four first exons were described by Hu et al. using 5'-RACE of cDNA isolated from T-47D cells, a human breast cancer cell line [158]. Of these, hE_{N2} (129 nt) and hE_{N3} (154 nt) are both expressed at low levels in the testis. hE_{N3} is also expressed at high levels in the liver [158]. Also found in the liver, hE_{N5} (132 nt) expression is detectable by RT-PCR analysis in the ovary [158]. Interestingly, hE_{N4} (134 nt) expression was not detectable by RT-PCR analysis in either the gonads or the liver [158]. The promoters for these novel human first exons have not been analyzed.

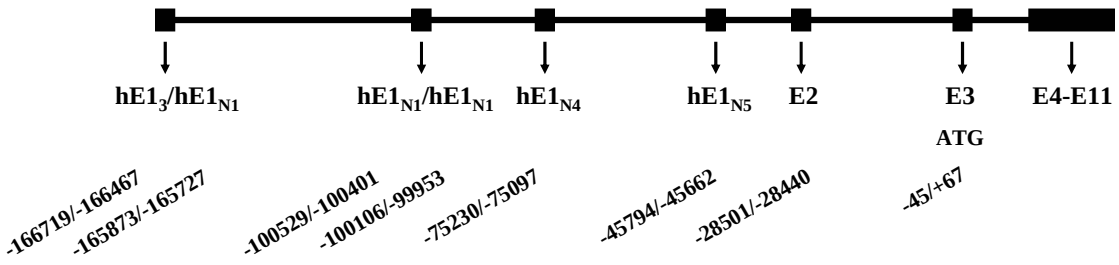

FIG 2.3. Structure of the human prolactin receptor gene (adapted from Hu et al. [153]). The human PRLR gene spans 167 kb on chromosome 5p13. The relative localization of the six alternative first exons and exons 2-11 are shown according to NT_006679.6. The translational start site (ATG) is located in exon 3. Locations and sizes of the exons are shown below (ATG=0).

CHAPTER III

THE ROLE OF ESTRADIOL IN UTERINE ADENOGENESIS

Introduction

Evidence accumulated from primate and subprimate species during the last century supports an unequivocal role for secretions from endometrial glands as primary regulators of conceptus (embryo/fetus and associated extra-embryonic placental membranes) survival, development, production of pregnancy recognition signals, and implantation/placentation [2, 3]. Exposure of neonatal ewes to a progestin from birth epigenetically ablates endometrial gland differentiation and produces an UGKO phenotype in the adult [12]. UGKO ewes are infertile and exhibit early pregnancy loss during the peri-implantation stage of conceptus elongation [12]. Therefore, mechanisms regulating endometrial gland differentiation and development, also termed adenogenesis, in the neonate determines, in part, the functional capacity and embryotrophic potential of the mature uterus [3, 41]. Although a functional role for endometrial glands has been established in many mammals, the developmental mechanisms regulating endometrial gland morphogenesis are not well understood. Uterine development after birth involves differentiation of the endometrial GE from the LE, specification of intercaruncular stroma, development of endometrial folds and, to a lesser extent, growth of endometrial caruncular areas and the myometrium [14, 15]. Endometrial gland development or adenogenesis in the ewe begins between PND 1 and 7 when shallow epithelial invaginations appear along the LE in presumptive intercaruncular areas. Between PND

7 and 14, the nascent GE buds proliferate into the stroma and form tubules or ducts that begin to coil and branch at the tips by PND 21. After PND 21, uterine adenogenesis primarily involves branching morphogenesis of tubular and coiled endometrial glands in the lower stroma (e.g. stratum spongiosum) adjacent to the inner circular layer of the myometrium. By PND 56, uterine morphogenesis is essentially complete, as the aglandular caruncular and glandular intercaruncular endometrial areas appear histoarchitecturally similar to that of the adult uterus [14]. Final maturation and growth of the ovine uterus does not occur until puberty [16].

In the neonatal ewe, pituitary PRL, E2-17β, and stromal growth factors, including FGF-7 and FGF-10, HGF, and IGF-I and IGF-II, with their respective epithelial receptors have been implicated as endocrine and paracrine regulatory systems controlling postnatal ovine endometrial adenogenesis [11, 14, 15]. Available evidence strongly supports a primary regulatory role for PRL in endometrial gland growth and branching morphogenesis [14]. Expression of both short and long forms of the PRL receptor (PRL-R) is restricted to the nascent GE buds on PND 7 and proliferating and developing GE from PND 14 to 56 [14]. Hypoprolactinemia in neonatal ewes retards endometrial gland development, whereas hyperprolactinemia increases endometrial gland development [Chapter V]. The precise roles of circulating E2-17β and uterine ERα in endometrial gland morphogenesis in the neonatal ovine uterus have not been evaluated. Postnatal uterine development is accompanied by expression of ERα in both the nascent and developing GE and endometrial stroma in rodents, pigs and sheep [14, 19-22, 25]. Studies in rodents indicate that endometrial adenogenesis is not dependent

on the ovary, adrenal gland, estrogen or uterine ERα [23, 30, 32, 110]. In contrast, endometrial adenogenesis in the neonatal pig is not dependent on the ovary [22], but is regulated by expression and activation of a functional ERα system [112].

Endometrial adenogenesis in the neonatal ewe is accompanied by abundant expression of ERα in emerging, proliferating and developing glands, as well as in the surrounding peri-glandular stroma [14]. In Fall born ewes, circulating concentrations of E2-17β are high at birth, increase from PND 7 to a peak on PND 28, and then decline to PND 56 [14]. The developing endometrial glands express abundant levels of ERα as well as PR, an estrogen-responsive gene [14]. During this period, the stroma is also ERα-positive and expresses both IGF-I and IGF-II [15]. The developing GE expresses the IGF-I receptor [15], and IGF-I can activate ERα in a ligand-independent manner in other model systems [24]. Available evidence in the neonatal ewe supports the working hypothesis that uterine ERα, activated by ligand-dependent or ligand-independent mechanisms, regulates endometrial gland morphogenesis in the neonatal ovine uterus. In order to test this hypothesis, this study was conducted to determine effects of estradiol-17β valerate (EV; an ERα agonist), CGS 20267 (a non-steroidal aromatase inhibitor), and EM-800 (an ERα antagonist) on uterine growth and endometrial gland development in the neonatal ewe.

Materials and Methods

Animals

All experiments and surgical procedures were in accordance with the Guide for the Care and Use of Agriculture Animals and approved by the University Laboratory

Animal Care Committee of Texas A&M University.

Experimental Design

Crossbred Suffolk ewes were mated to Suffolk rams between September and November. Pregnant ewes were maintained according to normal husbandry practices. Ewes used in the following experiments were born in February and March of 2001. Ewes (n=5 per treatment) were assigned randomly at birth (PND 0) to receive daily subcutaneous (s.c.) injections from PND 0 to PND 56 of: (1) saline and corn oil vehicle as a control (CX); (2) estradiol-17β valerate (EV; 50 μg/kg body weight (BW)) in corn oil; (3) EM-800 (125 μg/kg BW) in saline; or (4) CGS 20267 (125 μg/kg BW) in saline.

The selected dose of EV induces general uterine hyperplasia and precocious GE development in neonatal gilts [22, 112, 160]. The antiestrogen EM-800 fully impedes activities of ERα and ERβ, is a potent and pure antagonist of both ER subtypes [161], and is more potent than ICI 182,870 when injected subcutaneously in the mouse [162]. The EM-800 compound was kindly provided by Fernand Labrie (Universite Lavale, Quebec, Canada). The selected dose of EM-800 is equivalent to the amount of ICI 182,780 used to retard endometrial gland development in neonatal pigs [112]. The CGS 20267 (Letrozole; 4,4-[1,2,3-triazol-1yl-methylene] bis-benzonitrite) compound, a highly specific non-steroidal aromatase inhibitor selected to decrease endogenous estrogen production, was kindly provided by Norvartis Pharma AG (Basel, Switzerland). The selected dose of CGS 20267 was based on results from *in vivo* studies in baboons [163].

Beginning on PND 1, blood samples were collected by jugular venipuncture every 4 days into Vacutainer tubes (BD, Franklin Lakes, NJ) and then processed to obtain serum or plasma. On PND 14, the right ovarian pedicle was ligated with suture, and the ovary and oviduct removed. The right uterine horn was ligated with suture above the intercornual ligament, and the anterior portion of the right uterine horn above the ligature was removed, fixed in fresh 4% paraformaldehyde in PBS (pH 7.2) at room temperature for 24 h, and processed for histology. On PND 56, all ewes were weighed and necropsied. The left ovary was trimmed free of the mesovarium and weighed. The uterus was obtained and trimmed free of the broad ligament, oviduct and cervix. The entire left uterine horn was dissected from the remaining portion of the right uterine horn, weighed, and measured for length. Sections (~ 1 cm) from the mid-portion of the uterine horn were fixed in 4% paraformaldehyde and processed for histology.

Radioimmunoassay

Blood samples for serum were allowed to clot for 1 h at room temperature. Serum was then collected by centrifugation (3000 x g for 30 min at 4C), removed and stored at –20C. Blood samples for plasma were placed on ice immediately after collection. Plasma was then collected by centrifugation (3000 x g for 10 min at 4C), removed and then stored at –20C.

Concentration of PRL in serum was determined using reagents for the ovine PRL RIA provided by Dr. A.F. Parlow and the NIDDK National Hormone and Pituitary Program as described previously [14]. Purified ovine PRL (NIDDK-oPRL-I-3) was iodinated using the chloramine T reaction, and the assay conducted using methods and

reagents provided by the NIDDK Pituitary Hormones and Antisera Center. Assay sensitivity was 0.1 ng/ml, and the intra- and inter-assay coefficients of variation were 5% and 12%, respectively.

Concentration of estradiol in plasma were determined by a double-antibody RIA procedure (Ultra-Sensitive estradiol assay, DSL-4800; Diagnostic Systems Laboratories, Inc., Webster, TX). The procedure entails use of rabbit anti-17β-estradiol (polyclonal) serum and iodinated estradiol. The primary antiserum cross-reacts 2.4%, 0.6%, 0.2%, 2.6%, 0.2% and 3.4% with estrone, estriol, 17α-estradiol, 17β-estradiol-3-glucoronide, estradiol-3-sulfate and D-equilenin, respectively. The estradiol standard curve (ranged from 1.76 to 1600 pg/tube) was prepared from 1,3,5 (10)-Estratrien-3,17beta-diol (17β-estradiol; E950, Batch H239; Steraloids, Inc., Wilton, NH). Goat anti-rabbit gamma globulin serum and polyethylene glycol were used as the precipitating second antibody reagent. The sensitivity of the assay was 3 pg/tube. The intra- and inter-assay coefficients of variation for the assay were 4.3% and 5.4%, respectively. Radioimmunoassay data were analyzed using AssayZap Version 2.0 software (Biosoft, Cambridge, UK).

Histology and Morphometry

After fixation, uterine tissues were changed to 70% ethanol for 24 h and then dehydrated and embedded in Paraplast Plus (Oxford Labware, St. Louis, MO). Uteri were sectioned (5 μm) and stained with hematoxylin and eosin as described previously [12]. Uterine sections (n=4) from each ewe were photomicrographed, and images were analyzed using Scion Image software (Scion Corporation, Frederick, MD) as described

[Chapter V]. Measurements were standardized using the image of a stage micrometer at the same magnification. The number of superficial ductal invaginations of GE from LE into the stroma was determined. Endometrial gland number was determined by counting the total number of uterine glands in a complete cross-section of the uterine horn. A gland cross-section with a visible open lumen was counted as a single uterine gland. Endometrial gland density was determined by counting the number of glands in a 200 μm^2 area of the stratum compactum and stratum spongiosum areas of the intercaruncular endometrium. The number of ductal gland invaginations, endometrial gland number, and gland density estimates were generated for at least three areas within five non-sequential sections from each uterine horn. Intra- and inter-section repeatability estimates for determination of ductal gland invagination number and endometrial gland number by a single observer was 0.85 and 0.8, respectively. In the endometria of uteri from CX and EV ewes, the thickness or width of the endometrium and myometrium (inner circular and outer longitudinal layers) as well as LE cell height were measured using the Scion Image software from multiple points (n=3 to 4) of at least 10 non-sequential uterine sections.

In Situ Hybridization Analysis

Location of mRNA in uterine tissue sections was determined by in situ hybridization as described previously [164]. Deparaffinized, rehydrated, and deproteinated sections (5 μm) of the uterus were hybridized with radiolabeled sense or antisense cRNA probes generated from linearized plasmid templates using in vitro transcription with [α-^{35}S]UTP. Plasmid templates were partial cDNAs for: ovine ERα

[165]; ovine IGF-I, IGF-II and IGF-IR [15]; and bovine long PRLR [166]. After hybridization and digestion with ribonuclease A, slides were exposed overnight to Kodak BioMax X-ray film (Rochester, NY). Slides were then dipped in Kodak NTB-2 liquid photographic emulsion, exposed at 4C for one to four weeks depending on signal intensity as judged from autoradiographs, developed in Kodak D-19 developer, counterstained with hematoxylin, dehydrated, and protected with coverslips.

Immunohistochemistry

Immunoreactive proliferating cell nuclear antigen (PCNA) and ERα proteins were localized in cross-sections (5 μm) of the uterus using the appropriate mouse antibodies and a Super ABC Mouse/Rat IgG Kit (Biomeda, Foster City, CA) as described previously [14]. Mouse monoclonal antibody to PCNA (M0879; clone PC10) was purchased from DAKO (Carpinteria, CA). Rat monoclonal antibody to human ERα (H222) was kindly provided by Dr. Geoffrey Greene (University of Chicago, Chicago, IL). The final working antibody concentration was 2 μg/ml for PCNA and 5 μg/ml for ERα. Antigen retrieval utilizing boiling citrate buffer was performed as described previously for PCNA detection [11, 14]. Antigen retrieval using limited pronase digestion was performed as described previously for ERα detection [165]. The chromagen used for peroxidase localization was 3,3'-diaminobenzidine tetrahydrochloride from Sigma Chemical Co. (St. Louis, MO). Negative controls were performed in which the primary antibody was substituted with the same concentration of purified normal mouse IgG from Sigma Chemical Co. Multiple tissue sections from

each ewe were processed as sets within an experiment. Assessment of staining intensity and effects of treatment were evaluated by two independent observers.

Photomicroscopy

Representative photomicrographs of tissues analyzed by in situ hybridization or immunohistochemistry were taken using a Nikon Eclipse 1000 photomicroscope (Nikon Instruments Inc., Lewisville, TX) fitted with a Nikon DXM1200 digital camera. Digital images were assembled using Adobe Photoshop (Adobe Systems, Seattle, WA).

Statistical Analyses

All quantitative data were subjected to least-squares analysis of variance (LS-ANOVA) using General Linear Models (GLM) procedures of the Statistical Analysis System [167]. Plasma E2-17β and serum PRL levels were log transformed prior to least squares regression analyses. Ovarian weight, uterine horn weight, and uterine horn length data were analyzed using bodyweight as a covariate. Histomorphometrical data were analyzed using an overall model that included main effects of treatment, day, treatment by day interaction, section and area. If a treatment by day interaction was detected, data were reanalyzed within day to determine effects of treatment. Preplanned comparisons used to determine treatment effects on a within-day basis were CX vs EM-800, CX vs CGS 20267, and CX vs EV. In all analyses, error terms used in tests of significance were identified according to the expectation of the mean squares for error. Data are presented as least-square means (LSM) of untransformed values with overall standard errors (SE).

Results

Circulating Level of Estradiol-17β and PRL

Circulating concentrations of E2-17β in plasma were affected (P<0.01) by treatment, day and their interaction. In CX ewes (Fig. 3.1), E2-17β levels were highest between PND 1 and PND 9, declined to PND 13, increased slightly to PND 29, and then declined slightly to PND 56 (cubic effect of day, P=0.03). Overall, E2-17β levels in EM-800 ewes were not different (P>0.10) from CX ewes. However, circulating concentrations of E2-17β were lower (effect of treatment, P=0.07) in ewes receiving CGS 20267, particularly between PND 5 and 13 (quadratic effect of day, P=0.09). As expected in EV ewes, plasma E2-17β was higher on PND 1 than in CX ewes and increased thereafter (quadratic effect of day, P=0.02). Treatment of ewes with EV, EM-800 or CGS 20267 did not affect (P>0.10) circulating concentration of PRL in serum as compared to CX ewes (data not shown).

Treatment with EM-800 Antiestrogen Retards Endometrial Gland Morphogenesis

As summarized in Table 3.1, uterine weight and horn length on PND 56 were not affected (P>0.10) by EM-800 or CGS treatments. Treatment of ewes with EV from birth decreased (P<0.01) uterine weight, uterine horn length, and ovarian weight on PND 56. Ovarian weight was 200% greater (P>0.01) in CGS-treated ewes, but not different (P>0.10) in EM-800 compared to CX ewes. The ovaries from CX and EM-800 ewes contained numerous small vesicular follicles (data not shown). The ovaries of CGS ewes also contained follicles as well as one or more corpora lutea in three of the five treated ewes. In contrast, the ovaries of EV ewes were small and devoid of vesicular

follicles.

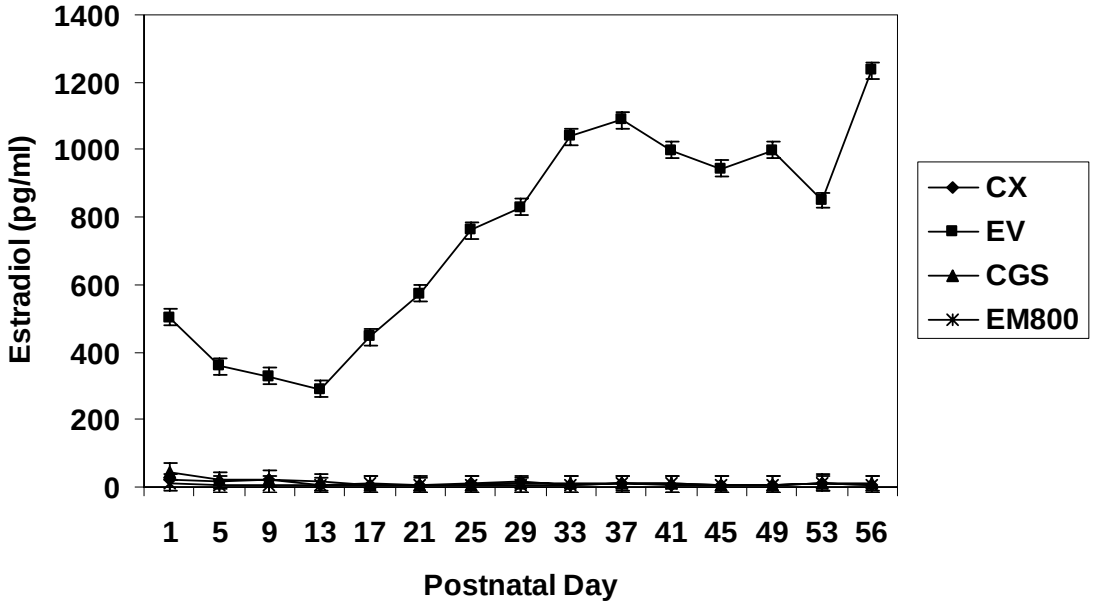

FIG 3.1. Concentrations of estradiol-17β in plasma from neonatal ewes assigned to the four treatment groups, as indicated by the legend, between PND 1 and PND 56. The Y scale is logarithmic.

Table 3.1. Effects of treatment on ovarian weight, uterine weight and uterine horn length on PND 56 for ewes treated with corn oil (CX), estradiol valerate (EV; ERα agonist), EM-800 (ERα antagonist), and CGS 20267 (aromatase inhibitor) from birth.

Treatment	Ovarian Weight (g)	Uterine Weight (g)	Uterine Horn Length (cm)
CX	0.8	2.5	6.0
EV	0.3[a]	1.2[a]	4.0[a]
EM-800	1.0	2.7	5.9
CGS 20267	1.6[a]	2.7	6.3
SE	0.2	0.3	0.2

[a] Significant difference ($P<0.01$) compared with CX.

On PND 14, the intercaruncular endometrium in CX ewes contained tubular and slightly coiled endometrial glands radiating from the uterine lumen into the upper stroma (Fig. 3.2). The endometrial LE appeared to be pseudostratified and columnar. On PND 56, the intercaruncular endometrium contained numerous coiled and branched glands in the intercaruncular endometrium extending from the LE through the stroma to the inner circular layer of smooth muscle of the myometrium. In CX ewes, the number of superficial ductal gland invaginations and endometrial glands increased ($P<0.01$) between PND 14 and PND 56 (Table 3.2). Treatment of ewes with CGS 20267 from birth did not result in detectable effects on uterine development or endometrial adenogenesis (Fig. 3.2). The number of ductal gland invaginations and endometrial glands were not different ($P>0.10$) for CGS compared to CX ewes on either PND 14 or PND 56.

Treatment of ewes with EM-800 from birth altered endometrial gland morphogenesis (Fig. 3.2). On PND 14, uteri from EM-800 ewes appeared histologically similar to CX ewes, except for a slight reduction in coiled endometrial glands in the stratum compactum. The number of ductal gland invaginations and endometrial glands were not different ($P>0.01$) in EM-800 compared to CX ewes on PND 14 (Table 3.2). However, the intercaruncular endometrium of EM-800 ewes on PND 56 tended to have fewer ($P<0.10$) endometrial glands that were less branched, and ductal gland invaginations were clearly lower ($P<0.01$) than for CX ewes.

As summarized in Table 3.2, endometrial gland density in the stratum compactum area of the intercaruncular endometrium adjacent to the LE was affected by

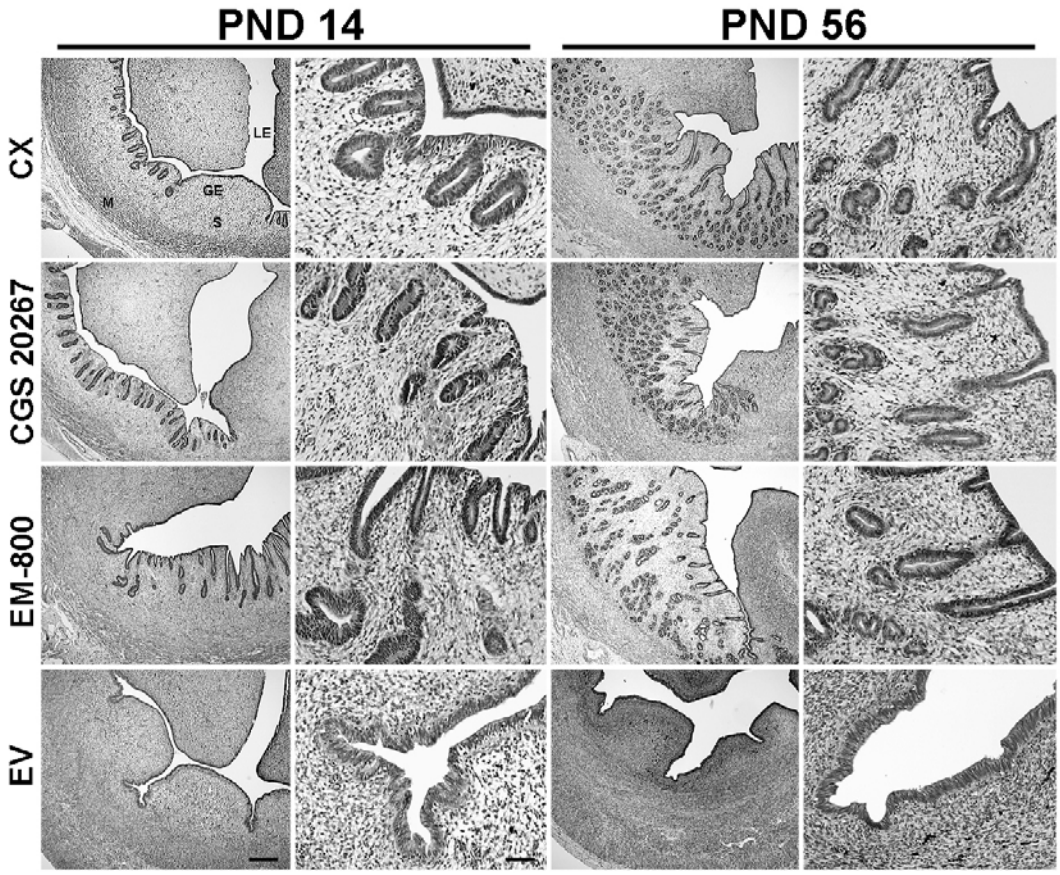

FIG 3.2. Representative photomicrographs of uteri on PND 14 and PND 56 in ewes. Effects of treatment are described in the text and summarized in Table 2. Tissues were prepared and stained using hematoxylin and eosin. Legend: GE, glandular epithelium; LE, luminal epithelium; M, myometrium; S, stroma. Bars represent 500 μm at low magnification and 50 μm at high magnification.

treatment ($P<0.01$), but not day ($P>0.10$). On PND 14 and PND 56, gland density was not different ($P>0.10$) in CX as compared to CGS ewes. In contrast, treatment of ewes from birth with EM-800 decreased ($P<0.01$) gland density in the stratum compactum on PND 14 and PND 56. Endometrial gland density in the stratum spongiosum area of the intercaruncular endometrium adjacent to the inner circular layer of myometrium was not affected ($P>0.10$) by CGS treatment, but treatment with EM-800 decreased ($P<0.01$) endometrial gland density on PND 56.

Table 3.2. Histomorphometrical measurements of uteri on PND 14 and PND 56 in ewes treated with corn oil (CX), estradiol valerate (EV; ERα agonist), EM-800 (ERα antagonist), and CGS 20267 (aromatase inhibitor) from birth. Legend: SC, stratum compactum; SS, stratum spongiosum.

	PND 14					PND 56				
Measurement	**CX**	**EV**	**EM-800**	**CGS 20267**	**SE**	**CX**	**EV**	**EM-800**	**CGS 20267**	**SE**
Ductal Gland Invaginations (number/section)	40	0 [a]	39	38	4	66	0 [a]	37 [a]	56	3
Gland Number (per section)	68	0 [a]	68	69	6	498	0 [a]	391 [b]	606	45
SC Gland Density (number/200 μm^2)	4.4	0 [a]	3.5 [a]	4.2	0.2	4.2	0 [a]	3. 5 [a]	4.3	0.2
SS Gland Density (number/200 μm^2)	0	0	0	0	0	11.0	0 [a]	8.7[a]	11.7	0.3

[a] Effect of treatment within PND ($P<0.05$) compared to CX.
[b]Effect of treatment within PND ($P<0.10$) compared to CX.

Treatment with EV Inhibits Uterine Growth and Endometrial Gland Differentiation

Treatment of ewes from birth with EV affected uterine development and endometrial adenogenesis. The endometrium from uteri of EV ewes on both PND 14 and PND 56 did not contain any histologically discernable endometrial glands (Fig. 3.2). The LE of the presumptive intercaruncular endometrial areas appeared hypertrophic, columnar and more ruffled than for CX ewes. In uteri from EV ewes, the stroma appeared more compact on PND 14 and was markedly denser on PND 56 as compared to CX ewes. The dense endometrial stroma in EV ewes on PND 56 lacked the characteristic stratum compactum and stratum spongiosum layers observed for the intercaruncular endometrium of CX ewes.

The effect of EV exposure on different uterine tissues was determined using

histomorphometry. Overall, endometrial thickness was affected ($P<0.001$) by day, treatment and their interaction. In CX ewes, endometrial thickness increased between PND 14 and PND 56. In contrast, EV treatment decreased ($P<0.01$) endometrial thickness on PND 14 (CX vs EV, 219 vs 178$\pm$5 μm) and PND 56 (318 vs 138$\pm$5 μm). In CX ewes, myometrial thickness increased ($P<0.05$) between PND 14 and PND 56. Treatment with EV increased ($P<0.01$) myometrial thickness on both PND 14 (CX vs EV, 224 vs 335$\pm$11 μm) and PND 56 (291 vs 355$\pm$11 μm). Overall, height of the LE was affected by treatment ($P<0.0001$), day ($P=0.05$) and their interaction ($P<0.01$). In uteri from PND 14, LE height was greater ($P<0.01$) in EV than CX ewes (CX vs EV, 2.9 vs 5.0$\pm$0.1 μm). Similarly, treatment with EV from birth increased ($P<0.01$) height of the LE on PND 56 (CX vs EV, 2.4 vs 5.1$\pm$0.1 μm).

Treatment with EV Does Not Affect Uterine Cell Proliferation

In order to determine how EV affects uterine growth and differentiation, expression of PCNA protein was determined in uteri from CX and EV ewes (Fig. 3.3). PCNA is a highly conserved DNA polymerase accessory protein essential for DNA synthesis, expressed during late G1 and S phases of the cell cycle, and a marker of cell proliferation [168]. In CX ewes, immunoreactive PCNA expression was present in all cell types of PND 14 uteri. Highest levels of PCNA protein were detected in the LE, GE and stroma of the intercaruncular endometrial areas. By PND 56, overall levels of PCNA expression were lower in endometrium of CX ewes. In EV ewes, expression of PCNA protein was not different on PND 14 compared to CX ewes. On PND 56, PCNA protein expression was particularly abundant in the upper portion of the stroma in the

uteri from EV ewes, similar to that observed in the stratum compactum of the intercaruncular endometrium of uteri from CX ewes. In addition, the endometrial LE of EV ewes contained a higher abundance of PCNA protein in the presumptive intercaruncular endometrial areas.

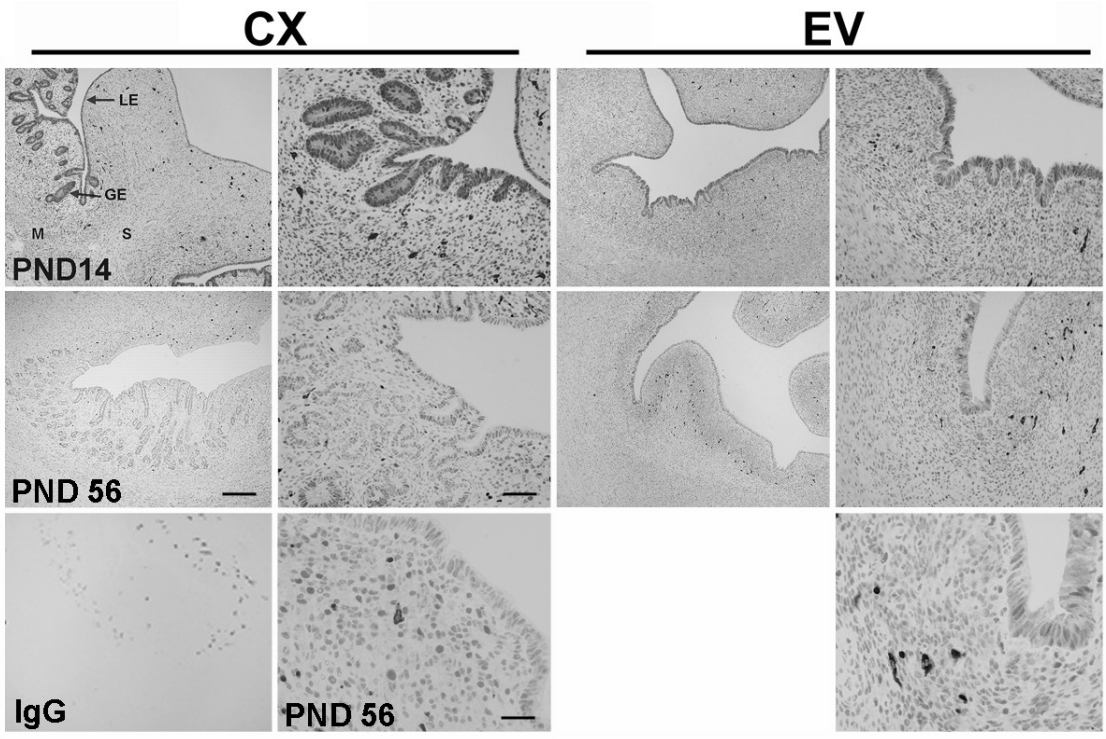

FIG 3.3. Representative photomicrographs depicting the distribution of immunoreactive PCNA protein in uteri from control and EV- treated ewes on PNDs 14 and 56. Immunoreactive protein was detected using mouse anti-PCNA monoclonal antibody and a BioStain Super ABC kit. Nuclear staining was not observed when irrelevant mouse IgG was used (see inset). Legend: GE, glandular epithelium; LE, luminal epithelium; M, myometrium; S, stroma. Bars represent 100 μm at high magnification and 50 μm at low magnification.

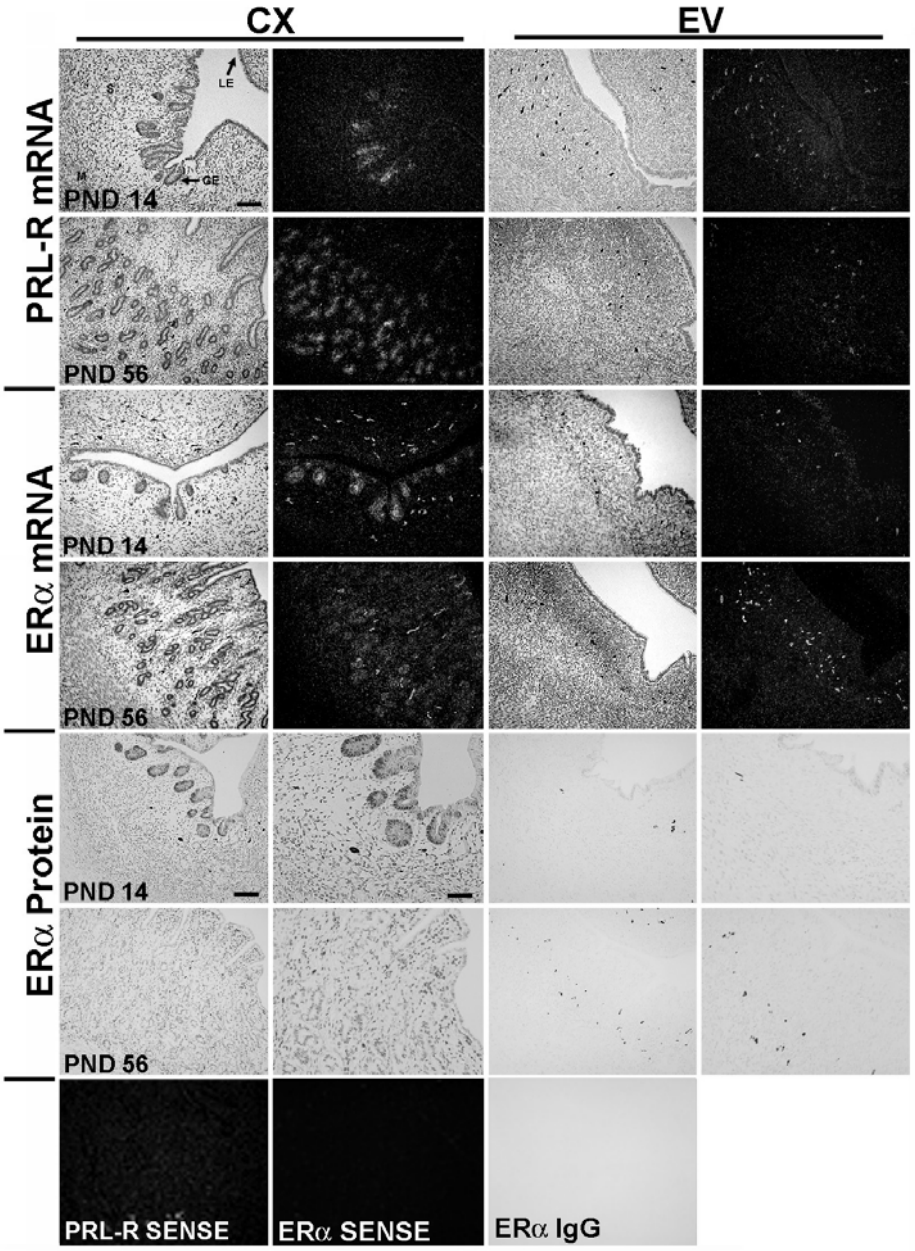

FIG 3.4. Representative photomicrographs depicting expression of PRLR mRNA and ERα mRNA and protein in uteri of control and EV treated ewes on PND 14 and 56. Top panel: In situ localization of PRLR mRNA; Middle panel: In situ localization of ERα mRNA; and Bottom panel: immunolocalization of ERα protein using rat-anti-human ERα monoclonal antibody. Nuclear staining was not observed when irrelevant rat IgG was substituted for primary antibodies. Cross-sections of uterine wall were hybridized with radiolabeled antisense or sense PRL-R or ERα cDNA probes. Protected transcripts were visualized by liquid emulsion autoradiography and were imaged under bright- and dark-field illumination. The inset panels illustrate the sense or IgG control. Many uteri contained pigmented melanocytes that are black in brightfield and white in darkfield photomicrographs. Legend: GE, glandular epithelium; LE, luminal epithelium; Mel, melanocytes; M, myometrium; S, stroma. Bars represent 50 μm at low magnification and 100 μm at high magnification.

Treatment with EV Suppresses PRLR and ERα Expression

The PRLR is a specific and restricted marker of GE phenotype in the neonatal and adult ovine uterus [14, 18]. Therefore, PRLR mRNA expression was determined in CX and EV uteri (Fig. 3.4). The uteri of many ewes contained darkly pigmented melanocytes that appear white in darkfield photomicrographs. In uteri from CX ewes, PRLR mRNA was detected only in the nascent budding and tubular glands on PND 14 and only in the coiled and branched glands on PND 56. There was an absence of PRLR mRNA in the superficial ductal glands in uteri from CX ewes on PND 56. In uteri from EV ewes, PRLR mRNA expression was not detected in any uterine cell type.

On PND 14 in CX ewes, expression of ERα mRNA and protein was most abundant in the endometrial GE with lower levels in LE and stroma (Fig. 3.4). In contrast, ERα expression on PND 56 in CX ewes was low in GE and LE, but abundant in the stroma. In uteri from EV ewes, ERα expression was markedly reduced in the endometrial LE and essentially absent in stroma and myometrium on both PND 14 and PND 56.

Treatment with EV Reduces Stromal IGF-I and IGF-II mRNA in the Endometrium

In CX ewes, IGF-I mRNA was detected only in the uterine stroma and predominantly in the intercaruncular endometrium (Fig. 3.5). Overall levels of IGF-I mRNA expression increased in uteri from CX ewes between PND 14 and PND 56. In EV ewes, stromal IGF-I mRNA expression was markedly decreased in PND 14 uteri and completely absent in PND 56 uteri as compared to the sense control.

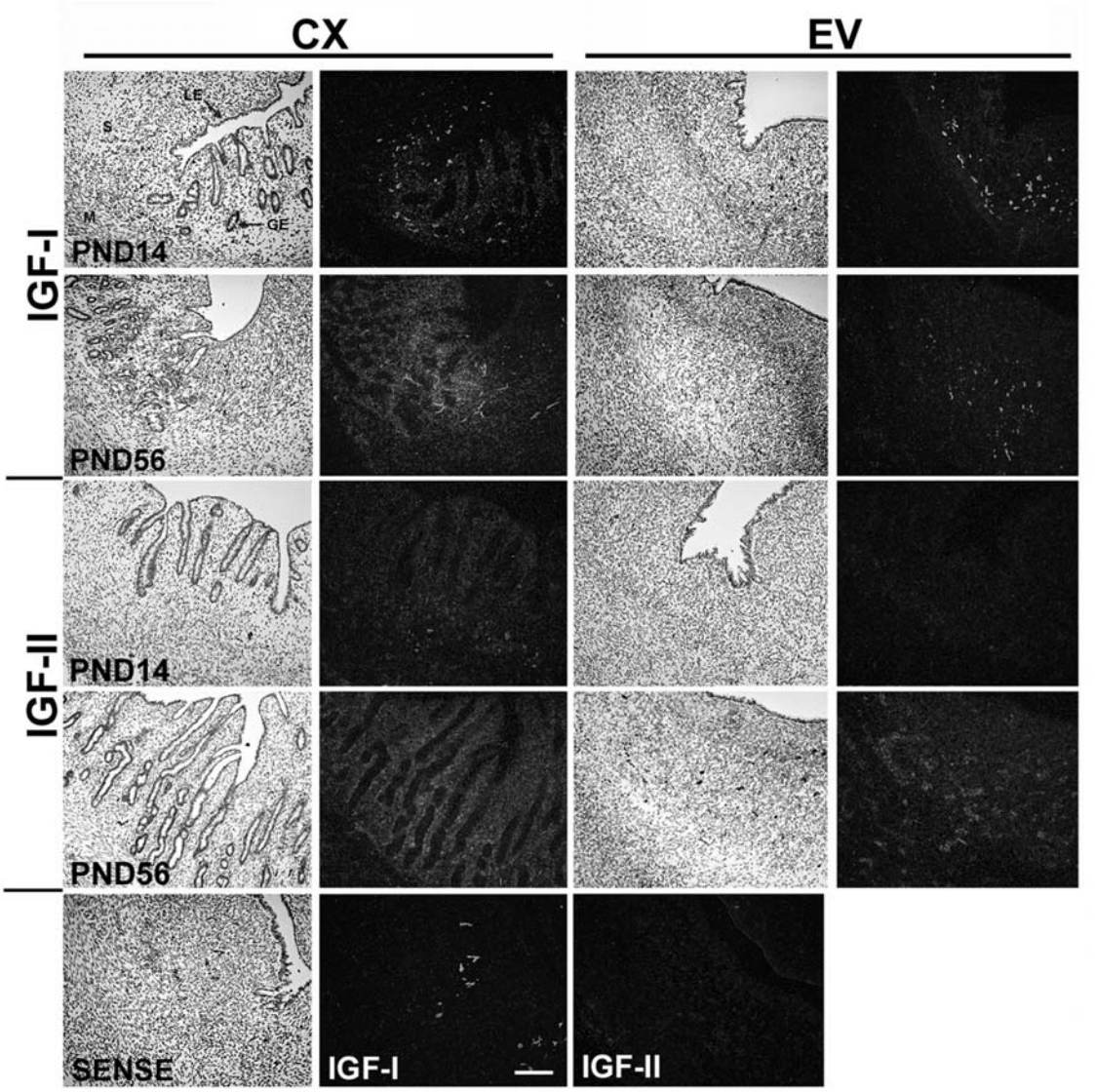

FIG 3.5. Expression of IGF-I and IGF-II mRNAs in uteri from CX and EV treated ewes on PND 14 and PND 56. Cross-sections of uterine wall were hybridized with radiolabeled antisense or sense ovine IGF-I or ovine IGF-II cRNA probes. Protected transcripts were visualized by liquid emulsion autoradiography and were imaged under bright- and dark-field illumination. Many uteri contain pigmented melanocytes that are black in brightfield and white in darkfield photomicrographs. Legend: GE, glandular epithelium; LE, luminal epithelium; M, myometrium; S, stroma. Bar represents 100 μm.

Expression of IGF-II mRNA was also detected only in the endometrial stroma and increased between PND 14 and PND 56 in uteri from CX ewes (Fig. 3.5). In uteri from PND 14 EV ewes, IGF-II mRNA expression was not detected in any uterine cell

type. However, IGF-II mRNA expression was detected in the stroma of uteri from PND 56 EV ewes. As compared to uteri from PND 56 CX ewes, the expression pattern of IGF-II mRNA was not as abundant and uniform, but appeared variegated. Expression of IGF-I receptor mRNA was detected in all endometrial cell types on both PND 14 and PND 56 and was not affected by treatment with EV (data not shown).

Discusssion

In the present study, average plasma E2-17β levels were maximal on PND 1 (~25 pg/ml) and ranged from a low of 6 pg/ml on PND 13 to 16 pg/ml on PND 29 in CX ewes. The circulating concentrations of E2-17β in the present study using Spring born ewes were lower than those previously reported by this laboratory for Fall born ewes [14]. It is possible that this difference is due to seasonal effects, as marked differences in circulating levels of PRL at birth and on PND 0 to PND 35 were found in neonatal ewes that may have reflected effects of photoperiod in utero [37]. Treatment with CGS 20267, a non-steroidal aromatase inhibitor, decreased circulating concentrations of E2-17β in plasma. Although circulating levels of E2-17β were not completely suppressed in CGS-treated ewes, CGS 20267 decreased circulating concentrations of E2-17β in baboons from 1-2 ng/ml to 0.1 ng/ml within 48-72 h post-treatment [169]. In the present study, ovarian weight was 200% greater in CGS than CX ewes on PND 56, which can be attributed to the presence of corpora lutea (CL) on the ovaries of three of the five ewes treated with CGS 20267. In women with anovulatory infertility, oral administration of 2.5 mg CGS 20267 was effective in inducing ovulation [170]. The ovary of the neonatal ewe normally contains large numbers of growing and vesicular follicles that increase

from birth to PND 28 and then decline significantly by PND 84 [16]. The ovaries of Spring born ewes do not usually contain CL, because they are prepubertal and born during the period of seasonal anestrus.

Treatment of ewes with CGS 20267 did not affect ovine uterine gland morphogenesis between birth and PND 56 in the present study. These results do not support our initial working hypothesis that changes in circulating E2-17β regulate endometrial gland differentiation and morphogenesis in the neonatal ovine uterus. In the ewe, removal of the ovary at birth does not affect uterine gland development on PND 14 [28]. Similarly, the ovary and E2-17β do not play a role in endometrial gland development in either the rodent or pig. Although circulating estrogens increase between PNDs 9 and 11 in the rat [103], initial postnatal uterine growth and endometrial adenogenesis are both ovary- and adrenal-independent [23, 110]. In the neonatal gilt, ovariectomy at birth inhibits uterine growth after PND 56, but does not affect genesis of uterine glands or related endometrial morphogenetic events prior to PND 120 [22]. Available evidence indicates that prepubertal uterine development and endometrial adenogenesis is an estrogen-independent process in mammals.

Genesis of endometrial glands in porcine [22], rodent [19-21, 25] and sheep [14] uteri involves coordinated changes in epithelial phenotype that are marked by ERα expression in nascent and proliferating endometrial GE. In the present study, treatment of neonatal ewes with EM-800, an antagonist of both ERα and ERβ, did not affect the initial stage of gland genesis between birth and PND 14 that involves budding differentiation of the GE from the LE and formation of tubules. However, EM-800

treatment retarded coiling and branching morphogenetic development of the endometrial glands between PND 14 and PND 56. Further, histomorphometry indicated that EM-800 treatment prevented the increase in superficial ductal gland invaginations that occurs between PND 14 and PND 56 in CX ewes. These results support a portion of our working hypothesis that expression and functional ERα activation regulate endometrial gland morphogenesis in the ewe, but modifies our hypothesis to indicate a specific role(s) in gland genesis and coiling and branching morphogenesis between PND 14 and PND 56 rather than initial stages of gland tubulogenesis between birth and PND 14. Indeed, daily administration of the anti-estrogen ICI 182,870 (125 μg per kg BW) from birth does not affect endometrial adenogenesis in neonatal ewes [K.M. Taylor and T.E. Spencer, unpublished results]. Similarly, inhibition of ERα activation by ICI 182,870 in neonatal rats from PND 10-14 has no effect on endometrial adenogenesis [32]. Homozygous ERα null mice (αERKO) have hypoplastic uteri that contain all characteristic cell types in reduced proportions [30]. In contrast to rodents, activated ERα regulates, in part, endometrial gland morphogenesis in pigs, because administration of ICI 182,780 to gilts from birth retarded endometrial adenogenesis on PND 7 and PND 14 [112]. The lack of involvement of uterine ERα in endometrial gland morphogenesis in rodents may be attributed to the lack of tightly coiled and branched endometrial glands in their uteri as compared to the sheep and pig.

Results from the present study indicated that the uterine ERα system regulates, in part, the coiling and branching morphogenetic development of the endometrial glands following the initial period of gland genesis that occurs between birth and PND 14 in the

ewe. The activation of ERα appears to be ligand-independent rather than ligand-dependent [24]. Activation of ERα by growth factors, such as IGF-I, involves direct serine phosphorylation by mitogen activated protein kinase (MAPK) pathways [171]. In the neonatal ovine uterus, both IGF-I and IGF-II mRNAs were expressed in the endometrial stroma and myometrium, with IGF-I predominantly present in the intercaruncular endometrial stroma [15]. Interestingly, IGF-I mRNA is nearly undetectable in ovine endometrium at birth and becomes strikingly abundant in the intercaruncular stroma surrounding the differentiating, developing, and proliferating endometrial glands between PND 7 and PND 56 [15]. In the neonatal ovine uterus, the IGF-I receptor is expressed in all uterine cell types, and phosphorylated extracellular regulated (ERK1 and ERK2) MAPKs are particularly abundant in the endometrial GE [15]. Therefore, IGF-I and perhaps IGF-II may regulate endometrial gland coiling and branching morphogenesis via ligand-independent activation of ERα that may account for the effects of EM-800 in the present study.

The present study is the first to indicate that inappropriate exposure of the developing neonatal ovine uterus to EV from birth disrupts uterine development and epigenetically ablates endometrial gland morphogenesis. Transcription of the PRLR gene is localized exclusively to nascent and developing endometrial glands where it plays a role in proliferation and development of the GE [14]. Therefore, absence of PRLR mRNA in EV treated uteri clearly suggests that EV inhibited the genesis of endometrial glands. The effects of EV in the present study are similar to those observed in rodents, but opposite to that reported for pigs. The same dose of EV administered to

gilts from birth to PND 6 or PND 13 increased uterine weight and induced precocious development of endometrial glands [112, 160]. In gilts, thickness of the endometrium, but not the myometrium, was increased by EV treatment. In contrast, results from the present study indicated that treatment of ewes with EV from birth decreased endometrial thickness and increased myometrial thickness on both PND 14 and PND 56. The anti-adenogenic effect of EV in the neonatal ovine uterus is similar to that reported for rats in that administration of estrogens to neonatal rats during the period of normal gland genesis (PND 10-14) induced a dose-related delay in the onset of appearance of glands [84]. Similarly, administration of tamoxifen, a mixed ER agonist/antagonist, to neonatal rats on PNDs 1-5 or PNDs 10-14 elicited a dose-related inhibition of uterine gland genesis that persisted to PND 26 or PND 60, respectively [172]. However, tamoxifen administered on PND 20-24, which is after the age of normal gland genesis, did not alter the number of preexisting glands. The observed differences in effects of inappropriate exposure to estrogen on uteri of sheep and rodents as compared to pigs may be due to differences in effects of ovarian steroids on steroid receptor gene expression in endometrial epithelia and myometrium of the adult uterus [173]. Collectively, studies in the sheep, pig and rodent reinforce the concept that postnatal uterine development occurs during a critical period during which endocrine disruptors can exert irreversible negative epigenetic effects on uterine development that determines uterine function in the adult.

The mechanism whereby exposure to EV inhibits endometrial adenogenesis is not fully understood. In the present study, treatment with EV from birth almost completely suppressed ERα expression in the uterus. Similarly, treatment of ewes with

a 19-norprogestin from birth ablates endometrial adenogenesis and suppresses ERα expression [11]. However, results from the present study indicate that expression and activation of a functional ERα system is not required for endometrial adenogenesis between birth and PND 14. Further, results from the analyses of PCNA protein expression indicates that the anti-adenogenic effects of EV are not due to inhibition of cell proliferation in the endometrial epithelia or stroma. Interestingly, PCNA expression in endometrium of EV ewes on PND 56 appeared to be greatest in the subepithelial stroma and correlates with PCNA staining in the deep stroma surrounding the proliferating and differentiating GE during normal uterine development [14]. In developing lung epithelium, bud outgrowth is not accompanied by induction of localized cell proliferation [174], but appears to involve remodeling of the basement membrane [175]. Thus, EV may suppress alterations in the epithelial-mesenchymal interface or extracellular matrix that have been proposed to support initiation of endometrial adenogenesis [10, 12, 28, 176]. Treatment of neonatal rats and mice with EV induces hypertrophy of the LE in both mice and rats [32, 114]. Similarly, EV exposure in the present study induced LE hypertrophy combined with compaction of the stroma, resulting in a 66% decrease in endometrial thickness by PND 56 in EV ewes. The disorganized, variegated nature of IGF-II expression in the compacted stroma of uteri from PND 56 EV ewes is distinctly different from its temporal and spatial pattern of expression during normal development of the intercaruncular endometrial stroma into two layers termed the stratum compactum and stratum spongiosum [14]. Given that the first step in uterine gland development involves differentiation of GE and invagination

of nascent glands into underlying stroma, one may speculate that the extreme hypertrophic state of LE induced by ERα agonists, such as EV and tamoxifen, prevents invagination of GE physically, as a consequence of alterations in cell shape and associated changes in cell-cell, and cell-ECM relationships that would otherwise support this process [177, 178]. Under such conditions, epithelial cells could be unable to recognize, integrate and respond normally to cooperative signals that normally drive gland genesis [32, 68, 84].

The process of uterine morphogenesis is governed by a variety of hormonal, cellular and molecular mechanisms, many of which remain to be defined [3, 41, 179]. Results from our previous studies supported the hypothesis that E2-17β and uterine ERα comprise a regulatory system to stimulate and maintain endometrial gland morphogenesis in the neonatal ovine uterus [14, 15]. Results from the present study do not support a role for E2-17β as a regulator of endometrial gland morphogenesis. However, results clearly support the hypothesis that expression and functional activation of ERα by ligand-independent mechanisms is required for proper endometrial gland coiling and branching morphogenesis in the neonatal ewe. Further, results from EV-treated ewes support the hypothesis that epithelial-stromal interactions are important for endometrial gland differentiation. Future studies will be directed at determining the roles of these critical interactions and stromal-derived factors, such as IGF-I and IGF-II, in endometrial gland morphogenesis using the neonatal ewe as a model system.

CHAPTER IV

OVARIAN REGULATION OF ENDOMETRIAL GLAND MORPHOGENESIS

Introduction

Uterine adenogenesis in the ewe begins after birth and involves the emergence, proliferation and differentiation of endometrial glands, specification of intercaruncular stroma, development of endometrial folds and, to a lesser extent, growth of endometrial caruncular areas and the myometrium [3, 11, 13-15]. Uterine gland development or adenogenesis is initiated between PND 1 and 7 when shallow epithelial invaginations appear along the endometrial LE in presumptive intercaruncular areas. Between PND 7 and 14, the nascent GE buds proliferate, grow into the stroma and form tubules or ducts that begin to coil and branch at the tips by PND 21. After PND 14, endometrial adenogenesis primarily involves coiling and branching morphogenetic growth of tubular endometrial glands from the upper stroma (e.g. stratum compactum) underneath the LE into the lower stroma (e.g. stratum spongiosum) adjacent to the inner circular layer of the myometrium. By PND 56, uterine morphogenesis is essentially complete, as the aglandular caruncular and glandular intercaruncular endometrial areas appear histoarchitecturally similar to that of the adult uterus [14]. Final maturation and growth of the ovine uterus does not occur until after puberty and endocrine events of pregnancy [16].

Jost [101] first established the concept that prenatal urogenital tract development in female mammals is an ovary-independent based on results from studies of rabbits.

Since then, studies of several species revealed that uterine development and endometrial adenogenesis can proceed normally in the absence of the ovary and, by default, ovarian steroids for varying periods of time during early postnatal life. In the prepubertal ewe, the ovary contains growing and vesicular ovarian follicles at birth that decline to PND 14, increase and peak in number on PND 28, remain high from PND 42 to PND 56, and decline thereafter [26, 27]. These changes in ovarian follicles correlate with the ontogeny of endometrial gland development in the ewe lamb [14]. However, ovariectomy of the ewe at birth does not affect uterine wet weight [27] or the initial stages of endometrial gland tubulogenesis [28] on PND 14, but does affect uterine growth after PND 14 [180]. Postnatal uterine growth and endometrial adenogenesis are ovary- and steroid-independent in rodents [30-32] and pigs [23]. Similarly, recent results indicate that postnatal uterine growth and endometrial adenogenesis are estrogen-independent from birth to PND 56, although coiling and branching morphogenesis after PND 14 is, in part, dependent on activated ERα [Chapter III]. Although the ovary plays a role in postnatal uterine growth, the role of the ovary in endometrial gland development after PND 14 has not been investigated in the ewe.

Recent results from studies of the neonatal ovine uterus implicate follistatin, activins, and activin receptors as autocrine and paracrine regulators of endometrial gland morphogenesis [181]. Activins and inhibins are members of the transforming growth factor (TGF) β superfamily and regulate growth and differentiation of many branched epitheliomesenchymal organs via autocrine, paracrine and perhaps endocrine mechanisms [182-187]. Activins and inhibins are dimeric proteins [188, 189]. Activin

consists of two β subunits, βA and βB, that homodimerize or heterodimerize to form activin A (βA:βA), activin B (βB:βB), or activin AB (βA:βB). Inhibin consists of an α-subunit that heterodimerizes with an activin β-subunit to form either inhibin A (α:βA) or inhibin B (α:βB). The biological activity of activins is mediated by receptor complexes consisting of Type IA (ActRIA) or Type IB (ActRIB) receptor and Type II (ActRII) receptor. One of the key features that distinguish the effects of activins from those of TGFβ is that binding of activins to their receptors can be blocked if activin binds to follistatin or if inhibin α-subunit binds to activin receptors [190-192]. Follistatin binds to activins with high affinity and neutralizes their activity [193-195]. Inhibin α-subunit, activins and follistatin are synthesized and secreted by granulosa cells of ovarian follicles in the neonate and the adult [188, 189, 196-199]. Therefore, these ovarian factors could act in an endocrine manner to regulate uterine growth and endometrial adenogenesis via the activin-follistatin system to compliment endocrine and paracrine effects of the activin-follistatin system in the in the neonatal ovine uterus.

Available evidence in the ewe and other domestic and laboratory animals supports the working hypothesis that endometrial adenogenesis is not regulated by the ovary and, thus, ovarian factors. In order to test this hypothesis, the present studies were conducted to determine: (1) effects of removing the ovary at PND 7 on subsequent uterine growth and endometrial adenogenesis on PND 56; (2) effects of ovariectomy on the activin-follistatin system in the uterus; and (3) expression of the activin-follistatin system in the neonatal ovary.

Materials and Methods

Animals and Experimental Design

All experiments and surgical procedures were in accordance with the Guide for the Care and Use of Agriculture Animals and approved by the University Laboratory Animal Care Committee of Texas A&M University. Crossbred Suffolk ewes were mated to Suffolk rams between the months of September and November 2001. Pregnant ewes were maintained according to normal husbandry practices. Ewes used in the following experiments were born between the months of February and March 2002. In Study One, ewes were assigned randomly at birth or PND 0 to undergo either a sham surgery as a control (CX) or bilateral ovariectomy (OVX) on PND 7 (n=6 per treatment). Beginning on PND 0, blood samples were collected by jugular venipuncture every 7 days into Vacutainer tubes without anticoagulant (Becton-Dickinson, NJ). On PND 56, all ewe lambs were weighed and necropsied. The uterus was obtained, trimmed free of the broad ligament, oviduct and cervix, and weighed. Sections (~ 1 cm) from the mid-portion of each uterine horn were fixed in fresh 4% paraformaldehyde at room temperature for 24 h and processed for histology. The remainder of the uterus was frozen in liquid nitrogen and stored at –80C. In Study Two, ewes (n=45) were assigned randomly at birth to be ovariohysterectomized on PND 0 (n=6), 7 (n=4), 14 (n=5), 21 (n=5), 28 (n=5), 35 (n=5), 42 (n=5), 49 (n=5) or 56 (n=5). A portion of the ovary was fixed in 4% paraformaldehyde for histology, and the remainder of the ovary was frozen in liquid nitrogen and stored at –80C.

Radioimmunoassay

Blood samples were allowed to clot for 1 h at room temperature. Serum was then separated by centrifugation (3000 x g for 30 min at 4C), removed and stored at –20C. Concentrations of PRL in serum were determined using reagents for the ovine PRL RIA provided by Dr. A.F. Parlow and the NIDDK National Hormone and Pituitary Program as described previously [14]. Purified ovine PRL (NIDDK-oPRL-I-3) was iodinated using the chloramine T reaction, and the assay conducted using methods and reagents provided by the NIDDK Pituitary Hormones and Antisera Center. Assay sensitivity was 0.1 ng/ml, and the intra- and inter-assay coefficients of variation were 5% and 12%, respectively.

Concentrations of E2-17β in plasma were determined using methods described previously [14]. Assay sensitivity was 3 pg/ml, and the intra-assay and inter-assay coefficients of variation were 5% and 12%, respectively. Assay results were calculated using the AssayZap Version 3.1 program (Biosoft, Ferguson, CA).

Histology and Morphometry

After fixation, ovarian and uterine tissues were changed to 70% ethanol for 24 h and then dehydrated and embedded in Paraplast Plus (Oxford Labware, St. Louis, MO). Uteri from Study One were sectioned (5 μm) and stained with hematoxylin and eosin as described previously [11]. Sections (n=4) of the uterus from each ewe were photomicrographed, and images were analyzed using Scion Image software (Scion Corporation, Frederick, MD) as previously described [Chapter V]. Measurements were standardized using the image of a stage micrometer at the same magnification. The

number of superficial ductal invaginations of GE from the LE into the stroma was determined. Endometrial gland number was determined by counting the total number of uterine glands in a complete cross-section of the uterine horn. The observation of a gland cross-section with a visible open lumen was counted as a single gland. Endometrial gland density was determined by counting the number of glands in a 200 μm^2 area in the stratum compactum and stratum spongiosum areas of the intercaruncular endometrium. The number of ductal gland invaginations, endometrial gland number, and gland density estimates were generated for at least three areas within four non-sequential sections from each uterine horn. Intra- and inter-section repeatability estimates for determination of ductal gland invaginations and endometrial gland number by a single observer was 0.85 and 0.8, respectively. The thickness or width of the endometrium and myometrium (inner circular and outer longitudinal layers) in the intercaruncular endometrial areas was measured using the Scion Image software from multiple points (n=3 to 4) of at least 10 non-sequential uterine sections. Ovaries from Study Two were sectioned (5 μm) and stained with Masson's trichrome as described previously [100].

Semi-quantitative Reverse Transcription PCR (RT-PCR) Analysis

Expression of mRNAs for βA subunit, βB subunit, ActRIA, ActRII and follistatin was assessed in uterine total RNA using semi-quantitative RT-PCR with methods [3, 15], and primers [181] as described previously[3, 15]. Total cellular RNA was isolated from frozen uteri using Trizol (Gibco-BRL, Grand Island, NY) according to

manufacturer recommendations. Briefly, cDNA was synthesized from total cellular RNA (5 μg) isolated from neonatal uteri using random (Life Technologies, Gaithersburg, MD) and oligo-dT primers and SuperScript II Reverse Transcriptase (Life Technologies). Newly synthesized cDNA was acid-ethanol precipitated, resuspended in 20 μl of water, and stored at -20C. The cDNAs were diluted (1:1 or 1:10) with water prior to use in PCR. Primers were designed to amplify partial cDNAs for ovine follistatin, βA subunit, βB subunit, ActRIA, ActRII, ActRIA, and ActRII as descrived previously [181]. β-Actin primers were ACGAAGATCCTTCACGGAACG (forward) and GAAGGTGGTCTCGTGAATGC (reverse), which amplified a 270-base pair product. PCR reactions were performed using AmpliTaq DNA polymerase (Applied Biosystems, Foster City, CA) and Optimized Buffer D (Invitrogen, Carlsbad, CA) for β-actin; Optimized Buffer E (Invitrogen) for AcyRIB; Optimized Buffer F (Invitrogen) for follistatin, ActRIA and ActRII; and Optimized Buffer J (Invitrogen) for βA-subunit and βB-subunit according to manufacturer recommendations. The amount of cDNA template, annealing temperature, and number of cycles used for PCR were initially optimized to ensure that final PCR conditions were within the linear range of amplification for each primer pair. Follistatin and βA-subunit PCR reactions contained 1.5 μl of cDNA (1:10); βB subunit reactions had 2.5 μl of cDNA (1:1); ActRIA reactions had 2 μl of cDNA (1:10); ActRII reactions had 3 μl of cDNA (1:10); and β-actin reactions had 1 μl of cDNA (1:10). All PCR reactions were performed at 95C for 30 sec, 55-59C for 1 min, and 72C for 1 min. Cycle number was: 25 for β-actin; 27 for

ActRII; 30 for follistatin, βA-subunit and ActRIA; and 35 for βB-subunit. In negative-control reactions, RT cDNA was substituted by inclusion of uterine total RNA or water. Following PCR, equal amounts of reaction product were analyzed using a 2% agarose gel, and PCR products visualized by ethidium bromide staining. The amount of DNA present was quantified by measuring the intensity of light emitted from correctly sized bands under UV light using an AlphaImager (Alpha Innotech Corporation, San Leandro, CA), and data are expressed as relative light units. The β-actin values were used as covariates in statistical analyses to correct for differences in amounts of cDNA used for each samples. All RT-PCR products were cloned into pCRII (InVitrogen) and fully sequenced in both directions to confirm identity.

In Situ Hybridization Analysis

Expression of mRNAs in the uterus and ovary was determined by in situ hybridization as described previously [181]. Briefly, deparaffinized, rehydrated, and deproteinated cross-sections (5 μm) of the uterus from each ewe were hybridized with radiolabeled sense or antisense cRNA probes generated from linearized plasmid templates containing partial cDNAs using in vitro transcription with [^{35}S-α]UTP. Partial cDNAs for ovine inhibin α subunit, βA subunit, βB subunit, ActRIA, ActRII and follistatin were generated by RT-PCR. After hybridization, washing and ribonuclease A digestion, slides were dipped in NTB-2 liquid photographic emulsion (Kodak, Rochester, NY), stored at 4C for 2 to 28 days, and developed in Kodak D-19 developer. Slides were then counterstained with Gill's modified hematoxylin (Stat Lab, Lewisville, TX), dehydrated through a graded series of alcohol to xylene, and protected with a

coverslip. Images of representative fields were recorded using a Nikon Eclipse 1000 photomicroscope (Nikon Instruments Inc., Lewisville, TX) fitted with a Nikon DXM1200 digital camera.

Immunohistochemistry

Expression of immunoreactive follistatin, inhibin α subunit, βA subunit, βB subunit, ActRIA, ActRIB and ActRII were detected in cross-sections (5 μm) of the ovary and uterus from each ewe using specific antibodies and a Super ABC Mouse/Rat Immunoglobulin G (IgG) Kit (Biomeda, Foster City, CA). Mouse anti-human monoclonal antibody to follistatin (catalog # MAB669), ActRIA (catalog # MAB637), ActRIB (catalog # MAB222) and ActRII (catalog # MAB3391) were from R&D Systems, Inc. (Minneapolis, MN). Mouse anti-human antibody to inhibin α subunit (catalog # MCA951S), βA subunit (catalog # MCA950S), and βB subunit (catalog # MCA1661) were purchased from Serotec, Inc. (Raleigh, NC). The working antibody concentration employed for immunohistochemistry was 6.7 μg/ml for follistatin, 400 ng/ml for inhibin α-subunit, 200 ng/ml for βA-subunit, 200 ng/ml for βB-subunit, 1 μg/ml for ActRIA, 2 μg/ml for ActRIB, and 1 μg/ml for ActRII. Negative controls were performed in which the primary antibody was substituted with the same concentration of normal mouse IgG from Sigma Chemical Company (St. Louis, MO). Antigen retrieval using a boiling citrate buffer was performed for all antibodies according to manufacturer's recommendations. Multiple tissue sections from each ewe were processed as sets within an experiment.

Relative staining intensity for immunoreactive protein expression were assessed in sections of the uterus and ovary from each ewe visually by two independent observers and scored as follows: absent (-; i.e., no staining above IgG control), weak (+), moderate (++), or strong (+++) [15]. If histologically discernable in the uterus, intercaruncular endometrial tissues, including LE, stroma, and GE, caruncular endometrial tissues, including LE and stroma, and myometrium were scored. In the ovary, cumulus cells (COC), granulosa cells (GC), oocyte (O), and theca cells (TC) were scored. Representative photomicrographs were taken using a Nikon Eclipse 1000 photomicroscope fitted with a Nikon DXM1200 digital camera.

Statistical Analyses

All quantitative data were subjected to least-squares analysis of variance (LS-ANOVA) using General Linear Models (GLM) procedures of the Statistical Analysis System [167]. Serum E2-17β and PRL levels were log transformed prior to least squares regression analyses. Uterine wet weight data were analyzed using body weight as a covariate. Histomorphometrical data were analyzed using an overall model that included main effects of treatment, day, treatment by day interaction, section and area. In all analyses, error terms used in tests of significance were identified according to the expectation of the mean squares for error. RT-PCR data were subjected to one-way ANOVA utilizing the β-actin values as a covariate in the model to correct for differences in amounts of RT cDNA analyzed for each uterus. A probability (P) value of 0.10 or less was accepted as indicating significance. Data are presented as least-square means (LSM) of untransformed values with overall standard errors (SE).

Results

Circulating Concentrations of E2-17β and PRL Are Unaffected by Ovariectomy

Circulating concentrations of E2-17β in plasma were low and affected by day ($P<0.10$), but not treatment ($P>0.10$) or their interaction ($P>0.10$). Serum E2-17β levels were highest on PND 0 (10±1.5 pg/ml), declined to PND 7 (3±1.5 pg/ml), and remained low to PND 56 (Fig. 4.1).

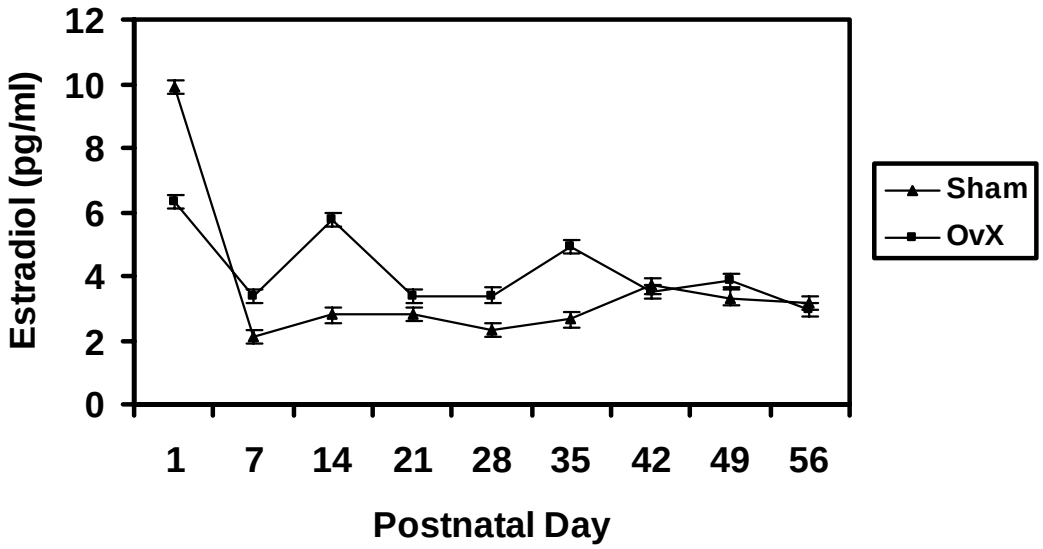

FIG 4.1. Concentrations of estradiol-17β in plasma from neonatal ewes that either underwent a sham surgery (CX) or ovariectomy (OVX) on PND 7, as indicated by the legend, between PND 1 and PND 56.

OvariectomyRretards Uterine Growth and Endometrial Gland Morphogenesis

As summarized in Table 4.1, uterine wet weight was 52% lower ($P<0.01$) in OVX compared to CX ewes on PND 56. The intercaruncular endometrium of CX ewes contained numerous coiled and branched glands extending radially from the LE through

the stroma to the inner circular layer of myometrium (Fig. 4.2). In contrast, the intercaruncular endometrium of OVX ewes contained substantially lower numbers of coiled and branched endometrial glands.

TABLE 4.1. Weights and histomorphometrical measurements of uteri from control (CX) and ovariectomized (OVX) ewes on PND 56.

Measurement	**CX**	**OVX**	**SE**	**P-value**
Uterine Wet Weight (g)	3.8	2.0	0.4	0.007
Ductal Gland Invaginations (number/section)	71	67	3	0.30
Endometrial Glands (total number/section)	789	439	80	0.0001
Stratum Compactum Gland Density (number/200 μm^2)	5.0	5.0	0.2	1.0
Stratum Spongiosum Gland Density (number/200 μm^2)	10.6	8.3	0.3	<0.0001
Endometrial Thickness (μm)	600	467	21	<0.0001
Myometrial Thickness (μm)	506	428	22	0.014

These histological observations were confirmed by histomorphometrical analyses and results are summarized in Table 4.1. The total number of endometrial glands in the uterine wall was reduced ($P<0.0001$) by 44% in ovariectomized ewe lambs. The number of gland invaginations from the LE and density of glands in the stratum compactum stroma adjacent to the LE were not affected ($P>0.10$) by ovariectomy. However, density of glands in the stratum spongiosum stroma adjacent to the inner circular layer of myometrium was reduced ($P<0.001$) by 22% in OVX ewes. In the intercaruncular endometrium, the thickness and width of the endometrium, and the myometrium were reduced ($P<0.05$) by 22% and 16%, respectively, in uteri of OVX ewes.

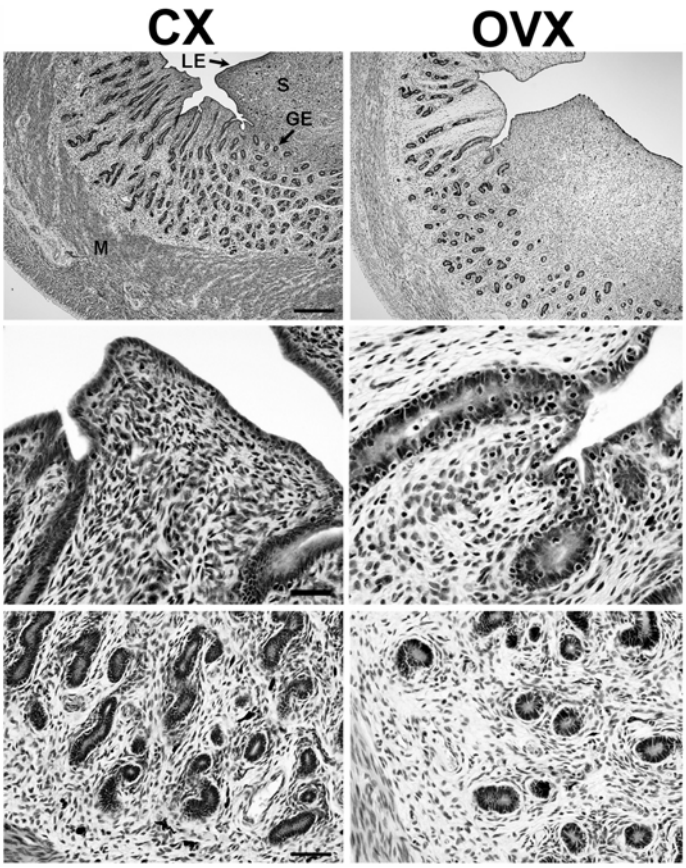

FIG 4.2. Representative photomicrographs illustrating the histoarchitecture of uteri from control (CX) and ovariectomized (OVX) ewes on PND 56. Tissues were prepared and stained using hematoxylin and eosin. Legend: GE, glandular epithelium; LE, luminal epithelium; M, myometrium; S, stroma. Bars represent 500 μm at low magnification and 50 μm at high magnification.

Expression of the Follistatin-Activin System in the Uterus Is Altered by Ovariectomy

Semi-quantitative RT-PCR analyses were conducted using total RNA isolated from uteri of CX and OVX ewes to determine steady-state levels of activin-follistatin system components. The number of PCR cycles was optimized for each primer pair to ensure amplification within the linear range of detection as representatively illustrated by follistatin (Fig. 4.3A). As illustrated in Figure 4.3B, each of the primer pairs used for RT-PCR amplified a single product of the expected size [181]. A partial cDNA for

ActRIB was detected abundantly in total RNA isolated from the neonatal ovary, but at extremely low amount in the neonatal ovine uterus (data not shown). The amplified products were sequenced to confirm identity (data not shown). As compared to mRNA levels in uteri of CX ewes (Table 4.2), uteri of OVX ewes had substantially lower levels of activin βA subunit, ActRIA, ActRII and follistatin on PND 56. In contrast, the level of activin βB-subunit mRNA was greater in uteri of OVX compared to CX ewes on PND 56.

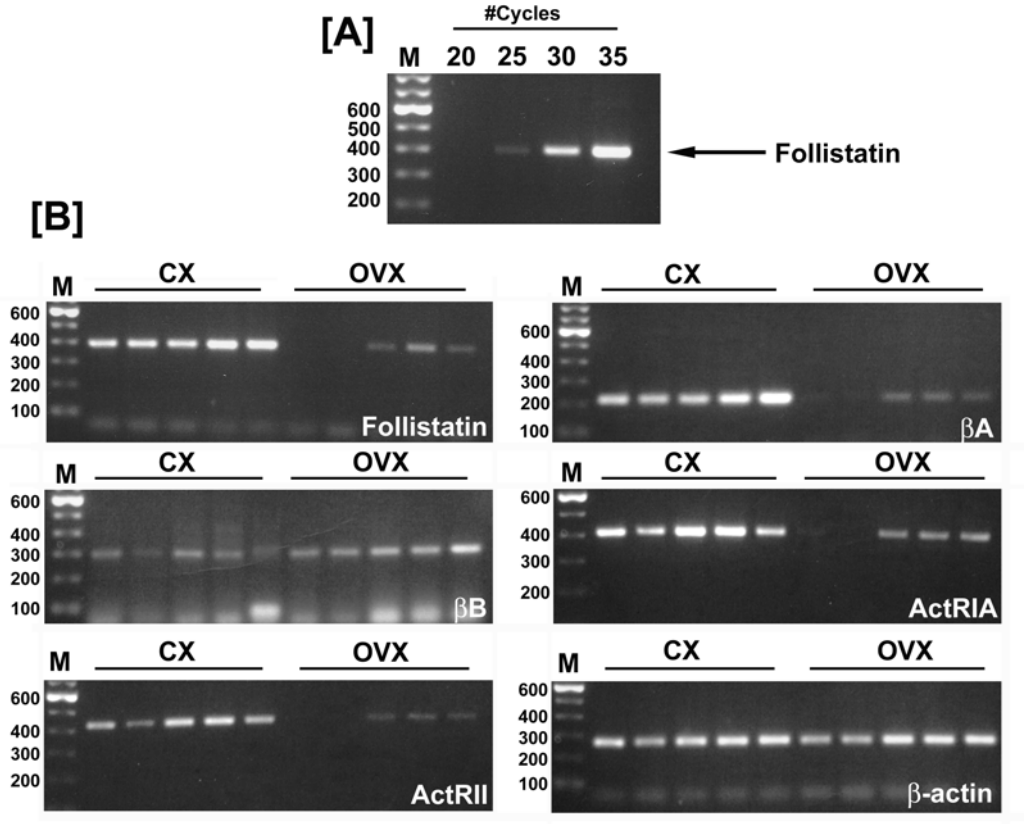

FIG 4.3. Semi-quantitative RT-PCR analysis of the mRNAs for the follistatin-activin system in total RNA isolated from uteri of sham control (CX) and ovariectomized (OVX) neonatal ewes on PND 56. [A] Representative analysis of the effects of cycle number on yield of follistatin cDNA. [B] Expression of mRNAs for follistatin, βA-subunit, βB-subunit, ActRIA, ActRII and β-actin in the ovine uterus. PCR products were separated in a 2% agarose gel and stained with ethidium bromide. Positions of the 100 bp DNA marker (M) ladder are shown. Results of analyses of changes in band intensity due to treatment are summarized in Table 2.

TABLE 4.2. RT-PCR analysis of the activin-follistatin system in total RNA from uteri of control (CX) and ovariectomized (OVX) ewes on PND 56.

	Relative Light Units (x 10^3)[a]			
mRNA	CX	OVX	SE	P-value
Follistatin	5,243	835	464	0.003
βA-subunit	6,886	993	704	0.006
βB-subunit	1,262	2,441	244	0.011
ActRIA	7,948	1,772	800	0.001
ActRII	3,425	470	326	0.004

[a] Measurement of cDNA synthesized in PCR reactions were made from ethidium bromide stained agarose gels. Data are presented as LSM with SE.
[b]Data were analyzed by one-way LS-ANOVA.

In situ hybridization and immunohistochemical analyses were performed to localize expression of follistatin-activin system mRNAs and protein in the uteri from CX and OVX ewes (Figs. 4.4 and 4.5). Results of immunohistochemical analyses were quantified and are summarized in Table 4.3. Expression of inhibin α subunit mRNA or protein was not detected in the neonatal ovine uterus (data not shown). As compared to CX ewes, uteri of OVX ewes had lower levels of βA subunit expression, particularly in the endometrial LE, GE and myometrium (Fig 4.4A and Table 4.3). In contrast, the expression of βB subunit was more abundant in the endometrial LE and GE of OVX ewes (Fig 4.4B). Follistatin mRNA and protein levels were lower in uteri of OVX ewes, particularly in the endometrial stroma and myometrium (Fig 4.4C).

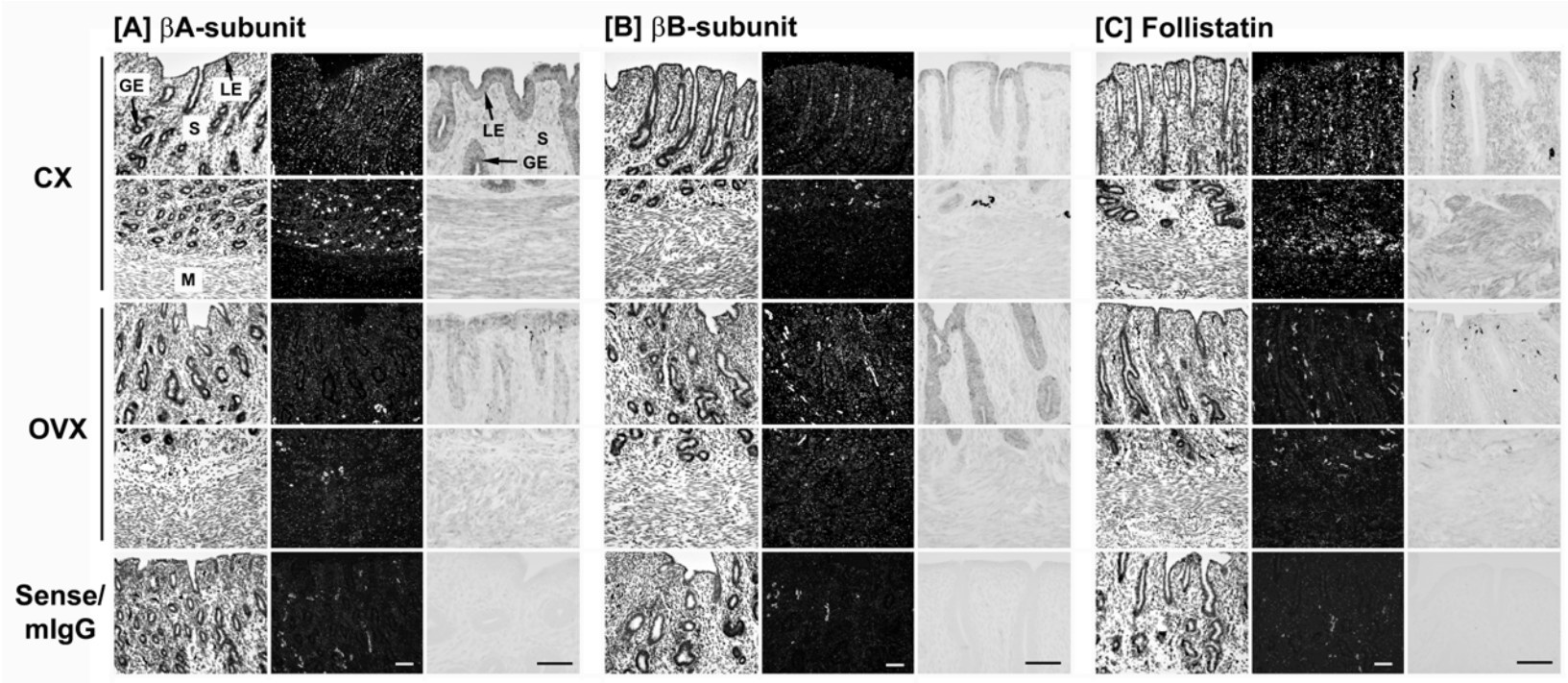

FIG 4.4. Representative photomicrographs indicating the distribution of βA-subunit [A], βB-subunit [B], and follistatin [C] mRNA and protein in uteri from CX and OVX ewes on PND 56. In situ localization of mRNA in the uterus is presented in brightfield and darkfield illumination (left panel). Representative photomicrographs of immunohistochemical results are presented for the upper and lower portions of the uterine wall (right panel). As a negative control, mouse IgG (mIgG) was substituted for the primary antibody. Legend: GE, glandular epithelium; LE, luminal epithelium; M, myometrium; S, stroma. Bar represents 50 μm.

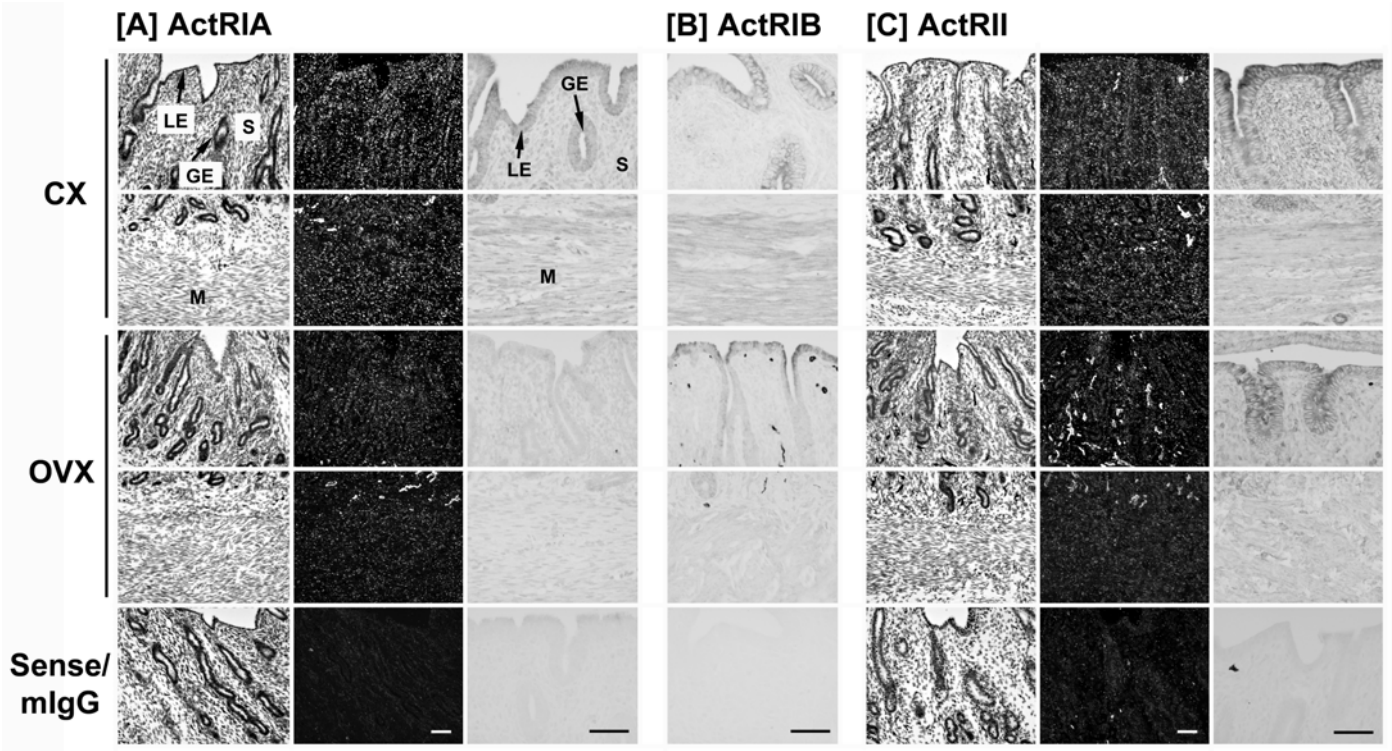

FIG 4.5. Representative photomicrographs depicting the distribution of ActRIA [A], ActRIB [B], and ActRII [C] expression in uteri from CX and OVX ewes on PND 56. For both ActRIA and ActRII, in situ localization of mRNA in the uterus is presented in brightfield and darkfield illumination (left panel). Representative photomicrographs of immunohistochemical results are presented for the upper and lower portions of the uterine wall. As a negative control, mIgG was substituted for the primary antibody. Legend: GE, glandular epithelium; LE, luminal epithelium; M, myometrium; S, stroma. Bar represents 50 μm.

TABLE 4.3. Distribution and relative abundance of immunoreactive βA-subunit, βB-subunit, follistatin, ActRIA, ActRIB and ActRII protein in uteri from CX and OVX ewe lambs.

		Intercaruncular endometrium				Caruncular endometrium		
		LE	GE: Shallow	GE: Deep	Stroma	LE	Stroma	Myometrium
βA-subunit	CX	+++	+++	+++	+	+	+	++
	OVX	++	++	++	+	+	+	+
βB-subunit	CX	++	++	++	+	+	+	+
	OVX	+++	+++	+++	+	+	+	+/++
Follistatin	CX	-/+	-	-	++/+++	-	+++	+++
	OVX	-/+	-	-	+	-	+	-/+
ActRIA	CX	+++	+++	++/+++	+	+	+	+/++
	OVX	++	+	+	+	-/+	+	-/+
ActRIB	CX	+++	+++	++	+	+	+	++/+++
	OVX	++	+	+	+	+	+	+
ActRIIA/B	CX	+++	+/++	+/++	++	+	++	+
	OVX	++	+/++	+/++	+/++	+/++	+/++	+

LE, luminal epithelium; GE, glandular epithelium.
βA-subunit, βB-subunit, follistatin, ActRIA, ActRIB and ActRIIA/B protein staining intensity was evaluated visually as absent (-), weak (+), moderate (++), or strong (+++).

Overall, expression of ActRIA and ActRIB was lower in the uteri of OVX ewes (Fig. 4.5, A and B). Specifically, ActRIA and ActRIB protein levels were reduced in both the endometrial glands and myometrium of OVX compared to CX ewes (Table 4.3). The abundance of ActRIB mRNA was below the detectable limits of the in situ hybridization procedure (data not shown). The mouse anti-human ActRII antibody detects both ActRIIA and ActRIIB (R&D Systems, Inc., Minneapolis, MN). Although ActRII mRNA expression was lower in uteri of OVX ewes, immunoreactive ActRIIA/B protein abundance was not different between uteri from CX and OVX ewes (Fig. 4.5C).

Expression of Activin-Follistatin System Components in the Neonatal Ovary

As expected, the number of growing and antral follicles in the neonatal ovine ovary declined from PND 0 to PND 7, increased between PND 7 and 14, peaked on PND 28 and remained high to PND 56 (Fig. 4.6). On PND 28 and thereafter, a number of the follicles exhibited signs of atresia, including rupture and disorganization of the TC and GC layers. As expected, no corpora lutea were observed in the ovaries.

In the ovaries, inhibin α subunit mRNA and protein were detected only in GC and cells of the COC (Fig. 4.7A). Overall, expression of inhibin α subunit mRNA and protein increased in vesicular and Graafian follicles between PND 0 and PND 14 and remained abundant thereafter (Table 4.4). In the neonatal ovary, βA subunit mRNA and protein were detected in GC, COC, and the oocyte with low levels of protein in the TC (Fig 4.7B). The βB subunit mRNA and protein were detected in GC and COC (Fig. 4.7C). The most abundant levels of immunoreactive βB subunit protein were in the zona pellucida of the oocyte. Follistatin mRNA and protein expression were detected

predominantly in the GC and COC (Fig 4.7D), but immunoreactive follistatin protein was also present in TC and tunica muscularis of blood vessels.

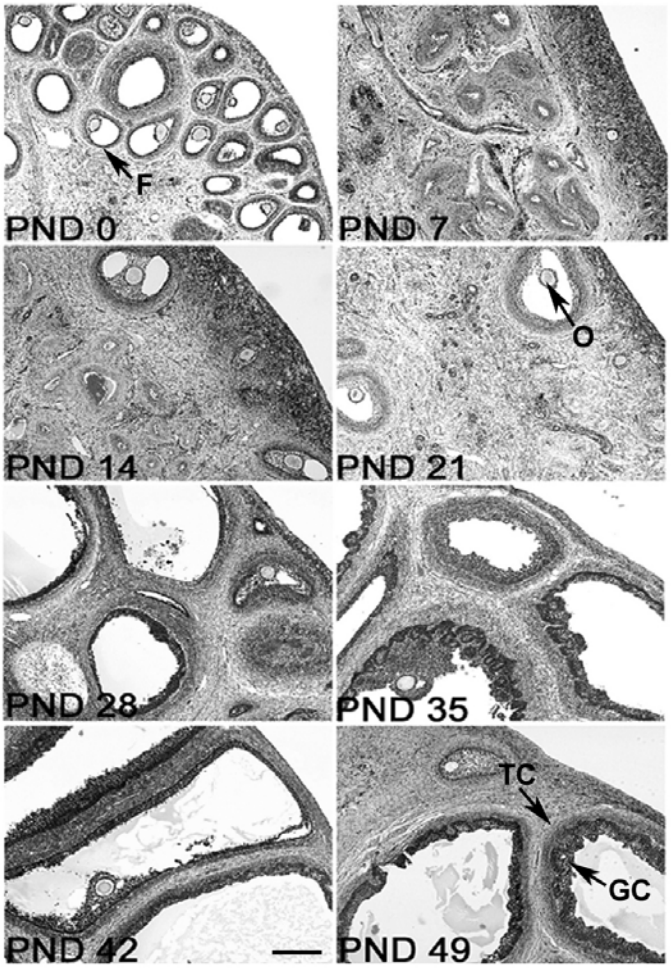

FIG 4.6. Representative photomicrographs illustrating the histoarchitecture of the ovary between PNDs 0 and 49 which corresponds to the period of postnatal uterine development in lambs. Tissues were prepared and stained using Masson's trichrome. Legend: F, follicle; GC, granulosa cells; TC, theca cells; O, oocyte. Bar represents 500 μm.

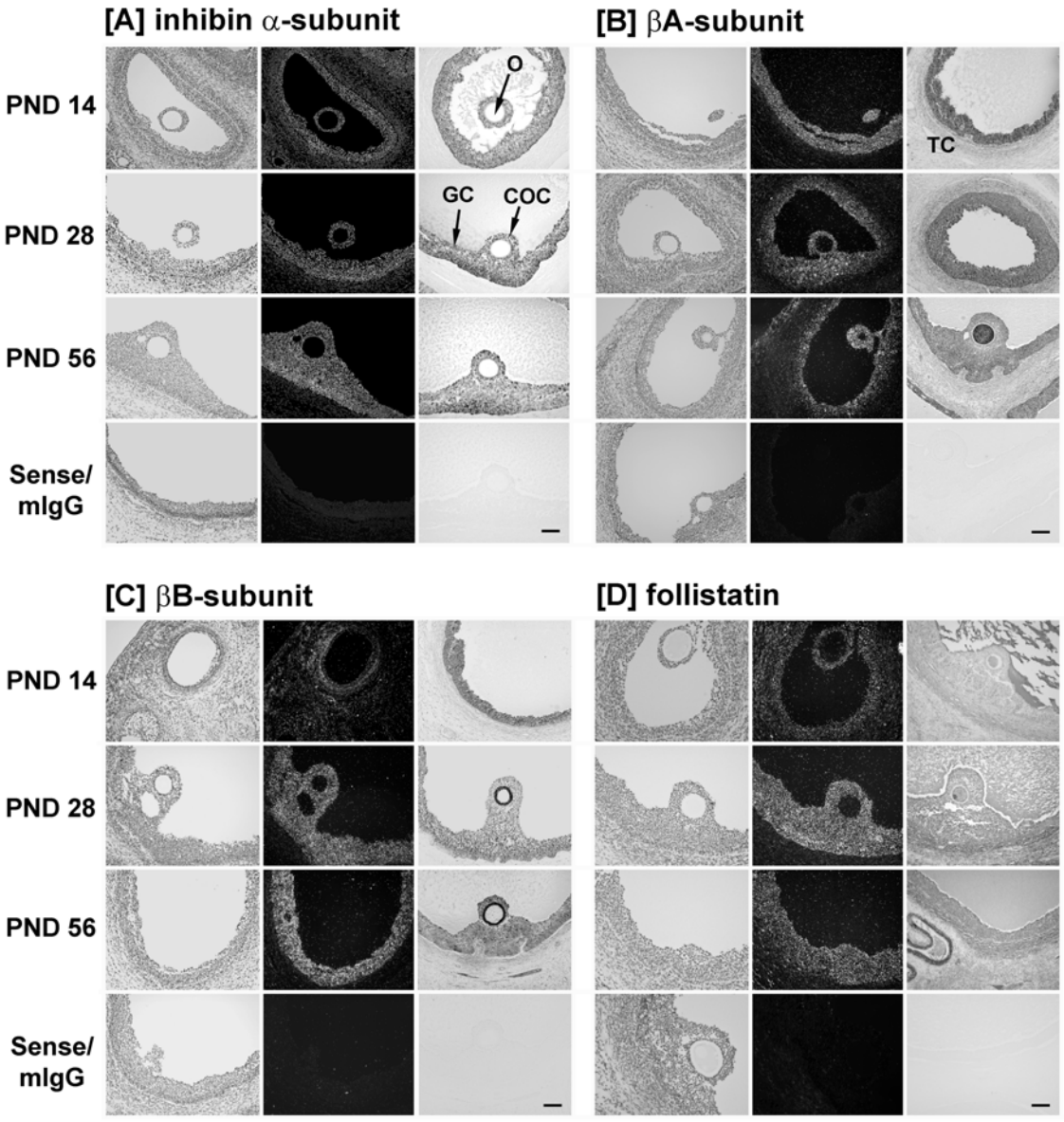

FIG 4.7. Representative photomicrographs indicate the distribution of inhibin α-subunit [A], βA-subunit [B], βB-subunit [C], and follistatin [D] mRNA and protein in ovaries from ewes on PND 14, 28 and 56. In situ localization of mRNA is presented in brightfield and darkfield illumination (left panel). Immunoreactive protein was detected using mouse monoclonal antibody and a BioStain Super ABC kit. Irrelevant mouse IgG was substituted for primary antibodies as a negative control. Legend: COC, cumulus oocyte cell complex; GC, granulosa cells; TC, theca cells; O, oocyte. Bar represents 100 μm.

TABLE 4.4. Distribution and relative abundance of immunoreactive α-subunit, βA-subunit, βB-subunit, and follistatin protein in the neonatal ovine ovary[1].

α-subunit

PND	GC	TC	COC	O
0	-	-	-	-
7	+/-	-	+	-
14	+++	-	+++	-
21	+++	-	+++	-
28	+++	-	+++	-
35	+++	-	+++	-
42	+++	-	+++	-
49	++	-	++	-
56	++	-	++	-

βA-subunit

PND	GC	TC	COC	O
0	+++	-	+++	+++
7	+++	-	+++	+++
14	+++	-	+++	+++
21	+++	-	+++	+++
28	+++	+/-	+++	+++
35	+++	+	+++	+++
42	+++	+	+++	+++
49	+++	+	+++	+++
56	++	+	+++	+++

Follistatin

PND	GC	TC	COC	O
0	++	+/-	++	++
7	++	+/-	+	++
14	++	+	+	++
21	+++	+	++	+++
28	+++	+	+++	+++
35	+++	++	+++	+++
42	+++	++	+++	+++
49	+++	++	+++	+++
56	+++	++/+++	+++	+++

βB-subunit

PND	GC	TC	COC	O (ZP)
0	++	-	++	+++
7	++	-	++	+++
14	++	-	++	+++
21	++	-	++	+++
28	++	-	++	+++
35	++	-	++	+++
42	++	-	++	+++
49	++	-	++	+++
56	++	-	++	+++

[1]PND, postnatal day; GC, granulosa cells; TC, theca cells; COC, cumulus oocyte complex; O, oocyte; ZP, zona pellucida. All protein staining intensity was evaluated visually as absent (-), weak (+), moderate (++), or strong (+++).

Discussion

Although uterine morphogenesis begins in the fetus, endometrial gland morphogenesis is a uniquely neonatal event [13, 14]. Ovariectomy of the neonatal ewe at birth does not affect the initial genesis and development of endometrial glands on PND 14 [28]. Similarly, ovariectomy of ewes on or before PND 4 had no effect on uterine wet weight on PND 14 [27]. Results of the present study confirm previous

reports that the ovary affects uterine growth after PND 14 [16, 180] and demonstrate that ovariectomy of the ewe on PND 7 reduced uterine wet weight by approximately 50% on PND 56. Liefer et al. [180] found a similar reduction in uterine weight on PND 44 in ewes ovariectomized on PND 4. In the present study, ovariectomy reduced growth of the endometrium and myometrium and the total number of endometrial glands in the uterus on PND 56. Development of the neonatal uterus involves reciprocal epithelial-mesenchymal interactions [3, 68, 134]. In the developing rodent uterus, the endometrial epithelium affects myometrial organization and growth [134]. In the neonatal ewe, estrogen or progestin treatment of neonatal ewes from birth epigenetically ablates endometrial adenogenesis, reduces uterine growth, and decreases endometrial and myometrial thickness [3]. In contrast, treatment of neonatal ewes with PRL from birth increases endometrial gland number as well as intercaruncular endometrial and myometrial thickness [Chapter V]. These results clearly indicate that effects of ovariectomy on intercaruncular endometrial and myometrial growth may result from decreased development of endometrial glands as well as changes in epithelial-stromal interactions.

In the present study, ovariectomy on PND 7 did not affect the number of superficial ductal invaginations of the GE from the LE nor the density of endometrial glands in the stratum compactum area of the stroma on PND 56. Results of the present study confirm those of Bartol et al. [28] that initial genesis and development of endometrial glands between birth and PND 14 is not dependent on the ovary or an ovarian factor(s). However, results of the present study clearly demonstrated that total

number of endometrial glands in the uterine wall and the density of the endometrial glands in the stratum spongiosum area of the stroma were reduced in uteri from OVX ewes which indicates that an ovarian-derived factor(s) regulates, in part, the coiling and branching morphogenesis stage of endometrial gland development that occurs between PND 14 and PND 56. Postnatal uterine growth and endometrial adenogenesis are ovary-, adrenal-, and steroid-independent in rodents [30-32]. In the neonatal gilt, ovariectomy at birth inhibits uterine growth after PND 56, but does not affect genesis of uterine glands or related endometrial morphogenetic events prior to PND 120 [23]. Collectively, available results indicate that the precise role of ovarian factor(s) in uterine growth and endometrial adenogenesis is species-specific.

The process of uterine morphogenesis is governed by a variety of hormonal, cellular and molecular mechanisms, many of which remain to be defined [3, 41]. In the neonatal ovine uterus, the PRL receptor gene is specifically expressed by the endometrial GE [14], and circulating PRL is a primary regulator of endometrial adenogenesis [Chapter V]. In the present study, ovariectomy on PND 7 did not affect circulating levels of PRL, indicating that effects of ovariectomy were not due to alterations in this endocrine regulatory system. Although changes in uterine ERα gene expression can be correlated with endometrial adenogenesis [14], uterine growth and endometrial gland development is an estrogen-independent process in the ewe between birth and PND 56 [Chapter III]. However, endometrial gland coiling and branching morphogenesis between PND 14 and PND 56 is dependent, in part, on expression and functional activation of uterine ERα [Chapter III]. In the present study, effects of

ovariectomy on uterine growth and development were not due to alterations in circulating E2-17β. Moreover, expression of ERα and PR protein was not different between uteri of CX and OVX ewes [K.D. Carpenter, K. Hayashi and T.E. Spencer, unpublished observations]. Therefore, the effects of ovariectomy on uterine growth and endometrial adenogenesis cannot be attributed to alterations in either PRL or the uterine ERα system.

The ovarian factor(s) that regulates uterine growth and endometrial adenogenesis is not known, but could be inhibin, follistatin or activins. In the neonatal ewe, the increase in ovarian weight between PND 14 and PND 56 is caused, in part, by the increase in number and size of antral follicles and the associated accumulation of follicular fluid [26]. The stimulus for initiation and maintenance of ovarian follicular growth after birth is not known. During this period, low levels of LH release in a pulsatile fashion can be detected, whereas FSH secretion is tonic [26, 180, 200]. The unregulated growth of ovarian follicles in the ewe after birth may be due to endocrine stimuli, such as LH and FSH, as well as intraovarian mechanisms. In the present study, ewes were born during seasonal anestrus and ovaries were collected before puberty, but inhibin α subunit, β subunits, and follistatin were expressed in nearly all growing and vesicular follicles. In the ewe, follistatin levels rise in the fetus during parturition and remain high in the neonate [196]. In contrast, immunoreactive inhibin levels are low at two weeks and then decline to fifteen weeks of life in the ewe lamb [198]. In the present study, abundant expression of β subunits and ActRs as well as follistatin and inhibin α subunit were detected in the neonatal ovary. These findings are similar to previously

reported results [197, 199]. Undoubtedly, these factors regulate follicular development in the prepubertal ovine ovary through their established roles in GC proliferation and control of pituitary hormones [188, 189].

Recent evidence from studies of the neonatal ovine uterus implicates follistatin, activins, and activin receptors as regulators of endometrial gland morphogenesis in the neonatal ovine uterus [181]. Follistatin, activins and inhibins regulate growth and differentiation of many branched epitheliomesenchymal organs via autocrine, paracrine and perhaps endocrine mechanisms [182-187, 201]. In general, exogenous activin inhibits gland development, whereas follistatin counteracts these inhibitory effects of activins by binding to the individual βA and βB subunits and preventing activin receptor activation [182, 190]. In a variety of cell types, expression of activin-follistatin system components can be modulated by activins, inhibin, and follistatin in a cell type-specific manner [202-206]. Activin can increase follistatin expression and differentially regulate ActR expression in pituitary cells [205]. In testicular tumor cells, activin regulates expression of ActRII and βA subunit and inhibits cell proliferation [204]. In rat Sertoli cells, activin increases expression of ActR and follistatin and increases cell proliferation [206]. In human GC, activin A increases βB subunit expression with no effects on βA mRNA or inhibin α subunit mRNA [203]. Available results support the working hypothesis that follistatin and activins from the ovary act on the uterus to regulate, in part, coiling and branching morphogenetic development of endometrial glands as well as overall uterine growth. This hypothesis is supported by findings in the present study that expression of specific components of the activin-follistatin system was affected by

ovariectomy and could be correlated with reduced endometrial gland development. Indeed, marked reductions in expression of follistatin, βA subunit, ActRIA, and ActRII genes and an increase in βB subunit expression were detected in uteri of ovariectomized ewes. Furthermore, these changes could be correlated with, but not completely accounted for, by the decreases in uterine size and endometrial gland development in ovariectomized ewes. One or more of the responsible ovarian factors likely is follistatin, activins, or inhibin.

Collectively, available results support the idea that a factor from the ovary regulates overall development, adenogenesis, and expression of the follistatin-activin system in the neonatal ovine uterus. It is tempting to speculate that the coordinate activities of the activin-inhibin-follistatin system in the ovary and uterus may be important in prolific breeds of ewes that possess an intrinsic high ovulation rate as well as a enhanced uterine capacity to maintain large litters [207]. Future experiments will be directed toward understanding the mechanistic aspects of the novel finding that an ovarian endocrine factor(s) includes a member of the activin-inhibin-follistatin system that may act in concert with autocrine-paracrine effects of the uterine activin-follistatin system to regulate coiling and branching morphogenesis of the endometrial glands during postnatal development of the ovine uterus.

CHAPTER V

PROLACTIN REGULATION OF NEONATAL OVINE UTERINE GLAND MORPHOGENESIS

Introduction

Postnatal uterine morphogenesis in the ewe involves the emergence, proliferation and differentiation of endometrial glands, specification of intercaruncular stroma, development of endometrial folds, and, to a lesser extent, growth of endometrial caruncular areas and the myometrium [3, 11, 14, 15]. Uterine gland development or adenogenesis is initiated between PND 1 and 7 when shallow epithelial invaginations appear along the LE in presumptive intercaruncular areas. Between PND 7 and 14, the nascent GE buds proliferate into the stroma and form tubules or ducts that begin to coil and branch at the tips by PND 21. After PND 21, uterine adenogenesis primarily involves branching morphogenesis of tubular and coiled endometrial glands in the stratum spongiosum adjacent to the inner circular layer of the myometrium. By PND 56, uterine gland morphogenesis is essentially complete, as the aglandular caruncular and glandular intercaruncular endometrial areas appear histoarchitecturally similar to that of the adult uterus [14]. Final maturation and growth of the ovine uterus may not occur until puberty [16] and during the first pregnancy, which involves extensive hyperplasia and hypertrophy of the endometrial glands [17, 18].

In the neonatal ewe, pituitary PRL, E2-17β, and stromal growth factors, including FGF-7 and -10, HGF, and IGF-I and -II, with epithelial receptors have been implicated as regulatory factors controlling endometrial adenogenesis [11, 14, 15].

Circulating levels of PRL are relatively high on PND 1, reach a maximum on PND 14, and then decline slightly to PND 56 [15, 37]. Expression of mRNAs for the short and long PRLR proteins is restricted to the nascent uterine GE buds on PND 7 and in proliferating and differentiating GE from PND 14 to 56 [15]. In the adult ovine uterus, PRLR expression is also restricted to the endometrial glands and not detected in other uterine cell types [18]. Prolactin, a member of the helix bundle peptide hormone/cytokine superfamily [141], regulates the growth and differentiation of a number of epitheliomesenchymal organs, including the pigeon crop sac, mammary gland, prostate, and uterus [33]. In the mammary gland, PRL and PRLR are required for development and differentiation of the lobuloalveolar portion of the GE [34-36]. Hyperprolactinemia elicits uterine glandular hyperplasia in the adult mouse, rabbit and pig [38-40]. The precise role of PRL in neonatal ovine uterine adenogenesis has not been elucidated.

Biological responses to PRL in other model systems is mediated by the PRLR and intracellular activation of several signal transduction systems, including signal transducers and activators of transcription (STAT) proteins 1, 3 and 5, IFN regulatory factor one (IRF-1), and the mitogen activated protein kinase (MAPK) cascade [148, 208, 209]. High levels of phosporylated ERK 1 and 2 MAPKs are also detected in nascent and proliferating endometrial glands of the neonatal ovine uterus [15]. Available evidence in the neonatal ewe supports the working hypothesis that PRL activates PRLR signaling pathways in the nascent and proliferating endometrial GE to stimulate and maintain their coiling and branching morphogenesis in the neonatal ovine uterus. In

order to test this hypothesis, studies were conducted in the neonatal ewe to determine effects of: (1) hypoprolactinemia on uterine adenogenesis; (2) hyperprolactinemia on uterine adenogenesis; (3) postnatal age on expression of STATs 1, 3 and 5 and IRF-1; and (4) PRL on activation of STAT and MAPK signal transduction pathways.

Materials and Methods

Reagents

Antibodies used in the present study included: monoclonal mouse anti-STAT 1 IgG (#610185), monoclonal mouse anti-STAT 3 IgG (#610189), and monoclonal mouse anti-STAT 5 IgG (#610191) from BD Transduction Laboratories (Lexington, KY); rabbit anti-phospho-STAT 1 IgG (Tyr 701; #9171), rabbit anti-phospho-STAT 3 IgG (Tyr 705; #9131), rabbit anti-phospho-STAT 5 IgG (Tyr694; #9351), rabbit anti-phospho-p44/42 MAPK IgG (Thr202/Tyr204; #9101), rabbit anti-p44/42 (ERK1/2) MAPK IgG (#9102), and rabbit anti-phospho-SAPK/JNK IgG (Thr183/Tyr185; #9251) from Cell Signaling Technology (Beverly, MA); rabbit anti-human IRF-1 IgG (sc-497) from Santa Cruz Biotechnology, Inc. (Santa Cruz, CA); peroxidase-labeled goat anti-mouse (#474-1806) and anti-rabbit IgG (#474-1506) from Kirkegaard & Perry Laboratories (Gaithersburg, MD); and normal rabbit IgG (#I5006) and normal mouse IgG (#I5381) from Sigma-Aldrich (St. Louis, MO).

Animals

All experiments and surgical procedures were in accordance with the Guide for the Care and Use of Agriculture Animals and approved by the University Laboratory Animal Care Committee of Texas A&M University.

Preparation of Recombinant Ovine Prolactin

Recombinant ovine PRL (roPRL) (GenBank Accession No. M27057) was prepared in Escherichia coli cells as described by Leibovich and colleagues [210]. The expressed protein, found in inclusion bodies, was refolded and purified to homogeneity on a Q-Sepharose column, yielding an electrophoretically pure fraction composed of over 98% monomeric protein of the expected molecular mass of approximately 23 kDa. The biological activity of the roPRL after proper renaturation was evidenced in vitro by its ability to stimulate proliferation of rat lymphoma Nb2 cells possessing PRLR, stimulate biological activity in HEK 293 cells transiently transfected with ovine PRLR, and induce progesterone secretion in primary cultures of luteal cells obtained from midpregnant ewes [210].

Experimental Design

Crossbred Suffolk ewes were mated to Suffolk rams in the Fall between the months of September and November of 2000 and 2001. Pregnant ewes were maintained according to normal husbandry practices and fed hay and corn. Ewes used in the following experiments were born in the Spring between the months of February and May of 2001 and 2002.

Study one

Biodegradable placebo and bromocryptine mesylate (100 mg) 21-day release pellets were obtained from Innovative Research of America (Sarasota, FL). Ten ewe lambs (n=5 per treatment) were assigned randomly at birth (postnatal day or PND 0) to be implanted with a placebo pellet as a control (CX) or 100 mg bromocryptine mesylate pellet (BROMO) that releases 100 mg over a 21-day period (approximately 4.8 mg per day). Biodegradable pellets were placed subcutaneously in the periscapular region every 20 days from birth. Blood samples were collected every 7 days beginning at birth by jugular venipuncture. On PND 56, all ewes were hemi-ovariohysterectomized. For removal of the right uterine horn and ovary, a hemostat was clamped perpendicular across the uterine horn at the bifurcation of the uterine horns. A scalpel blade was used to remove the right uterine horn, oviduct and ovary. Electrocautery was used to seal the opening of the remaining portion of the uterine horn. The uterine horn piece was then trimmed free of the broad ligament, oviduct and cervix. Sections (~ 1 cm) from the mid-region of the uterine horn were fixed in fresh 4% paraformaldehyde in PBS (pH 7.2) for 24 h at room temperature and processed for histology.

Study two

Crossbred Suffolk ewes (n=5 per treatment) were assigned randomly on PND 0 to receive twice daily injections (0700 h and 1800 h) of sterile saline vehicle as a control (CX) or roPRL (1 mg per kg body weight) from PND 1 to PND 56 to determine effects on uterine gland development. Body weight of the ewes was measured every 4 days and

used to adjust treatments. Blood samples were collected every 8 days beginning on PND 1 by jugular venipuncture. On PND 14, all ewes were subjected to mid-ventral laparotomy. The right ovarian pedicle was ligated, and the ovary and oviduct removed. One-half of the ipsilateral anterior uterine horn was then removed and fixed in 4% paraformaldehyde for histology. On PND 56, all ewes were weighed and necropsied. The left ovary was trimmed free of the mesovarium and weighed. The uterus was obtained and trimmed free of the broad ligament, oviduct and cervix. The entire left uterine horn was dissected free of the partial right uterine horn and weighed. Sections from the mid-region of the uterine horn were fixed in paraformaldehyde for histology.

Histology and Morphometry

After 24 h of fixation in 4% paraformaldehyde, uterine tissues were changed to 70% ethanol for 24 h and then dehydrated and embedded in Paraplast Plus (Oxford Labware, St. Louis, MO). Uteri were sectioned (4-6 μm) and stained with hematoxylin and eosin as described previously [11]. Sections (n=4) of the uterus from each ewe were photomicrographed, and images were analyzed using Scion Image software (Scion Corporation, Frederick, MD). Measurements were standardized using the image of a stage micrometer at the same magnification. In the intercaruncular endometrium, the thickness or width of the endometrium and myometrium (inner circular and outer longitudinal layers) was measured using the Scion Image software from multiple points (n=3 to 4) of each uterine section. The number of superficial ductal invaginations of the GE into the stroma was counted in each section. Endometrial gland number was determined by counting the total number of uterine glands in a complete cross-section of

the uterine horn using methods described previously [67]. Gland number estimates were generated for at least 10 non-sequential sections from each uterine horn. The observation of a gland cross-section with a visible open lumen was counted as a gland. Intra- and inter-section repeatability estimates for determination of gland number by a single observer was 0.85 and 0.8, respectively. Data are presented as total gland number per uterine horn cross-section. Gland density was determined in the stratum compactum and stratum spongiosum of the intercaruncular endometrium. The number of glands in a 200 μm^2 area was counted in four areas of four sections for each uterine horn. Data are presented as total gland number per 200 μm^2 area.

Photomicroscopy

Representative photomicrographs were taken using a Nikon Eclipse 1000 photomicroscope (Nikon Instruments Inc., Lewisville, TX) fitted with a Nikon DXM1200 digital camera.

Radioimmunoassay

Blood samples were allowed to clot for 1 h at room temperature. Serum was then collected by centrifugation (3000 x g for 30 min at 4C), removed and stored at -20C for hormone analyses. Concentrations of PRL in serum were determined using reagents for the ovine PRL RIA provided by Dr. A.F. Parlow and the NIDDK National Hormone and Pituitary Program as described previously [14]. Purified ovine PRL (NIDDK-oPRL-I-3) was iodinated using the chloramine T reaction, and the assay conducted using methods and reagents provided by the NIDDK Pituitary Hormones and Antisera Center. Assay

sensitivity was 0.1 ng/ml, and the intra- and inter-assay coefficients of variation were 5% and 12%, respectively.

Concentrations of E2-17β in the serum were determined by RIA as described previously [14]. Assay sensitivity was 1 pg per tube, and the intra-assay and interassay coefficients of variation were 8% and 14%, respectively. Assay results were calculated using the AssayZap Version 3.1 program (Biosoft, Ferguson, CA).

Statistical Analyses

All quantitative data were subjected to least-squares analysis of variance (LS-ANOVA) using General Linear Models (GLM) procedures of the Statistical Analysis System [167]. For serum PRL and E2-17β measurements, statistical models included the main effects of treatment, PND, and their interaction. Statistical models for analysis of morphometry data in Study One included main effects of treatment, ewe within treatment, tissue section, microscopic field within tissue section, and the appropriate interactions. Models for Study Two included main effects of treatment, ewe within treatment, PND, tissue section, microscopic field within tissue section, and the appropriate interactions. Initial analyses indicated that uterine wall location, tissue section, and microscopic field within section were not significant sources of variation. In some cases, data were log transformed to alleviate heterogeneity of error variance. Data are presented as least-square means (LSM) with overall standard errors (SE).

Results

Hypoprolactinemia Retards Endometrial Adenogenesis (Study One)

This study tested the hypothesis that lowering circulating levels of PRL with bromocryptine mesylate, a dopamine D2 receptor agonist and inhibitor of PRL secretion in the ewe [34], would retard or prevent endometrial adenogenesis. Ewes received a biodegradable pellet that released placebo as a control (CX) or bromocryptine mesylate (BROMO) every 20 days beginning at birth. Circulating levels of PRL were affected by treatment ($P<0.0001$) and PND ($P<0.10$), but not their interaction (Fig. 5.1). In CX ewes, serum levels of PRL were high on PND 1, increased to a maximum on PND 14, and decreased thereafter ($P<0.10$, cubic). In BROMO ewes, serum PRL levels were lower on PND 1 and increased two-fold ($P<0.10$, linear) to PND 56, but always remained markedly lower (~4.5-fold) than CX ewes. Treatment with BROMO did not affect ($P>0.10$) serum levels of E2-17β compared to CX ewes (data not shown).

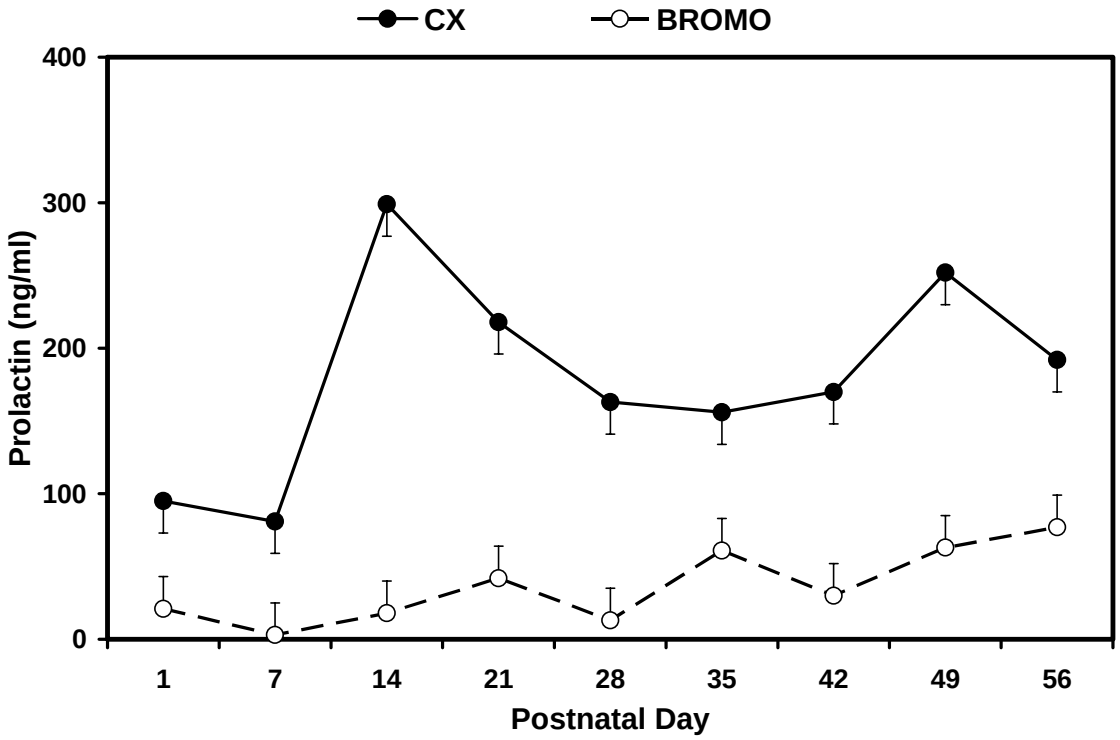

FIG 5.1. Concentrations of PRL (LSM ± SEM) in serum from neonatal ewes implanted every 20 days with either a placebo pellet as a control (CX) or bromocryptine mesylate (BROMO) pellet from birth to PND 56.

Histological analyses of the uterine wall indicated that the endometrium of CX ewes contained large numbers of coiled and branched glands in the intercaruncular endometrium (Fig. 5.2). In contrast, the endometrium of BROMO ewes lacked the large numbers of characteristically coiled and branched glands in the lower stroma. As summarized in Table 5.1, the number of primary ductal invaginations of the GE into the stratum compactum stroma was lower ($P<0.06$) in the endometrium of BROMO-treated as compared to CX ewes. Endometrial gland number was lower ($P<0.001$) in the endometrium of BROMO-treated as compared to CX ewes. Endometrial gland density was lower ($P<0.001$) in the stratum spongiosum, but not in the stratum compactum

endometrium, of BROMO-treated ewes. Endometrial and myometrial thicknesses were not affected (P>0.10) by treatment.

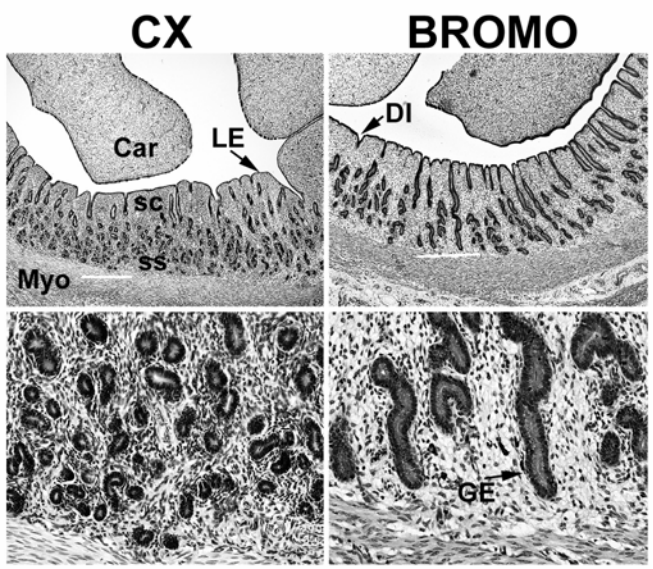

FIG 5.2. Representative photomicrographs depicting effects of treatment with placebo pellets as a control (CX) or bromocryptine mesylate (BROMO) pellets from birth (PND 0) on uterine wall development at PND 56. Uterine tissue sections were prepared and stained with hematoxylin and eosin. Photomicrographs are shown at low (4X) magnification (top) with the area denoted by the white bar at a higher (20X) magnification (bottom). Note the reduction in coiled and branched endometrial glands in the stratum spongiosum of BROMO-treated ewes. Legend: Car, Caruncle; DI, ductal gland invagination; LE, lumenal epithelium; GE, glandular epithelium; sc, stratum compactum; ss, stratum spongiosum; Myo, myometrium.

TABLE 5.1. Effects of bromocryptine treatment on endometrial gland ductal invaginations, gland number, gland density, and thickness of both endometrium and myometrium (Study One).

Measurement	Treatment		SE
	CX	BROMO	
Ductal Invaginations (number/section)	70.4	51.8[a]	1.3
Gland Number (per section)	695	455 [a]	30
Gland Density (number/200 μm^2)			
Stratum Compactum	5.7	5.8	0.2
Stratum Spongiosum	13.0	9.4 [a]	0.3
Endometrial Thickness (μm)	457	464	34
Myometrial Thickness (μm)	295	276	15

[a] Effect of treatment (P<0.10)

Hyperprolactinemia Increases Endometrial Gland Development (Study Two)

This study tested the hypothesis that hyperprolactinemia elicits uterine gland hyperplasia in the neonatal ovine uterus. Ewes were treated from PND 0 to PND 56 with either saline vehicle as CX or roPRL (2 mg/kg body weight/day). Ewes were hemi-ovariohysterectomized on PND 14, and the remaining uterine horn and ovary were removed on PND 56. Serum levels of PRL were affected (P<0.01) by PND, treatment, and their interaction (Fig. 5.3). In CX ewes, serum levels of PRL were high on PND 1, reached a maximum on PND 17, and decreased thereafter (cubic effect of day, P<0.05). Overall, treatment of neonatal ewes with roPRL increased (P<0.01) circulating levels of PRL. In roPRL ewes, serum levels of PRL were higher than CX ewes on PND 1 (P<0.01, day x treatment) and increased between PNDs 1 and 56 (quadratic effect of day, P< 0.10). Treatment with roPRL did not affect (P>0.10) serum levels of E2-17β as

compared to CX ewes (data not shown). As summarized in Table 5.2, weights of the ovary and right uterine horn were not affected (P>0.10) by treatment on PND 56.

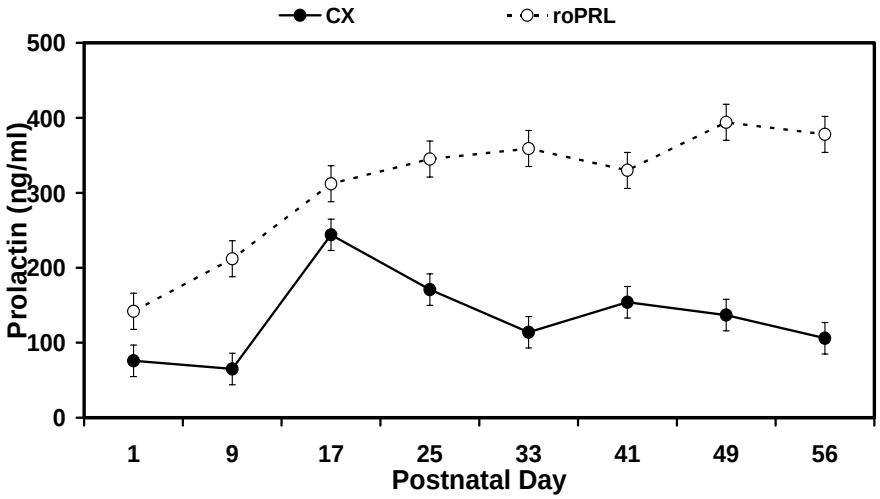

FIG 5.3. Concentrations of PRL (LSM ± SEM) in serum from neonatal ewes treated with either saline vehicle as a control (CX) or recombinant ovine prolactin (roPRL) from PNDs 1 to 56.

Treatment of neonatal ewes with roPRL affected uterine gland morphogenesis (Fig. 5.4). On PND 14, the endometrium of CX ewes contained nascent glands that were mostly tubular. On PND 56, the endometrium of CX ewes contained large numbers of coiled and branched endometrial glands, particularly in the stratum spongiosum. As summarized in Table 5.2, the number of primary superficial ductal invaginations of the GE into the stratum compactum increased (P<0.01) between PND 14 and PND 56 in CX ewes, but was not affected (P>0.10) by treatment with roPRL regardless of PND. In contrast, endometrial gland number and density were affected (P < 0.01) by PND, treatment and their interaction. In CX ewes, endometrial gland numbers increased (P<0.001) almost 13-fold from PND 14 to PND 56. Administration of roPRL tended to

increase (P=0.09) endometrial gland number on PND 14 and increased (P<0.01) it by 63% on PND 56. Similarly, endometrial gland density was increased (P<0.05) by roPRL on PND 14. On PND 56, endometrial gland density was greater (P<0.05) in the stratum spongiosum, but not stratum compactum endometrium, in roPRL-treated as compared to CX ewes. Endometrial and myometrial thicknesses were affected (P<0.10) by PND, treatment, and their interaction. The thicknesses of the endometrium and myometrium were not different (P>0.10) on PND 14. However, treatment with roPRL increased (P<0.10) the thicknesses or widths of the endometrium and myometrium on PND 56.

Immunoreactive STATs 1, 3 and 5 Are Present in the Developing Endometrial Glands (Study Three)

Immunoreactive STATs 1, 3 and 5 were detected in the nucleus and cytoplasm of most uterine cell types in the neonatal ewe (Fig. 5.5). STAT 1 protein was detected in all cell types on PND 1, but was more abundant in the LE. On PND 14 and thereafter, STAT 1 protein was detected in the developing GE. STAT 3 protein was detected in the LE and stroma. Expression of STAT 3 protein was particularly abundant in the LE and nascent and developing GE. In the stroma, STAT 3 protein expression was most abundant in immune cells as compared to stromal cells. STAT 5 protein was detected in all uterine cell types on PND 1, but was most abundant in the stroma and LE. STAT 5 protein was detected in the nascent and developing GE throughout development. Negligible levels of background were detected in negative controls wherein the primary antibodies were replaced with an equal amount of non-specific mouse IgG.

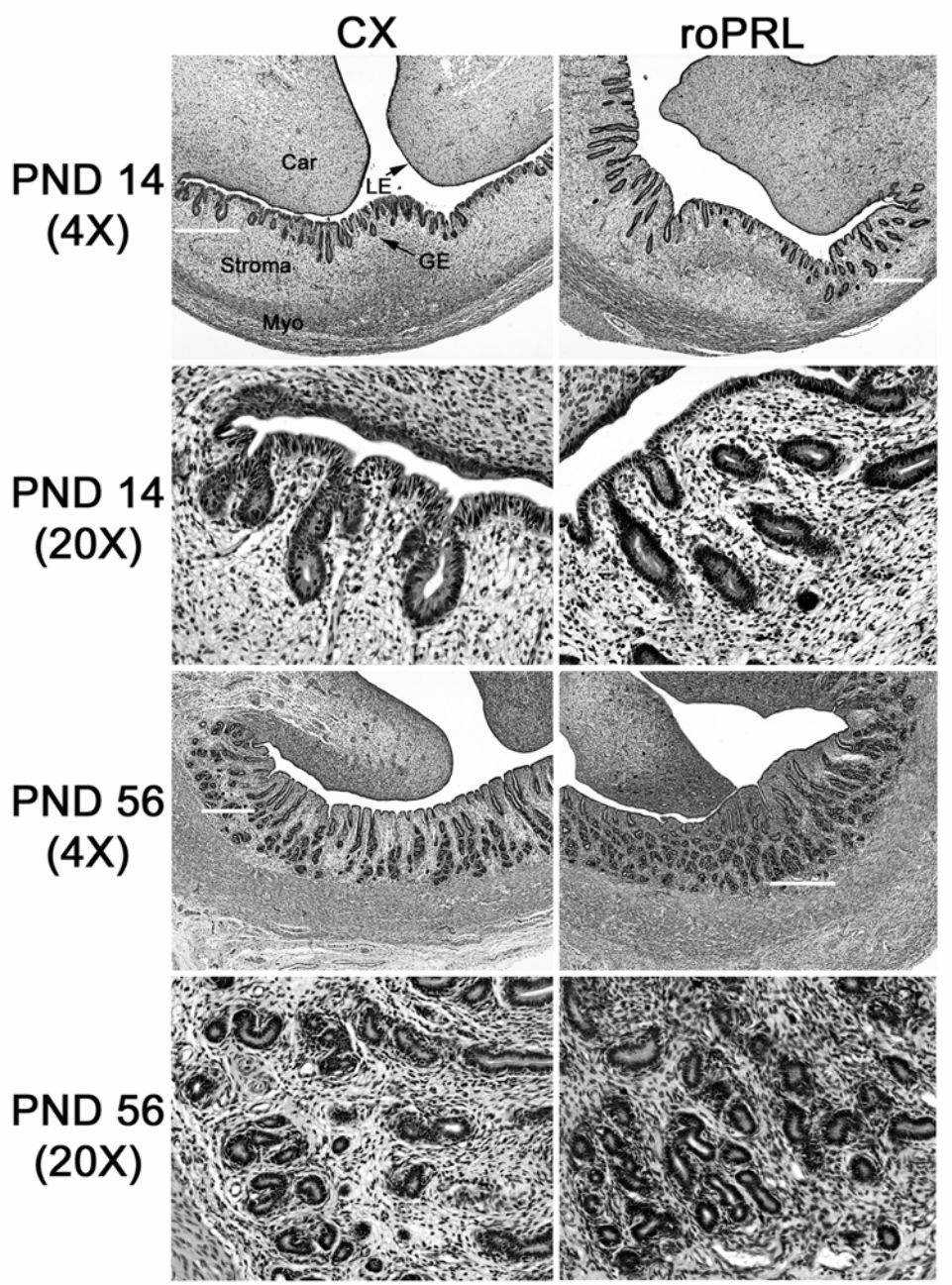

FIG 5.4. Representative photomicrographs depicting effects of treatment with vehicle as control (CX) or recombinant ovine prolactin (roPRL) on PND 14 and PND 56. Ewes were assigned at birth to receive treatment with saline vehicle as a CX or roPRL from PNDs 1 to 56. On PND 14, ewes were hemi-ovariohysterectomized, and the remaining uterine horn and ovary removed on PND 56. Uterine tissue sections were prepared and stained with hematoxylin and eosin. Photomicrographs are shown at low (4X) magnification (top) with the area denoted by the white bar at a higher (20X) magnification (bottom). Note the increase in coiled and branched endometrial glands in the stratum spongiosum of roPRL-treated ewes on PND 56, but not on PND 14. Legend: LE, lumenal epithelium; GE, glandular epithelium; Myo, myometrium.

TABLE 5.2. Effects of day and prolactin treatment on endometrial gland ductal invaginations, gland number, gland density, and thickness of both endometrium and myometrium (Study Two).

	PND 14			PND 56		
Measurement	CX	roPRL	SE	CX	roPRL	SE
Ductal Invaginations (number/section)	52	55	4	64	70	4
Gland Number (per section)	36	61*	7	450	732*	32
Gland Density (number/200 μm^2)						
Stratum Compactum	4.4	5.9	0.3	8.9	9.0	0.4
Stratum Spongiosum	-	-	-	15.4	18.7*	0.6
Endometrial Thickness (μm)	359	383	14	492	563*	17
Myometrial Thickness (μm)	289	292	11	353	464*	19
Ovarian Weight (g)	n.d.[1]	n.d.	n.d.	1.2	0.8	0.1
Right Uterine Horn Weight (g)	-	-	-	2.3	2.1	0.2

* Effect of treatment within PND ($P<0.10$); [1] n.d. = not determined

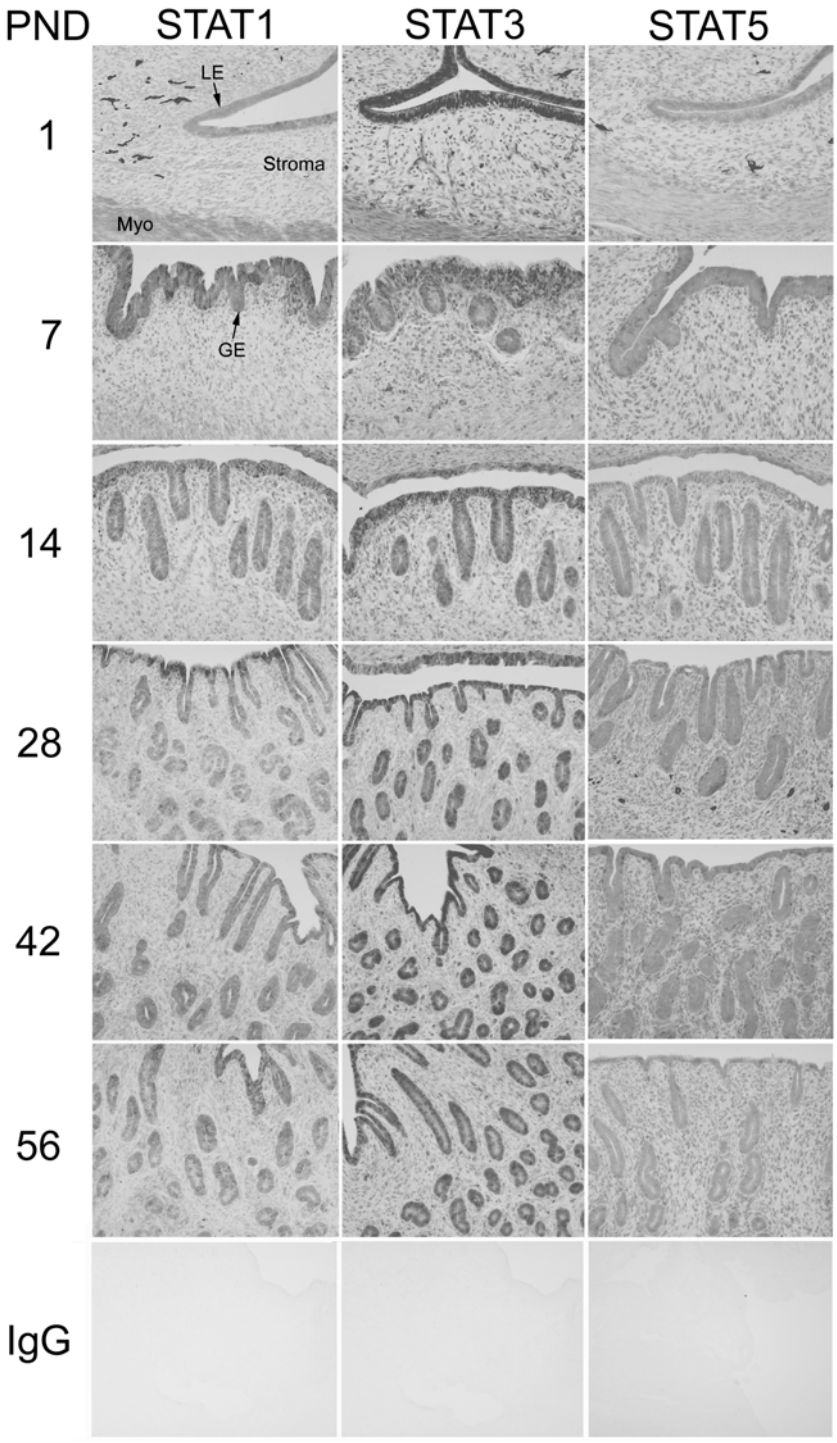

FIG 5.5. Expression of STAT 1, STAT 3 and STAT 5 proteins in the developing neonatal ovine uterus. Immunoreactive STAT proteins were detected using mouse anti-human STAT 1, 3 or 5 antibodies and a Biostain Super ABC Kit. Specific cellular staining was not observed when irrelevant mouse IgG was substituted for primary antibodies. All photomicrographs are shown at 40X. Legend: LE, lumenal epithelium; GE, glandular epithelium; Myo, myometrium.

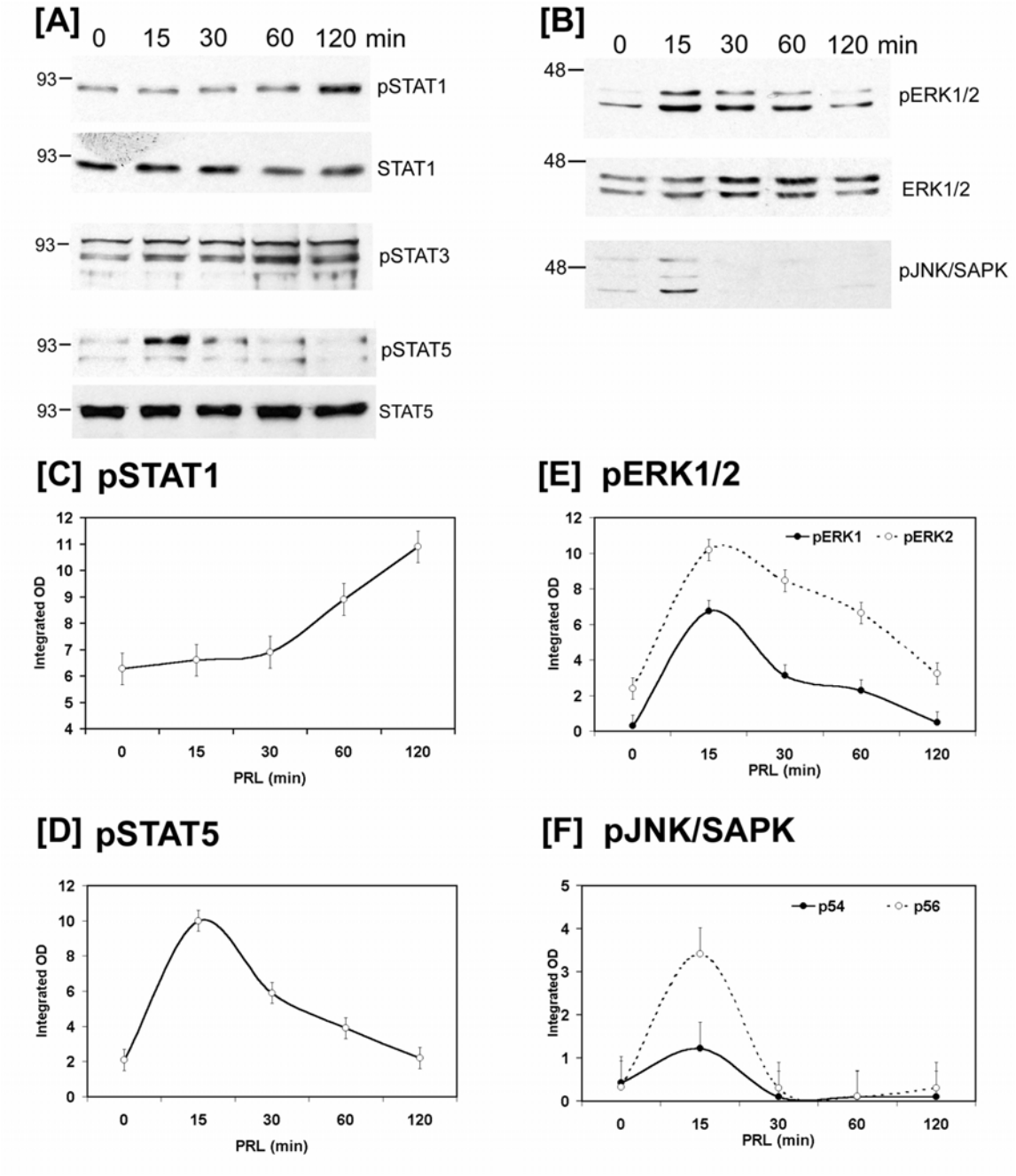

FIG 5.6. Effects of prolactin treatment of PND 28 ovine uterine explants on phosphorylation of STAT, ERK1/2 and SAPK/JNK proteins. Whole uterine explants from PND 28 ewes were treated with roPRL (500 ng/ml) for 0, 15, 30, 60 or 120 min, and 40 μg of each lysate was separated by SDS-PAGE and analyzed for phosphorylated STATs 1, 3, and 5 (panel A) or ERK1/2 and JNK/SAPK (panel B) by Western Blotting. Positions of the prestained molecular weight markers are shown on the right. Effects of PRL on expression of STAT and MAPK proteins in uterine explants are shown in panels C-F. Data are presented as LSM with SE. Representative results are from the analyses of uterine explant cultures from five ewes.

Although IRF-1 protein was detected in immune cells, immunoreactive IRF-1 protein was not detected in the endometrial glands or in any other uterine cell types regardless of neonatal age (data not shown). In situ hybridization analyses of the neonatal ovine uterus also confirmed these results using a homologous full-length ovine IRF-1 cRNA probe and methods described previously [211]. IRF-1 mRNA was not detected in any uterine cells, but was present in immune cells (data not shown).

Prolactin Stimulates Phosphorylation of STATs 1 and 5, ERK 1 and 2, and JNK/SAPK (Study Four)

In order to investigate PRL signaling pathways in the neonatal ovine uterus, uteri from PND 28 ewes were explanted into serum-free medium and stimulated with 500 ng/ml purified native oPRL. The explants were harvested at specific times, and effects of PRL on STAT, ERK 1 and 2, MAPK, and JNK/SAPK signaling pathways determined by Western blot analysis of proteins isolated from whole uterine explants (Fig. 5.6). Levels of tyrosine phosphorylated STAT 1 were increased by PRL ($P<0.05$, quadratic) after 30 min post-treatment (Fig. 5.6A and 5.6C). Treatment of uterine explants with PRL elicited a transient increase ($P<0.01$, cubic) in levels of tyrosine phosphorylated STAT 5 within 15 min post-treatment (Fig. 5.6A and 5.6D), but had no effect ($P>0.10$) on STAT 3 (Fig. 5.6A). The phospho-specific antibody used for this study detected both STAT 5a and STAT 5b. Within 15 min, PRL increased ($P<0.01$, cubic) levels of threonine and tyrosine phosphorylated ERK 1 and 2 MAPKs (Fig. 5.6B and 5.6E). Similarly, PRL also stimulated an increase ($P<0.10$, cubic) in levels of threonine and tyrosine phosphorylated JNK/SAPK by 15 min post-treatment (Fig. 5.6B and 5.6F).

Discussion

Results from each of the present studies strongly support the hypothesis that PRL regulates the critical process of endometrial gland morphogenesis in the developing uterus of the neonatal ewe. As observed previously [14], serum PRL levels in CX ewes in both Study One and Two were relatively high on PND 1, reached a maximum around PND 14, and then declined. Serum levels of PRL on PND 56 are much greater than in adult ewes during most of the estrous cycle and pregnancy [212]. The temporal changes in circulating levels of PRL in the neonatal ewe parallel the ontogeny of endometrial glands in the developing intercaruncular endometrium of the uterine wall [14]. Hypoprolactinemia was induced in neonatal ewes by treatment with bromocryptine mesylate, which markedly reduced (~4.5-fold) circulating levels of PRL to an average of 36 ng/ml. These findings are consistent with the ability of bromocryptine to markedly inhibit, but not completely ablate, PRL release from the pituitary in sheep [34]. Unfortunately, an effective antagonist of the PRLR is not available [213]. Hypoprolactinemia decreased endometrial gland number and density in the PND 56 uterus. Histologically, the uteri of BROMO-treated ewes contained lower numbers of superficial ductal gland invaginations as well as coiled and branched endometrial glands in the endometrial stratum spongiosum near the myometrium. In the neonatal ewe, PRLR mRNA is most abundant in the proliferating, branching and differentiating GE between PNDs 21 and 56 [14, 15]. These findings are interpreted to support the hypothesis that PRL is a regulatory factor controlling endometrial gland coiling and branching morphogenesis in the developing neonatal ovine uterus. However, the

inability of BROMO treatment to completely inhibit PRL secretion may preclude determination of the precise role of PRL in the initial stages of endometrial adenogenesis.

Hyperprolactinemia causes uterine glandular hyperplasia in the adult mouse, rabbit and pig [39, 40]. Moreover, intrauterine administration of ovine placental lactogen (oPL), a PRL-like hormone that homodimerizes and signals through the PRLR [142], stimulates proliferation of endometrial glands in the adult ewe and, in particular, the coiled and branched glands in the stratum spongiosum of adult ewes [67]. In Study Two, treatment of ewes with roPRL from birth to PND 14 only slightly elevated circulating PRL levels, but increased endometrial gland number and density on PND 14. Indeed, the endometrium of roPRL-treated ewes on PND 56 contained more coiled and branched endometrial glands in the stratum spongiosum, but not stratum compactum. The budding, nascent and proliferating endometrial glands express mRNAs for the long and short PRLR forms on PNDs 7 and 14 [14]. Although all budding glands express PRLR on PNDs 7 and 14, only the GE in the stratum spongiosum express PRLR on PNDs 28 to 56 [14]. These temporal and spatial changes in PRLR mRNA expression are likely to be responsible for the differential effects of hyperprolactinemia on endometrial adenogenesis on PND 14 compared to PND 56. After the budded glands elongate to a more tubular form and begin coiling and branching morphogenesis by PND 21 [14], the ductal GE loses PRLR expression, thereby preventing it from responding to PRL. Indeed, the PRLR is expressed only in the endometrial glands of the stratum compactum in the adult ewe [18]. In mice with targeted disruption of the PRL gene, the

mammary glands display normal ductal tree formation, but fail to develop lobuloalveolar structure [35]. Similarly, mammary gland transplants from PRLR null mice into normal mice showed normal side branching and the formation of alveolar buds, but no lobuloalveolar development [36, 214]. These findings are different from the present studies and suggest that mechanisms whereby PRL regulates gland development is organ specific.

In Study Two, treatment of neonatal ewes with roPRL increased thickness of the endometrium and myometrium on PND 56. These effects of PRL are likely to be the results of increased numbers of endometrial glands. Development of the neonatal uterus involves reciprocal epithelial-mesenchymal interactions [3]. In the developing rodent uterus, the endometrial epithelium affects myometrial organization and growth [215]. Similarly, progestin treatment of neonatal ewes epigenetically ablates endometrial adenogenesis and reduces endometrial and myometrial thickness [90]. In Study Two, the thickness of the endometrium and myometrium increased between PND 14 and PND 56 in CX ewes, which correlates with coiling and branching morphogenetic development of the endometrial glands into the stratum spongiosum adjacent to the myometrium. These results support the idea that the endometrial glands regulate endometrial and myometrial growth during uterine development. Although estrogen can affect uterine growth and size in a number of species [3], the effects of bromocryptine and roPRL in Studies One and Two did not involve alterations in the circulating levels of E2-17β. Collectively, results from Studies One and Two strongly support the hypothesis that PRL

acts directly on the endometrial GE that express the PRLR, and regulates coiling and branching morphogenesis during postnatal development of the ovine uterus.

Biological responses to PRL in other model systems are mediated by the PRLR and intracellular activation of several signal transduction systems, including STATs 1, 3 and 5 proteins, IRF-1, and the MAPK cascade [148, 208, 209]. Prolactin binding to the PRLR activates janus kinase 2 (JAK2) and STATs 1, 3 and 5 [216, 217]. Although each of these STAT proteins have been ablated in mouse models, their roles in endometrial gland morphogenesis may be difficult to fully ascertain, because the mouse uterus lacks the extensive coiled and branched endometrial gland architecture characteristic of uteri from domestic animals and primates [3]. Results from Study Three indicated that STATs 1, 3 and 5 are present in the developing ovine uterus and, in particular, are expressed in the nascent and developing endometrial glands. In Study Four, PRL was determined to increase phosphorylation of STATs 5 and 1, but not STAT 3 in uterine explants from a PND 28 ewe. Interestingly, the effect of PRL on phospho-STAT 1 levels was more protracted and not observed until 60 min. Activation of the JAK2/STAT 5 cascade by PRL probably represents the hallmark of PRL signaling [218]. Functional development of the mammary gland epithelium during pregnancy depends on PRL signaling, and STAT 5a is essential for mammary gland alveolar proliferation and function [219-221]. Therefore, PRL signaling via the PRLR and STAT 5 may be critical for endometrial adenogenesis in the uterus during the neonatal period. However, the precise roles of STAT 5 are not known in neonatal ovine uterine gland development or

in adult uterine gland hyperplasia and hypertrophy that normally occurs in response to oPL in pregnant ewes [67].

In the PRL-responsive Nb2 T lymphoma cell line, PRL-mediated STAT 1 activation increases expression of the immediate-early gene IRF-1 [219, 222]. In the common marmoset monkey and human, the PRLR is also expressed predominantly in the endometrial glands along with JAK2, STAT 1 and IRF-1 [216, 223]. Further, treatment of proliferative phase endometrium from the monkey uterus increases expression of IRF-1 [216]. In the present study, IRF-1 mRNA and protein could not be detected in the endometrial glands of the developing neonatal ovine uterus, even though IRF-1 gene expression has been detected in the adult ovine uterus in response to conceptus interferon tau, a Type I interferon [211]. Therefore, IRF-1 does not appear to be a mediator of PRL actions on the endometrial GE in the neonatal ovine uterus.

Results from Study Four indicated that three members of the MAPK family are involved in the effects of PRL in the neonatal ovine uterus. Both ERK 1 and ERK 2 (also known as p44 and p42 MAPKs) function in a protein kinase cascade that plays a critical role in regulation of cell growth and differentiation [224, 225]. These two kinases share structural homology with the more recently discovered *c-Jun* N-terminal kinase/stress activated protein kinase (JNK/SAPK) family [226]. A variety of extracellular stimuli activate the JNK/SAPK pathway, including inflammatory cytokines, ultraviolet light and osmotic stress. In Nb2 cells, PRL activated JNK/SAPK and JNK/SAPK are important for mitogenic signaling and perhaps suppression of apoptosis [227]. In bovine mammary gland epithelial cells, PRL stimulation of cell

proliferation involves activation of JNK/SAPK and an increase in *c-Jun* content of the activator protein 1 (AP-1) transcriptional complex that leads to increased gene transactivation [228]. Recently, PRL signaling in the human endometrial glands was also shown to involve activation of ERK 1 and ERK 2 [229]. The results of Study 4 indicate that PRL increased phosphorylated ERK 1, ERK 2 and JNK/SAPK MAPKs. Previously, Taylor et al. [15] found high levels of phosphorylated ERK 1 and 2 in the nascent and proliferating endometrial glands that express PRLR in the developing neonatal ovine uterus. Collectively, results indicate that PRL stimulates several signaling pathways, including STATs 1 and 5, ERK 1 and 2 MAPKs, and JNK/SAPK, and is a major regulatory factor controlling endometrial gland morphogenesis in the neonatal ovine uterus.

CHAPTER VI

THE COMPLEX NATURE OF THE PROLACTIN RECEPTOR GENE AND DISCOVERY OF THE OVINE EXON 2

Introduction

Prolactin regulates the growth and differentiation of a number of epitheliomesenchymal organs, including the pigeon crop sac, mammary gland, prostate, and uterus [33]. In the mammary gland, PRL and PRLR are required for development and differentiation of the lobuloalveoli [34-36]. Hyperprolactinemia elicits uterine glandular hyperplasia in the adult mouse, rabbit and pig [38-40]. In the neonatal ewe, circulating levels of PRL are relatively high on PND 1, reach a maximum on PND 14, and then decline slightly to PND 56 [15, 37]. These temporal changes in circulating levels of PRL in the neonatal ewe parallel the ontogeny of endometrial glands in the developing intercaruncular endometrium of the uterine wall [14]. Additionally, expression of mRNAs for the short and long PRLR proteins is restricted to the nascent uterine GE buds on PND 7 and in proliferating and differentiating GE from PND 14 to 56 [15]. In the adult ovine uterus, PRLR expression is also restricted to the endometrial glands and not detected in other uterine cell types [18]. Intrauterine administration of ovine placental lactogen (oPL), a PRL-like hormone that homodimerizes and signals through the PRLR [142], stimulates proliferation of endometrial glands in the adult ewe and, in particular, the coiled and branched glands in the stratum spongiosum of adult ewes [67]. Moreover, hyperprolactinemia in the neonatal ewe increases the number of endometrial glands by 63% on PND 56 whereas hypoprolactinemia decreases the

number of endometrial glands present by 35% [Chapter V]. These results indicate PRL and the PRLR are involved in the regulation of postnatal endometrial gland development in the ovine uterus.

The GE specific nature of PRLR expression suggests that transcription of the PRLR gene is activated when the GE differentiates and buds from the LE. Therefore, transcription factors that regulate PRLR transcription may be key regulators of GE differentiation. The complete gene structure for PRLR has been determined in the human, rat, and mouse [145, 151, 154, 158, 159]. While there is variation among these species, many similarities exist including the location of the start codon in exon 3. Both the human [143] and the rat [144] PRLR genes are comprised of eleven exons, while the mouse PRLR gene contains thirteen [145]. In these species, the transcriptional start site is located in exon 3; therefore, exons 1 and 2 as well as part of exon 3 comprise the 5' untranslated region of the gene. Most mammals, including rats, express both long and short forms of the PRLR due to alternative splicing of exons 10 and 11, respectively [144]. Indeed, both the short and long forms of the PRLR are detected in the neonatal and adult ovine uterus [15, 18]. Alternative splicing of exons 10 and 11 also occurs in humans resulting in one long and two short isoforms [143, 146]. The mouse expresses four isoforms, one long and three short, also arising from alternative splicing of the 3' exons [145, 147]. The variant forms within a species are identical in their extracellular and transmembrane domain, but differ in the length of their cytoplasmic domains as well as the mechanisms through which they signal [143, 148]. The PRLR gene possesses a complex 5' genomic structure made up of multiple promoters and non-coding first exons

(Fig 6.1). These alternative first exons are differentially expressed depending on tissue type and developmental stage [149-153]. Exons 2 and 3 are highly homologous across species [145].

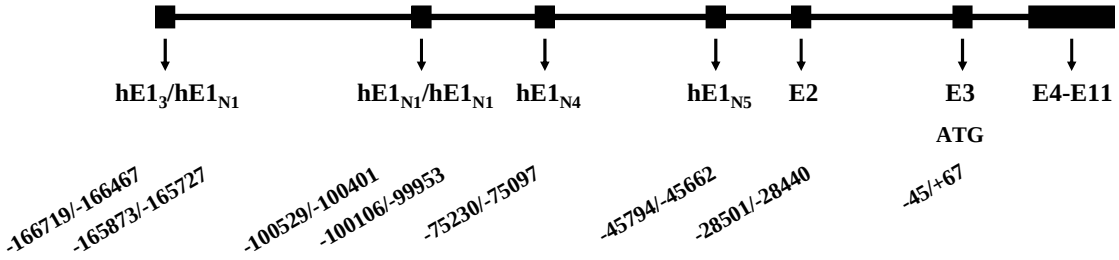

FIG 6.1. Structure of the 5' region of the human prolactin receptor gene (adapted from Hu et al. [153]). The human PRLR gene spans 167 kb on chromosome 5p13. The relative localization of the six alternative first exons and exons 2-11 are shown according to NT_006679.6. The translational start site (ATG) is located in exon 3. Locations and sizes of the exons are shown below (ATG=0).

The rat PRLR gene spans a 145kb region on chromosome 2 (2q16) [154] and contains four known first exons ($E1_1$, $E1_2$, $E1_3$, and $E1_4$) [150, 151]. The expression of each E1 is controlled by a separate, proximal promoter (PI, PII, PIII, and PIV) [151, 155]. Interestingly, canonical TATAA elements, found in most promoters, are absent from the PRLR promoters; however, they do contain TATA-like sequences [151]. Expression of $E1_1$ is primarily controlled by a SF1 binding domain in PI [154]. Thus, $E1_1$ is highly expressed in ovaries and has a low level of expression in the testis [151, 154]. Expressed only in the liver, $E1_2$ expression is controlled by HNF4 (hepatic nuclear factor-4), a transcription factor required for the expression of several liver specific genes [153]. The more ubiquitous expression pattern of $E1_3$ can be attributed to the presence of binding sites for the transcription factors C/EBPβ, a member of the CCAAT-enhancer binding protein family, and Sp1, a transcription factor that binds to GC-rich sequences

within PIII [152]. Hu et al. [151] detected high levels of $E1_3$ expression in testis where it was the predominant form with low levels being detected in ovaries and liver. A brain specific PRLR first exon, $E1_4$, was first described in the rat by Tanaka et al [150]. The mouse prolactin gene (Prlr) resides on chromosome 15 [157]. A total of five first exons and promoters span more than 60kb of the 5' region of Prlr [145]. Exons homologous to rat $E1_1$, $E1_2$, and $E1_3$ have been described as well as two novel first exons [145, 154]. The expression patterns of murine $E1_1$, $E1_2$ and $E1_3$ are similar to that seen in the rat. The two novel first exons were isolated by 5' rapid amplification of cDNA ends (5"-RACE) using liver cDNA [145]. They and their respective promoters have yet to be characterized. The PRLR gene spans 167kb on human chromosome 5 (5p13) [158] and contains six first exons ($hE1_3$, $hE1_{N1}$, $hE1_{N2}$, $hE1N_3$, $hE1_{N4}$, and $hE1_{N5}$) and promoters (hPIII, hP_{N1}, hP_{N2}, hP_{N3}, hP_{N4}, and hP_{N5} respectively) [158, 159]. Only one of the human first exons, $hE1_3$, is homologous to an E1 found in rats and mice [159], and, like rodents, its expression is controlled by C/EBP and Sp1 [158]. hE_{N1} is 147 nt long reaching from -252 to -106 [159]. The hP_{N1} promoter contains putative binding sites for the transcription factors ETS-1, Sp1, and AP2, as well as CRE [159]. The ETS element has been proven to be functional; however, Sp1 was not able to bind to this region [158]. The AP2 and CRE sites have not yet been examined. The remaining four first exons were first described using a human breast cancer cell line [158]. Of these, hE_{N2} and hE_{N3} are both expressed at low levels in the testis. hE_{N3} is also expressed at high levels in the liver [158]. Also found in the liver, hE_{N5} expression is detectable by RT-PCR analysis in the ovary [158]. Interestingly, hE_{N4} (134 nt) expression was not detectable

by RT-PCR analysis in either the gonads or the liver [158]. The promoters for these novel human first exons have not been analyzed.

Both long and short prolactin receptors are expressed in the endometrial GE of the neonatal and adult ovine uterus [14, 18]. The short form of PRLR results from a 39 base pair insertion 5' of exon 10 that contains two in-frame stop codons [230]. Although the coding regions of both long and short ovine PRLR have been cloned, the 5' end has been sequenced only -21 nt in front of the translational start site which is 23 nt shorter than the human exon 3 [230]. The objective of this study was to clone and characterize the 5' region of the ovine PRLR in order to identify potential transcription factors regulating cell type-specific expression of the PRLR within the endometrial glands of the ovine uterus.

Materials and Methods

Isolation of PRLR Clones

A Day 14 pregnant ovine endometrial cDNA library, constructed by Clontech (Palo Alto, CA, USA) using directional cloning into the pTriplEx2 phage vector and an EMBL3 λsheep genomic library (CLONTECH Laboratories, Inc., Palo Alto, CA) were used to screen for PRLR clones using radiolabeled probes under high stringency conditions. The first library screen was performed on the genomic library using a KpnI-NcoI fragment of a known sheep PRLR cDNA (AF041257) isolated by Bignon et al [230]. A second library screen was performed on the day 14 pregnant cDNA library using the same ovine PRLR fragment for a probe. This library was screened again using a bovine PRLR cDNA (NM174155) [149] that spanned from exon 3 to exon 10 as a

probe. Both the genomic and Day 14 pregnant cDNA libraries were also screened using radiolabeled overgo primers. Overgo primers were designed against exon 2 (5'-AAGAACGCTTCTGTTCATGGAGGC-3', 5'-AGCATCCTTAGCATTTGCCTCCAT-3') and a 47 nt region 5' to exon 2 (5'-AGGACGAGAGAGCCGAGGAGAGGA-3', 5'-TTGCCCAACTTCCCTCTCCTCTCC-3') of the 5'-RACE clones. Probes were synthesized using the DECAprime II kit (Ambion, Austin, TX) and P^{32}-dCTP. The ability of the radiolabeled primers to recognize and bind the gene of interest was verified by Southern blot analysis using the 5'-RACE products and standard techniques [231]. Plaque purification to homogeneity of several positive isolates and DNA isolation were performed using standard methods.

Southern Blot Analysis

Southern blot analysis were performed by standard techniques [231]. Briefly, digested DNA samples were separated by electrophoresis on a TAE gel containing agarose (1% w/v) and ethidium bromide (1μg/L) and transferred to a nitrocellulose membrane (Schleicher & Schuell BioScience, Keene, NH) by capillary blotting. The membranes were then hybridized with probes synthesized using the DECAprime II kit (Ambion, Austin, TX) and P^{32}-dCTP. Membranes were then washed under high stringency conditions. The blots were visualized using a Typhoon 8600 MultiImager (Molecular Dynamics, Piscataway, NJ).

Sequence Analysis

A 3.6 kb fragment of a PRLR genomic clone was sequenced by Agencourt Biosciences (Beverly, MA). The 5'-RACE clones were sequenced in both directions

using an ABI PRISM Dye Terminator Cycle Sequencing Kit and ABI PRISM automated DNA sequencer (Perkin-Elemer Applied Biosystems, Foster City, CA). Sequence alignment was conducted with the ClustalW alignment tool of the European Bioinformatics Institute (EMBL-EBI) available online at http://www.ebi.ac.uk/services.

Rapid Amplification of cDNA Ends (5'-RACE)

Total cellular RNA was isolated from frozen PND 28 and 56 uteri using the Trizol reagent (Gibco-BRL, Grand Island, NY) and analyzed for concentration and quality. The RNA (1 μg) was then used to synthesize cDNA using MMLV reverse transcriptase from the SMART RACE cDNA Amplification Kit (Clontech, Palo Alto, CA) according to the manufacturer's instructions. Ovine PRLR specific primers were based on the mRNA sequence published by Bignon et al (AF041257) [230]. Sequences were used to amplify upstream of exon 6 (5'-CACCTTCCTTGCGGTAAGTCAG-3') and exon 3 (5'-GACAGGTTCACAGGAGGCTCT-3'). The PCR conditions were as follows: 5 cycles of 94C for 5 sec followed by 72C for 3 min; 5 cycles of 94C for 30 sec, 70C for 30 sec followed by 72C for 3 min; and 25 cycles of 94C for 30 sec, 68C for 30 sec, and 72C for 3 min. The resulting products were gel purified on a 1.2% agarose gel and subcloned into the pCRII cloning vector using a T/A Cloning Kit (Invitrogen Live Technologies, Carlsbad, CA).

Results

Several clones (5B, 7A, and 16C) were purified to homogeneity from an EMBL3 λsheep genomic library using a KpnI-NcoI fragment that includes the translational start site from the 5'-end of a previously identified ovine cDNA (AF041257) [230]. The

clones were then analyzed by restriction digest and Southern blot analysis (Fig. 6.2). Of these, only one clone (16C) tested positive by Southern blot analysis when probed with the same KpnI-NcoI fragment that was used for the library screen. This 12.5kb fragment was analyzed and further mapped by restriction digests (Fig. 6.3A). A fragment of approximately 1.4kb was excised using the BglII restriction enzyme (Fig. 6.3B), subcloned into pCRII, and sequenced from both ends (Fig. 6.4). The resulting sequences were homologous to human chromosome 5, but not PRLR. EcoRV was used to remove 8.9kb from 16C, and the remaining ends were ligated (Fig. 6.3B). The remaining 3.6kb insert was sequenced by Agencourt Biosciences (Fig. 6.5). Sequence analysis revealed that nucleotides 1935 to 2047 were 81% homologous to the human PRLR exon 3. The KpnI-NcoI fragment was also used to screen an endometrial cDNA library from Day 14 pregnant sheep endometrium to potentially isolate an ovine cDNA that contained exons 1 and 2; however, no positive plaques were isolated (data not shown). This library was screened again with bovine PRLR cDNA (NM174155) [149], but also resulted in no positive plaques unfortunately (data not shown).

In an effort to clone exon 1 and 2, 5'-RACE was utilized. An initial 5'-RACE product was obtained from PND 56 endometrial cDNA using a primer designed against exon 6 of the ovine PRLR gene (AF041257) [230]. The band was gel purified and used as a template for nested 5'-RACE using a primer homologous to exon 3. The exon 3 primer was also used to obtain primary 5'-RACE products from PND 28 and 56 cDNA (Fig. 6.6). Each reaction yielded products of approximately 350nt in length which were gel purified and subcloned into pCRII. Sequence analysis revealed high homology

among the 5'-RACE products (99%), and between the products and the human PRLR gene (82%) (Fig. 6.7). The clones contained all of exon 3 and a 64 nt region homologous to human exon 2. The 5'-RACE clones also possessed a 47 nt region 5' of exon 2 that is not homologous to any known exon 1.

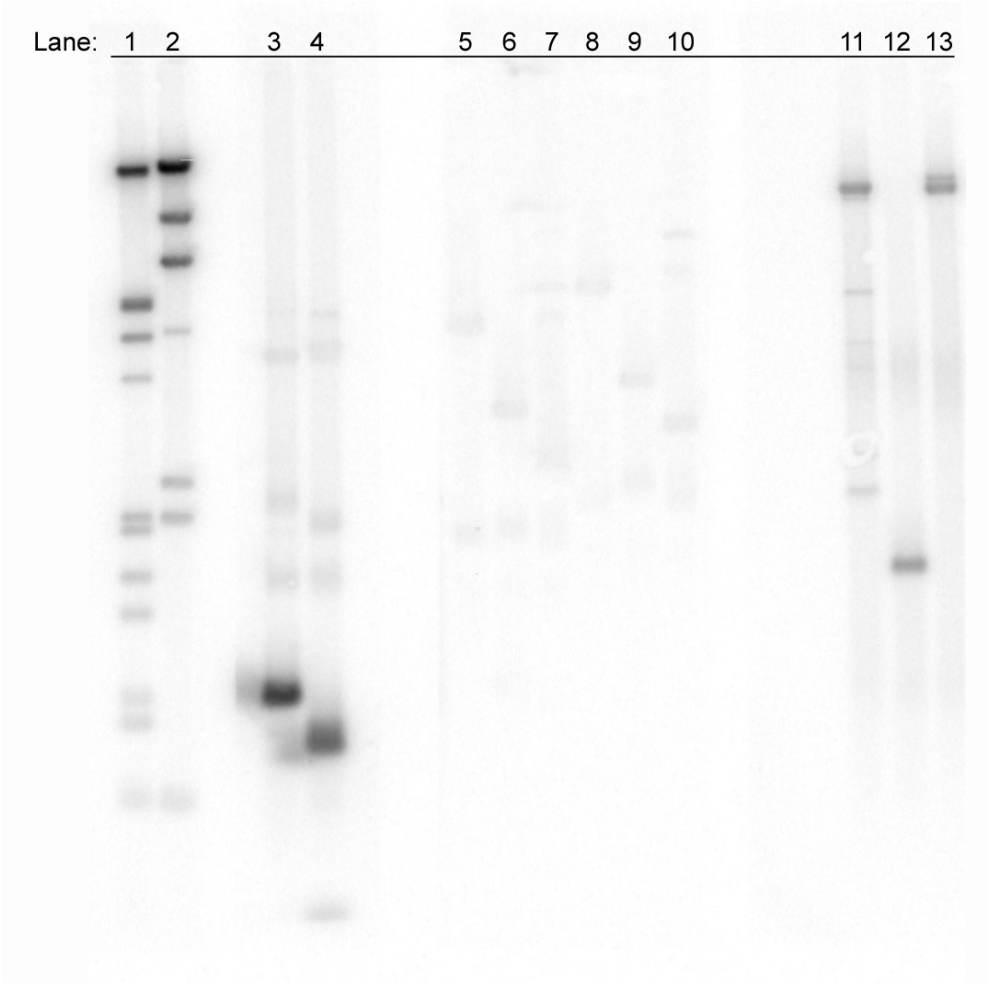

FIG 6.2. Southern blot analysis of clones isolated from an EMBL3 λsheep genomic library using the KpnI-NcoI fragment of an ovine PRLR cDNA. Lanes 1 and 2 are λ-HindIII and λ-HindIII/EcoRV ladders, respectively, hybridized with radiolabeled λ-DNA. Lanes 3 and 4 are the ovine cDNA from which the probes were synthesized. The cDNA was digested with KpnI+SmaI+SacI and BamHI+HindIII, respectively, as a positive control. Lanes 5 through 7 are clone 5B, lanes 8 through 10 are clone 7A, and lanes 11 through 13 are clone 16C. Each of these clones was digested with in order SacII, BglII+NotI, and XbaI+NotI. Lanes 3 through 13 were hybridized with the KpnI-NcoI fragment of an ovine PRLR cDNA. All DNA was digested, separated in an agarose gel, and blotted onto a nitrocellulose membrane. Membranes were then hybridized with radiolabeled probes, and washed under high stringency conditions.

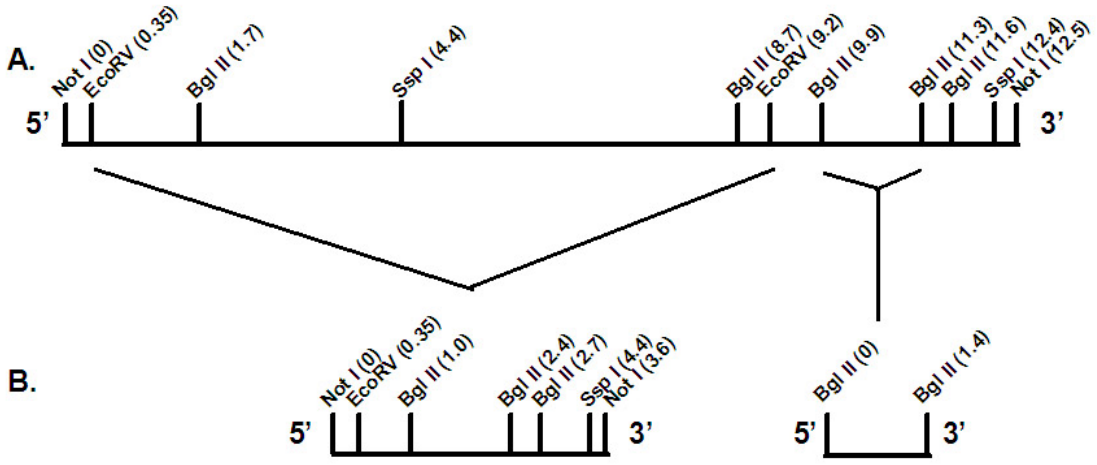

FIG 6.3. Restriction map of the 16C clone. A. The entire 16C insert was mapped with EcoRV, BglII, and SspI. NotI was used to excise the clone from the plasmid. B. Maps of the portions of 16C that were sequenced. EcoRV was used to remove 8.9kb from the insert. The ends were ligated, and the remaining 3.6kb was sequenced. BglII was utilized to excise a 1.4kb fragment of 16C that was positive for ovine PRLR by Southern blot analysis. The fragment was subcloned into pCRII and sequenced.

A.

TGCAGAATTCCAGCACACTGGCGGCCGTTACTAGTGGATCTATTGTTTTCCAAGAGTTGTTT
GGAGTCCAAAGAGGCTAATGAGTCTTTTCCAAATGTCTTTCAAAATCCTTTCTTCTTAAAAGG
ACATTTAGAGGCTTTGAAAATTGTTCCAAGGGTAAAAATAATATTAATAATAAATTTCTCAAAA
CTCTCAACCCCTGTAGGNGCAAAATTTGCTTAATTCTTCAAATGCAAAGGACTTTGAATTGTT
ACTGGGAATTGTCAATTTTTGCTTATGAGGATTTTCCAAAGGGTAAGAGTCATCACATGGAA
GTCCACTAGAGTTCACTACATGGNGGGGGGGNCTTGTCCGTGAGCTGGGACACTTCTAGA
GTCTTCAGAAGCANAACCTTCAAGAGAGCCTTCCCCCTTTTTCTTGGTGGCATCCATGGGG
CCAGGTGGGAGTTAAACTGNAAGCATCAACTTT

B.

GATGGNATATCTGCAGNAATTCCAGCACACTGGGCGGCCGTTACTAGTGGATCTATTGTTTT
CCAAGNAGTTGTTTGGAGTCCAAAGAGGCTAATGAGTCTTTTCCAAATGTCTTTCAAAATCC
TTTCTTCTTAAAAGGACATTTAGAGGCTTTGAAAATTGTTCCAAGGGTAAAAATAATATTAATA
ATAAATTTCTCAAAACTCTCAACCCCTGTAGGTTCAAAATTTGCTTAATTCTTCAAATGCAAA
GGACTTTGAATTGTTACTGGGAATTGTCAATTTTTGCTTATGAGGATTTTCCAAAGGGTAAGA
GTCATCACATGGAAGTCCACTAGAGTTCACTACATGGGNGGGGGCTTGTCCGTGAGCTGG
GACACTTCTAGAGTCTTCAGAAGCAGAACCTTCAAGAGAGCCTTCCCCCTTTTTCTTGGCGG
CNTCCATGGGGCCAGGTGGGAGTTAAACTGAAAG

FIG 6.4. Forward and reverse sequences of the BglII excised fragment of 16C. BglII was used to excise a 1.4kb fragment of 16C that was positive for ovine PRLR by Southern blot analysis. The fragment was subcloned into pCRII and sequenced. A. A Sp6 primer was used for forward sequencing. B. A T7 primer was used for reverse sequencing.

AAGAACAGAGGAGCCTTCTGGGCTACAATCCATAAGGTCACGAAGAGTCAGACACGACTCT
GCAGACGTGACTGACTGAGCACACACGCACGCACTAGTTTACGGGCTTGCACATGCGCATT
ACGCAGGACTGAGCATATTTTGACGGGGAAGTGAGCCAGATGTGAAAACAGCTAACAGATT
TACTGAGAAATGAGGGAATGGAGGAAATGGGAGTGTGAAGCTTTCGGAAATGTGCAGAGAT
TAATTCTAACTGATCTTAGGAATAAAATGCTTCCTGAAAGCACTTTTATTGGAAAATGTTATTT
AGAAGAGTTTCAGGTTTATTTTAGAACTTTTTCAGTCAGTGGGTAGCACACCCATCCCCAGG
CCAAGCTGAGATCACAAGATGTGCAGGACAAAGAACTCTTTCAGGCCTCAGTGGACCCAGT
GAAACTGGATTAGGGCGAACAACAGTGTTTAAGATCCTCGGAGGCAGGCATGGCCACTCTG
CTGTCTCTCTGCTTCATAATTTCTCAACTTCTACCCTTTCCGCTGCTTTCTTTTTCCTGTTCCA
TTTTCCAGTTTCAATCCCCAACATAAAACCCCGAACCTGTATCGTCACTGAGAATTCTATTTC
CAAGTATGTCTCAAGGGACATGATAGCAGGTGGAAAGAACTTCAAGAAGTTGTTTGTTAGGT
GATGTCTGGCTGGCAGATGGAGATCCACCCTCTGACCAGGAGGAGTTGGCAAAGCCTGGT
CTTTTCAAGGCTCATCAAGCAGCATTCAGCATTTTCCAACATCCCTGGATGGGCGGCCTTG
CTCCTGCATGCCCTTCCCCCAATTTTTAAAAAAAATGTAAAATTTAAAAGGAAAATGTAAGTC
ATGGGCTTCCAAGAATTTATACTTACTTCATCAGATCTATTGTTTTCCAAGAGTTGTTTGGAG
TCCAAAGAGGCTAATGAGTCTTTTCCAAATGTCTTTCAAAATCCTTTCTTCTTAAAAGGACAT
TTAGAGGCTTTGAAAATTGTTCCAAGGGTAAAAATAATATTAATAATAAATTTCTCAAAACTCT
CAACCCCTGTAGGTTCAAAATTTGCTTAATTCTTCAAATGCAAAGGACTTTGAATTGTTACTG
GGAATTGTCAATTTTTGCTTATGAGGATTTTCCAAAGGGTAAGAGTCATCACATGGAAGTCC
ACTAGAGTTCACTACATGGCTCACAGCCTTGTCCGTGAGCTGGGACACTTCTAGAGTCTTC
AGAAGCAGAACCTTCAAGAGAGCCTTCCCCCTTTTTCTTGGTGGCATCCATGGGGCCAGGT
GGGAGTTAAACTGAAAGCATCAACTTTTCAGCCTGCCTTATTTTTGGCTAGTAGATCAGAGT
CCTCCCAGAACAGTTCTATTGTAGGGCATGCAATCTGTATCACATAAAACAGGTGATCTATT
ATTGGGTGGCTTCACTGGTGGCTCAGACAGTAGAGAATTCACCTGCAATGCAGGAGACAAG
GTTTCAACCCTGGGTCAGGAAGATCCCCTGGAGAAGGGAATGGCTACCCACTCCAGTATTC
TTGCCTGAGAAATCCCGTGAACAGAGGAGCCTGGCAAGCTACAGTCCATGGGGTTTCAGA
GTCAGATACAACTGAGCAACTAACCCTGTGGGGTGCAAAGAGAACAATTTTTCCTTAGGGT
GTGTGCAAAGGAGCCCTTTGTGCTCAGCTGACCTTGAACGTTGTCTTCGGATGACCTCTGG
TGGTGGAATTTTTCCCAGCATATGCACAGCTATGTTTCTGAGCCAAGCTATCCTTGTTACATT
TTCCTACATTCCTTTCCTCCTGTTTTGTTATTCACATTCAGCAAGGAGCAAGAATCAGTTGCA
AACACTCAGAATAAAGTGGTGCATGTGCCTCACCAGACTTTTGGTGTTTCAAAAAGTTGCCT
GTGCCTTCTCTTTCAG**<u>TGAACCTCTGATATATTTCCTGTGGAAAGAGGAAGGAGCCAACAT
GAAGGAAAATGCAGCATCCAGAGTGCTTTTCATTCTGCTACTTTTTCTCTACGCCAGCCTT
CTGAATG</u>**GTAAGTAAGAGACTGTCCTGTTCTCTTTCACTTCCTGGGTTATTTGCACAAGAGG
AGGGGAGAATCCATCCCAGTCCTTTTGCAGCACAGTTACAGGAAATGAAAATGTCCATGGC
ATTTGCTTCTCTTCAATTATTTATAATATTATGGGGATTAAAATGAAGGCAAACAGTAATGCA
AAAGACTGGATGCAGTTAATGCCACATCCTGTCACCATGCTCTGACTTCCATCCTCATTCTG
GGAGTGCAGAGAAACAACCCTGCCAGGGACATATCACAGTCTCAGTCCAGGTTCTGTCCCT
TACTGGCTGTGCAACCTTGAGCCAGTTAACTTAGTTCCCGGGATTTACACTCTTTCAAAGTG
AGGAAAATGACGTTTCCTCCACCTCAGATGAAAAGTTGTGTGAGAAAAATCTTTGAAAACCT
GTGAAGAGATCTAAGGGGATTGCTGTTACATGGTGGAAAACAGGGACACTCAACTCTGCTA
GGCAGGAAATGAAATTCACAAGTAGACTAGCACATGCAAGCCTATGTGTGTACATTTCAGTG
TGTCTACCCCAGTCTATTTGTAAGTGTGTATACTTGTGTATATCTCTGTATCTATTAGCTTCC
CTGTACGTACCTGGTGGAAAATGCTCCTTTGTGTGTACCTATATGCATACCCATTTGTGGGT
GCATATTTCTGCATATGTATCTATGTGTGGACCAGTATCTACTTCTGTAAGTATGCAGCTGC
GTATATTGTTCCTCTGTGATCTGAGGGTGTGTTTCTGATATGAGCCCTTCTGTCTGAGCACG
TGTGTGTTGGGGGTGGGGAGTACCTCTGTGGTTGTCCCTGGGTTTGTGTGCATTGTACAGG
GAAAGTGAGACCATCCATTCACTGTAACCATCTCTTCTAAAGTGGGTGAAAGAAACATTTGA
CTAATTACATTTCACAGCGTTACCTTCCTCTCTTGAGTT

FIG 6.5. Sequence of the remaining 3.6kb of the 16C insert after a 8.9kb was excised using EcoRV and the resulting ends were ligated. Sequencing was performed by Agencourt Biosciences (Beverly, MA). The underlined region (nucleotides 1935-2047) is homologous to human exon 3.

TTCTCGAGGTACTGTTAATAACCAGTGAAATGTGAGAGAGAGAAGCTTTCAGAAAGAGAAAA
AGGAATGTGGAGATTGGTACAATCCATATGGAAACTTTAAGTATTCAACTAAGCCCCAAATA
ATCAGCAGTTGCCTTAATTGGCTTCTAAATATGCTCATTATTGAGCTGTAAACTTTGTGTGTT
TTTAAAATAAAAGCTTTTCCTTCCACCTCACACACTCCTCCCTAGCCGCAAGAAAAATCAAAC
AAAAAATCACTTCACCCTGTGAAATTGTCCTGAAGAAATATTCCCTAGAGGTCAAGCAACGT
TCCAAAATGGGCAGAGCTAAGCCCAGACTGGCTGGCATGAACAGTTTTCAG

FIG 6.5 (Continued)

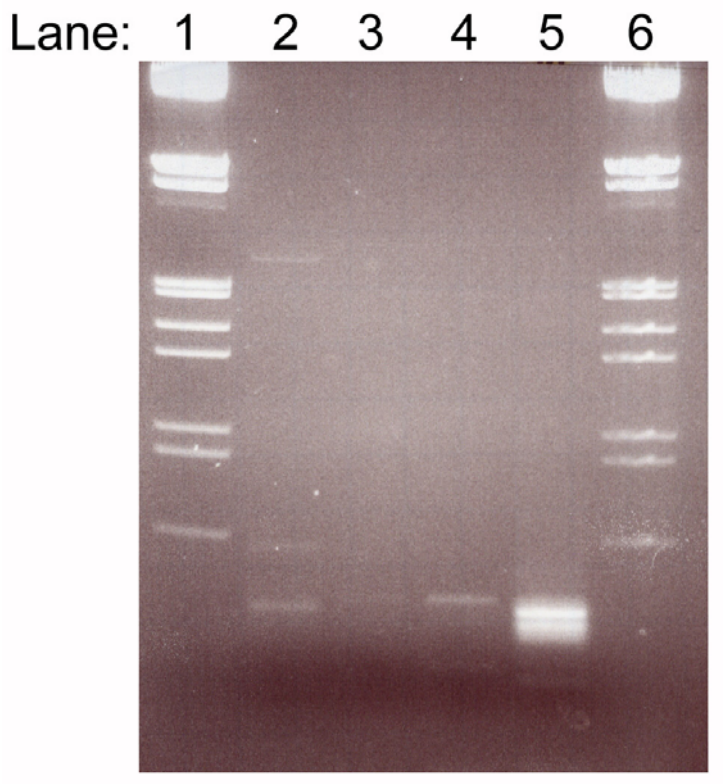

FIG 6.6. Products of 5'-RACE using a primer to exon 3 run on agarose gel. Lane 1 and 6 are λ-HindIII/EcoRV ladders. Lanes 2 through 4 contain 5'-RACE products using day 120 pregnant sheep endometrium, PND28, and PND56 mRNA as template, respectively. Lane 5 contains a nested 5'-RACE product using PND56 mRNA and a primer for exon 6 in the previous RACE. The resulting product was gel purified and used as a template for subsequent RACE analysis.

```
NM_000949       ----------------------------------------------CTAAAGAACTCTC
NPND56          -GGAGGACGAGAGAGCCGAGGAGAGGAGAGGGAAGTTGGGCAAACAGCTAAAGAACGCTT
PND56-5         -GGAGGACGAGAGAGCCGAGGAGAGGAGAGGGAAGTTGGGCAAACAGCTAAAGAACGCTT
PND28-7         GAGAGGACGAGAGAGCCGAGGAGAGGAGAGGGAAGTTGGGCAAACAGCTAAAGAACGCTT
                                                              ********* **

NM_000949       CTATTCATGGAGGCGAACACTGAGGATGCTTTCCACATGAACCCTGAAGTGAACTTCTGA
NPND56          CTGTTCATGGAGGCAAATGCTAAGGATGCTTTCCAAGTGAACCCTGA-GTGAACCTCTGA
PND56-5         CTGTTCATGGAGGCAAATGCTAAGGATGCTTTCCAAGTGAACCCTGA-GTGAACCTCTGA
PND28-7         CTGTTCATGGAGGCAAATGCTAAGGATGCTTTCCAAGTGAACCCTGA-GTGAACCTCTGA
                ** *********** **  ** *************  ********** ****** *****

NM_000949       TACATTTCCTGCAGCAAGAGAAGGCAGCCAACATGAAGGAAAATGTGGCATCTGCAACCG
NPND56          TATATTTCCTGTGGAAAGAGGAAGGAGCCAACATGAAGGAAAATGCAGCATCCAGAGTGC
PND56-5         TATATTTCCTGTGGAAAGAGGAAGGAGCCAACATGAAGGAAAATGCAGCATCCAGAGTGC
PND28-7         TATATTTCCTGTGGAAAGAGGAAGGAGCCAACATGAAGGAAAATGCAGCATCCAGAGTGC
                ** ********  * ***** * * ********************  *****   *

NM_000949       TTTTCACTCTGCTACTTTTTCTCAACACCTGCCTTCTGAATGGACAGTTACCTCCTGGAA
NPND56          TTTTCATTCTGCTACTTTTTCTCTTCGCCAGCCTTCTGAATGGACAGTCACCTCCTGAAA
PND56-5         TTTTCATTCTGCTACTTTTTCTCTTCGCCAGCCTTCTGAATGGACAGTCACCTCCTGAAA
PND28-7         TTTTCATTCTGCTACTTTTTCTCTTCGCCAGCCTTCTGAATGGACAGTCACCTCCTGAAA
                ****** ****************  * ** ****************** ******** **

NM_000949       AACCTGAGATCTTTAAATGTCGTTCTCCCAATAAGGAAACATTCACCTGCTGGTGGAGGC
NPND56          AACCCAAGCTTATTAAATGTCGGTCTCCTGGAAAGGAAACGTTCACCTGCTGGTGGGAGC
PND56-5         AACCCAAGCTTATTAAATGTCGGTCTCCTGGAAAGGAAACGTTCACCTGCTGGTGGGAGC
PND28-7         AACCCAAGCTTATTAAATGTCGGTCTCCTGGAAAGGAAACGTTCACCTGCTGGTGGGAGC
                ****  ** *  ********** *****    ******** ***************  **

NM_000949       CTGGGACAGATGGAGGACTTCCTACCAATTATTCACTGACTTACCACAGGGAAGG
NPND56          CCGGGGCAGATGGAGGACTTCCTACCAATTACACACTGACTTACCGCAAGGAAGG
PND56-5         CCGGGGCAGATGAAGGACTTCCTACCAATTACACACTGACTTACCGCAAGGAAGG
PND28-7         CCGGGGCAGATGGAGGACTTCCTACCAATTACACACTGACTTACCGCAAGGAAGG
                * *** ****** ******************  ************ ** ******
```

FIG 6.7. Sequence alignment of 5'-RACE products with human PRLR. NM000949, human PRLR cDNA sequence; NPND56, nested PND56; PND56-5, primary product from PND56 template; and PND28-6, primary product from PND28 template. Asterisks indicate nucleotides which are homologous among the four sequences.

Overgo primers were designed against exon 2 and the proceeding 48nt using the 5'-RACE clones as a template. The radiolabeled probes synthesized from the overgo primers were able to bind to the 5'-RACE product on a Southern blot analysis demonstrating their ability to recognize the target sequences (Fig 6.8A). Probes synthesized from the overgo primers were then used to screen an ovine genomic library. Two clones (3B and 14A) were purified to homogeneity were isolated using the exon 2 probe; however, no clones were isolated using the probe designed against the 5'-47bp

region. These clones were analyzed by restriction digests and Southern blot analysis (Fig 6.8B and 6.8C). Both clones were able to hybridize to the exon 2 probe and seemed to be duplicates. To potentially isolate a full-length PRLR cDNA clone, the overgo probes were also used to screen the Day 14 ovine endometrial cDNA library; however, no positive plaques were recovered from this screen (data not shown).

Discussion

The present studies were unable to isolate the predicted non-coding exons of the ovine PRLR gene; however, this is the first time PRLR exon 2 has been described in the sheep. Initially, the previously described ovine cDNA was used to screen an ovine genomic library. Of the clones that were isolated, only one tested positive by Southern blot analysis. Portions of the 16C clone were excised and further analyzed by sequencing. The resulting sequence contained a region homologous to the human PRLR exon 3 (NM000949) (Fig 6.4). Further analysis of the ovine PRLR cDNA (AF041257) revealed that it does not contain a 5'-untranslated region homologous to that found in other species. Therefore, the probe derived from the ovine cDNA did not contain exons 1 or 2, and the library was screened with a region homologous to exon 3. A Day 14 cDNA endometrial library was subsequently screened with the ovine PRLR probe and then a bovine probe that contained exons 3 through 10 to potentially isolate a full-length ovine cDNA; however, no positive clones were isolated. The failure to isolate a positive clone from the cDNA library may be due to the relatively low amount of PRLR-positive glandular epithelium as compared to total endometrial tissue in the Day 14 pregnant ovine uterus [18].

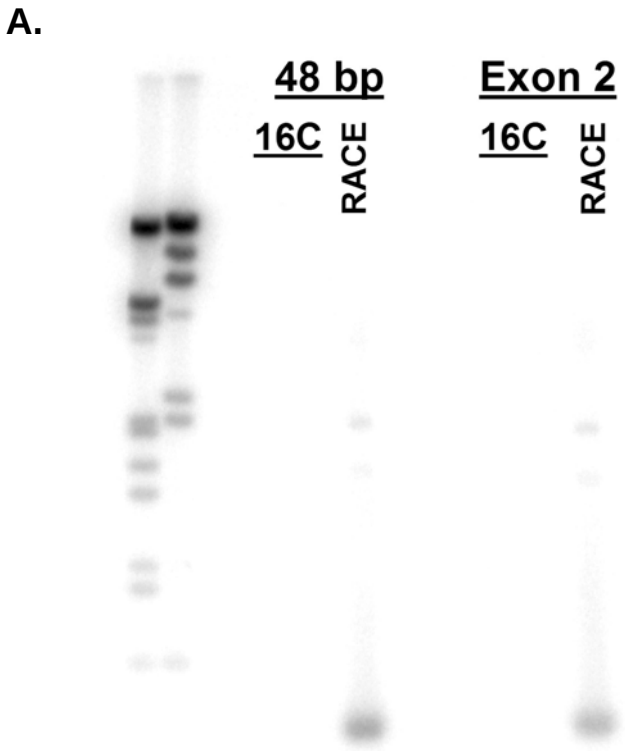

FIG 6.8. Southern blot analysis using radiolabeled overgo primers as probes. A. Overgo probes were tested for their ability to hybridize to DNA. The first two lanes λ-HindIII/EcoRV and λ-HindIII ladders, respectively, hybridized with radiolabeled λ-DNA. The overgo probes were designed against the 48nt upstream of exon 2 and exon 2 in the 5'RACE products. Both probes were tested for their ability to bind to the 16C clone and to the nested PND56 RACE product. 16C was digested with NotI, NotI+EcoRV, and EcoRV. The 5'-RACE product was excised from pCRII using EcoRI. B. Clone 3B was purified to homogeneity from an EMBL3 λsheep genomic library using the exon 2 specific overgo probe and analyzed by Southern blot analysis. Lanes 1 and 2 are λ-HindIII/EcoRV and λ-HindIII ladders, respectively, hybridized with radiolabeled λ-DNA. The remaining lanes are the 3B clone digested with: lane 3, HindIII; lane 4, KpnI; lane 5, SacI, lane 6, BamHI; lane 7, EcoRI; lane 8, XhoI; lane 9, ApaI; lane 10, BstXI; lane 11, SmaI; and lane 12, PstI. The exon 2 specific overgo probe was radiolabeled and hybridized to the membrane which was subsequently washed under high stringency conditions. C. Clone 14A was purified to homogeneity from an EMBL3 λsheep genomic library using the exon 2 specific overgo probe and analyzed by Southern blot analysis. Lanes 1 and 2 are λ-HindIII/EcoRV and λ-HindIII ladders, respectively, hybridized with radiolabeled λ-DNA. The remaining lanes are the 3B clone digested with: lane 3, HindIII; lane 4, KpnI; lane 5, SacI, lane 6, BamHI; lane 7, EcoRI; lane 8, XhoI; lane 9, ApaI; lane 10, BstXI; lane 11, SmaI; lane 12, PstI; and lane 13 NcoI. The exon 2 specific overgo probe was radiolabeled and hybridized to the membrane which was subsequently washed under high stringency conditions.

B.

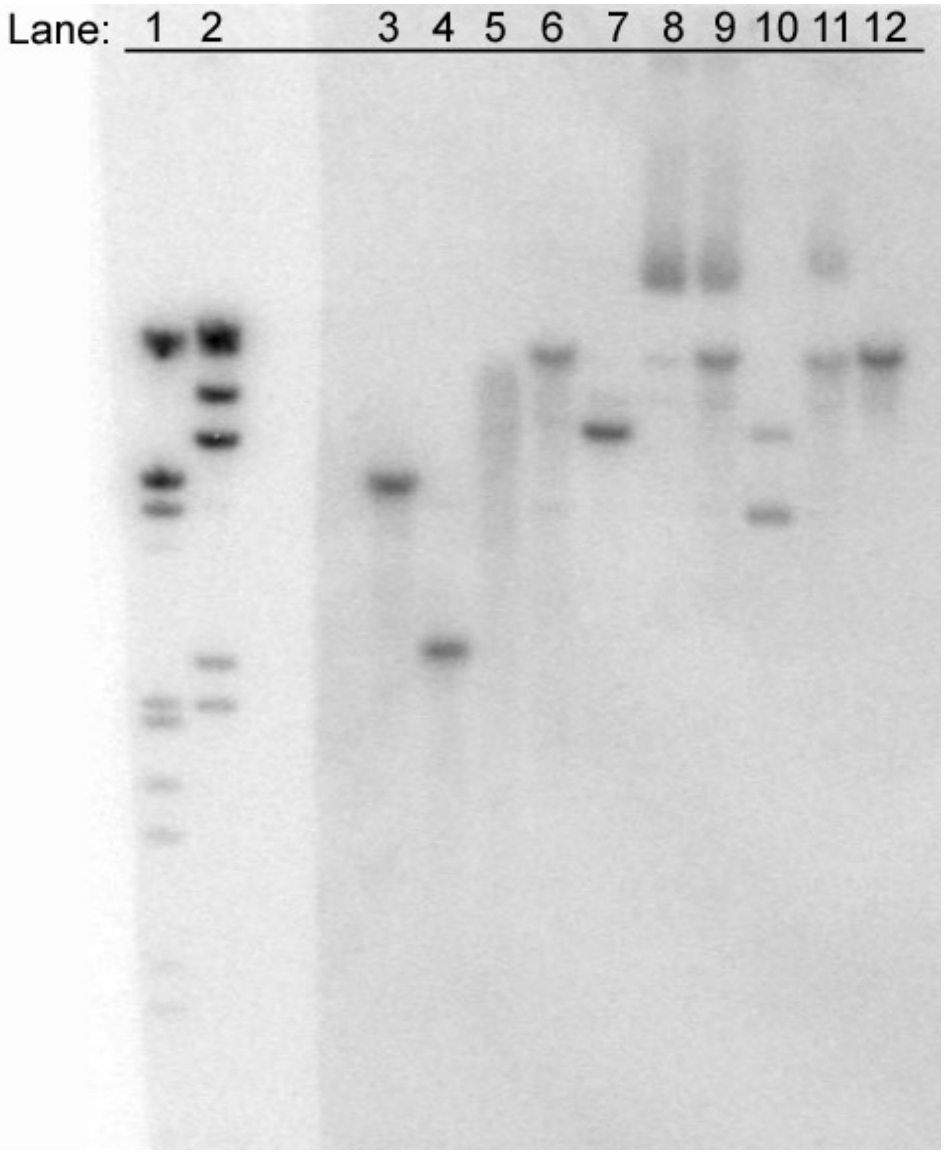

FIG 6.8 (Continued)

C.

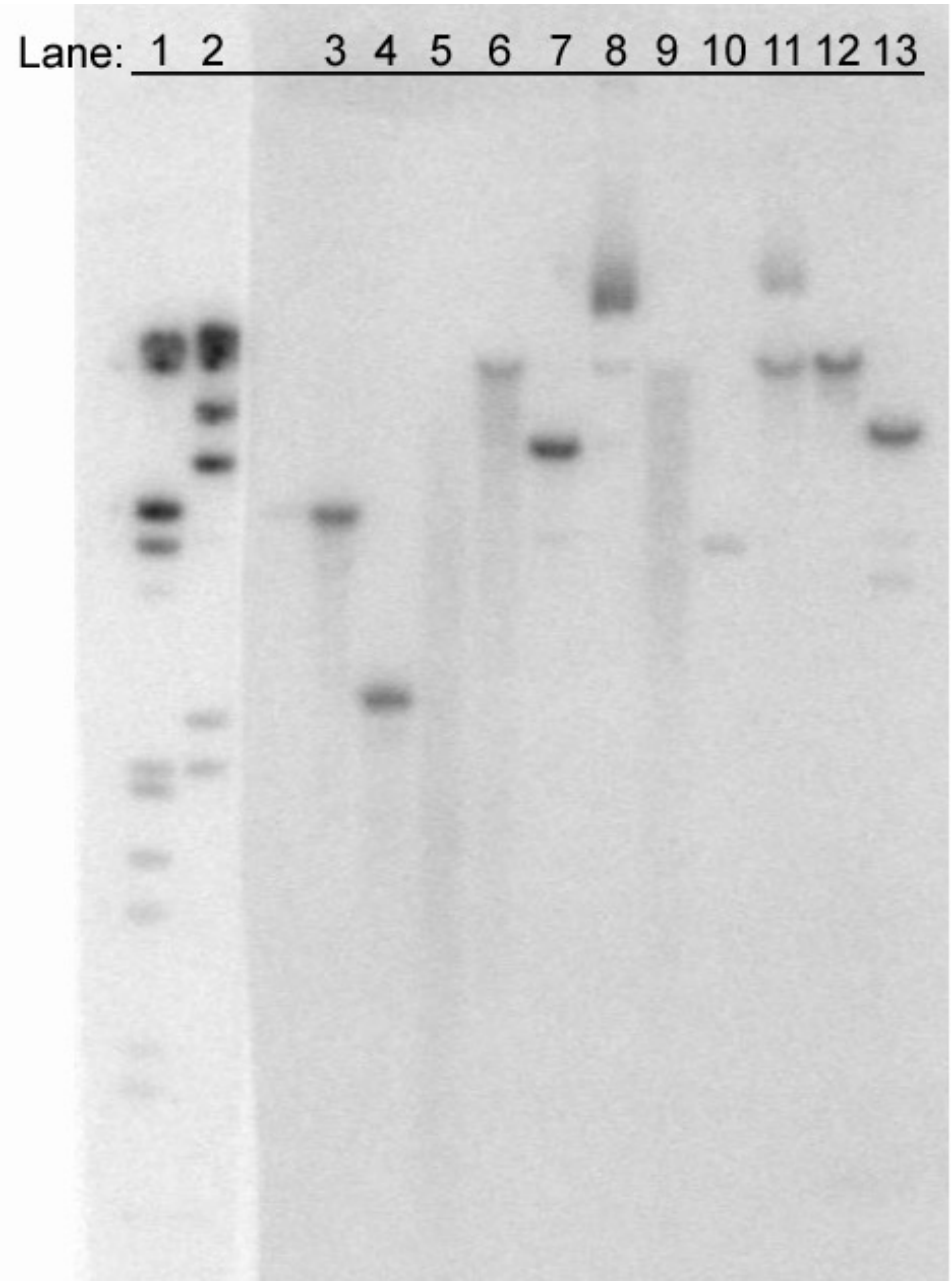

FIG 6.8 (Continued)

The complex nature of the 5'-region along with the total size of the PRLR genes described to date suggests that the ovine PRLR gene would be equally complex [145, 150, 151, 154, 158, 159]. The mouse, rat and human PRLR genes range from 168 to 145 kb in length and possess four to six first exons and promoters [145, 150, 151, 154, 158, 159]. Only one of these first exons, $E1_3$, is conserved throughout the three species described to date [145, 152, 158]. The expression of $E1_3$ has been shown to controlled by the transcription factors C/EBPβ resulting in an ubiquitous pattern of expression [152, 159]. This first exon, along with a probable steroid responsive PRLR mRNA, should have been detectable by 5'-RACE as it was the method used to clone the PRLR gene in other species. The 5'-RACE product did contain exon 2 and 3 as expected, but it only contained 48nt 5' of exon 2. Overgo probes were designed using the 5'-RACE products as a template and used to screen the ovine genomic and Day 14 pregnant cDNA libraries. Two clones recovered with the exon 2 overgo probe from the genomic ovine library did not contain enough 5' of exon 2 to include any exon 1. Screening of the ovine cDNA library was expected to yield a full-length PRLR mRNA; however, the failure to isolate a positive clone from the cDNA library may be due to the low amount of glandular epithelium that expresses PRLR mRNA in the day 14 pregnant ovine endometrium [18].

PRLR exon 2 is highly conserved across species. This is again seen in the sheep as the ovine exon 2 has 82% homology to human exon 2. Evaluation of the bovine genome and sequences not yet integrated has yielded several contigs that contain portions of the PRLR gene or the 5'-RACE products. A contig of approximately 62kb

(NW_621253) was found to contain exons 3 through 10. Unfortunately, no region homologous to exon 2 was found. Several contigs that are not yet integrated into the bovine genome build were found to be homologous to exon 2. One contig (ti# 51287359) contained a region 95% homologous to the 47 nt 5' region of the 5'-RACE clone. This 970 nt contig was used to search human expressed sequence tags (ESTs). Two human ESTs were identified (AI971975, and AA398543). These results suggest that as the bovine genome sequence is refined, it can be utilized to elucidate the structure of the ovine PRLR as many genes share a high degree of homology between the two species.

CHAPTER VII

CONCLUSIONS

Endometrial glands are essential for successful reproduction in all mammals studied to date. However, little is known of the mechanisms that regulate their development. Studies in other mammals have implicated E2-17β, ERα, PRL and PRLR as factors that mediate this critical developmental process. The current studies indicate that estrogens are detrimental to the uterine adenogenesis, but ERα, PRL and PRLR, as well as uterine and ovarian factors, including follistatin, activins, and inhibin, are required for normal glandular development (Fig 7.1).

Available evidence strongly supports the hypothesis that the functional capacity of the adult uterus is defined, to a significant extent, by developmental events associated with 'programming' of uterine tissues during prenatal and postnatal life [41, 70, 80, 81]. In all studied mammals, endometrial gland morphogenesis is a uniquely or primarily postnatal event. The timing of these developmental events varies among species and is subject to differences in uterine maturity at birth, e.g. gestation length, and perhaps the interval between birth and puberty [3]. For instance, postnatal development of the rodent uterus after birth begins with differentiation of the mesenchyme into endometrial stroma and myometrium, whereas the uterine mesenchyme in domestic animals and humans is already differentiated into endometrial stroma and myometrium at birth. Morphogenetic events common to postnatal development of uteri include: (1) organization and stratification of endometrial stroma; (2) differentiation and growth of the myometrium; and (3) coordinated development of the endometrial glands [3, 41, 79].

In humans, endometrial gland morphogenesis occurs with growth of the uterine lining during every menstrual cycle increasing the opportunities for aberrant development and alterations in uterine function. Disruption of this critical developmental process could be detrimental to subsequent pregnancies as seen in other species.

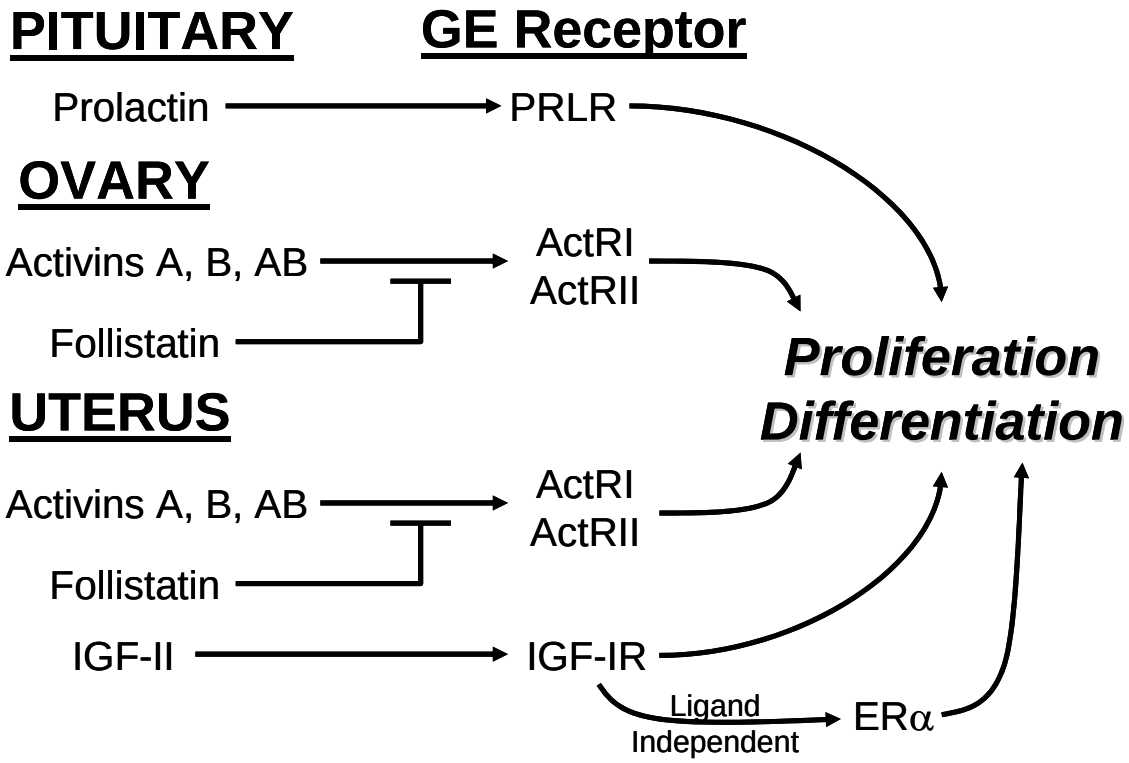

FIG 7.1. Working hypothesis of factors regulating uterine gland morphogenesis. Factors that influence uterine gland development may be produced by the pituitary gland (PRL), the ovary (activins and follistatin), or in the uterus itself (activins, follistatin and IGF-II). They are able to bind to their respective receptors (PRLR, ActRI, ActRII, and IGF-IR) in the luminal and glandular epithelia to regulate uterine adenogenesis. Follistatin inhibits the activation of ActRI and ActRII by binding activins and blocking their ability to bind theie receptors. Additionally, activated IGF-IR can activate ERα in a ligand-independent manner to influence endometrial gland development. Legend: PRL, prolactin; PRLR, prolactin receptor; ActRI, activin receptor-I; ActRII, activin receptor-II; IGF-II, insulin-like growth factor-II; IGF-IR, insulin-like growth factor receptor-I; ERα, estrogen receptor-alpha.

In the neonatal ewe, uterine development involves differentiation of the endometrial GE from the LE, specification of intercaruncular stroma, development of

endometrial folds and, to a lesser extent, growth of the aglandular caruncular areas and the myometrium [14, 15]. Endometrial adenogenesis in the ewe begins between PND 1 and 7 when shallow epithelial invaginations appear along the LE in presumptive intercaruncular areas. Between PND 7 and 14, the nascent GE buds proliferate into the stroma and form tubules or ducts that begin to coil and branch at the tips by PND 21. After PND 21, uterine adenogenesis primarily involves branching morphogenesis of tubular and coiled endometrial glands in the lower stroma (e.g. stratum spongiosum) adjacent to the inner circular layer of the myometrium. By PND 56, uterine morphogenesis is essentially complete, as the aglandular caruncular and glandular intercaruncular endometrial areas appear histoarchitecturally similar to that of the adult uterus [14]. Final maturation and growth of the ovine uterus does not occur until puberty [16].

Postnatal uterine development is accompanied by expression of ERα in both the nascent and developing GE and endometrial stroma in rodents, pigs, and sheep [14, 19-23]. In the UGKO ewe, the absence of ERα in the epithelium on PND 28 as a result of progestin treatment suggested a similar requirement for epithelial ERα expression in sheep [11]. In the present study, treatment of neonatal ewes with EM-800, an antagonist of ERα and ERβ, did not affect the initial stage of gland genesis between birth and PND14 [Chapter III]; however, EM-800 retarded the coiling and branching of the endometrial glands between PND 14 and PND 56 and prevented the increase in the number of ductal gland invaginations during this time [Chapter III]. These results suggest that ERα plays a role in the branching and coiling morphogenesis, but not in the

initial stages of gland tubulogenesis. Similarly, inhibition of ERα activation by ICI 182,870 in neonatal rats during the normal period of gland development (PND 10 to PND 14) had no effect on endometrial adenogenesis [112]. This is in contrast to pigs in which ICI 182,870 inhibited early endometrial gland development on PND 7 and PND 14 [24]. The activation of ERα appears to be ligand independent rather than ligand dependent as inhibition of estrogen synthesis with CGS 20267, an aromatase inhibitor, did not affect uterine gland morphogenesis [Chapter III]. Indeed, treatment of neonatal ewes with EV ablated adenogenesis and caused aberrant expression of growth factors, IGF-I and IGF-II [Chapter III], known to activate ERα in a ligand independent manner [171].

The effects of EV in the present study were similar to those observed in rodents but opposite those reported for pigs. The same dose of EV administered to gilts from birth to PND 6 or PND 13 increased uterine weight and induced precocious development of endometrial glands [24, 161]. In rats, administration of estrogens during glandular development induced a dose related delay in the onset of gland differentiation [84]. Similarly, administration of tamoxifen to neonatal rats on PNDs 1-5 or PNDs 10-14 elicited a dose related inhibition of uterine gland genesis [172]. EV treatment of neonatal ewes inhibited uterine adenogenesis and induced LE hypertrophy in the neonatal ewe [Chapter III] similar to results in mice and rats [112, 114]. This hypertrophic state of the LE may have prevented invagination of the GE physically, as a consequence of alterations in cell shape and associated changes in cell-cell, and cell-extracellular matrix relationships that would otherwise support this process [177, 178].

The antiadenogenic effect of EV treatment may also have been due to changes in expression patterns of growth factors and binding proteins in the stroma as aberrant spatial and temporal patterns of expression of both IGF-I and IGF-II were seen in the EV treated uteri [Chapter III]. Exogenous estrogens have also been shown to suppress the expression of IGF binding protein-3 (IGFBP-3) in ovine stromal cells [232]. The ability of IGFBP-3 to interact with IGFs and cell membranes makes it a potent modulator of IGF action [233]. Interestingly, this binding protein is able to inhibit cell growth independent of the IGF receptors [234]. Therefore, the reduction in IGFBP-3 expression in the neonatal ewe may have contributed to the hypertrophic state of the LE in response to EV treatment.

Similar results were seen when neonatal ewes were exposed to estradiol-benzoate (EB) during key developmental periods: PND 14-27 (period one) or PND 42-55 (period two) [232]. Low doses of EB (0 μg, 0.01 μg, and 0.1 μg) did not affect glandular development, but high doses (1 μg, and 10 μg) decreased the total number of glands present in a cross section as was seen in the present study [232]. The antiadenogenic effect of EB during these time periods was accompanied by a hypertrophic response and a reduction in ERα expression which was most pronounced in the GE [232]. Furthermore, expression of growth factors and their receptors were altered [232]. Collectively, these results support the hypothesis that neonatal exposure to estradiol inhibits normal endometrial gland development by inducing uterine hypertrophy and altering expression of many genes including ERα and growth factor networks which disrupts epithelial-mesenchymal interactions that regulate glandular development. The

mechanisms of estradiol inhibition of uterine adenogenesis as well as the long term effects of neonatal exposure to estradiol on adult uterine function and reproductive performance need to be investigated. Additionally, inhibition of ERα expression immediately after birth would elucidate the potential role of ERα in the budding of the GE from the LE, separating the receptor's function from that of estradiol-17β.

Studies of several species revealed that uterine development and endometrial adenogenesis can proceed normally in the absence of the ovary and, by default, ovarian steroids for varying periods of time during early postnatal life. In the prepubertal ewe, the ovary contains growing and vesicular follicles at birth that decline to PND 14, increase and peak in number on PND 28, remain high from PND 42 to PND 56, and decline thereafter [26, 27]. These changes in ovarian follicles correlate with the ontogeny of endometrial gland development in the ewe lamb [14]; however, ovariectomy of the ewe at birth did not affect uterine wet weight [27] or the initial stages of endometrial gland tubulogenesis [28] on PND 14, but affected uterine growth after PND 14 [180]. Postnatal uterine growth and endometrial adenogenesis are ovary- and steroid-independent in rodents [30-32] and pigs [23]. In the neonatal gilt, ovariectomy at birth inhibits uterine growth after PND 56 but does not affect genesis of endometrial glands or related endometrial morphogenetic events before PND 120 [23]. The number of superficial ductal invaginations of the GE from the LE and the density of endometrial glands in the stratum compactum area of the stroma on PND 56 were not affected by ovariectomy on PND 7 [Chapter IV]; however, the total number of endometrial glands in the uterine wall and the density of the endometrial glands in the stratum spongiosum

area of the stroma were reduced in uteri from ovariectomized ewes [Chapter IV]. These results indicate that an ovarian-derived factor(s) regulates, in part, the coiling and branching morphogenetic stage of endometrial gland development between PND 14 and PND 56. Collectively, available results indicate that the precise role of an ovarian factor(s) in uterine growth and endometrial adenogenesis is species-specific. Results presented here indicate that postnatal uterine growth and endometrial adenogenesis are estrogen-independent from birth to PND 56, although coiling and branching morphogenesis after PND 14 is, in part, dependent on activated ERα [Chapter III]. Additionally, circulating levels of estradiol as well as expression of ERα and PR were not different between ovariectomized and control ewes [Chapter IV]. Therefore, the effects of ovariectomy on uterine growth and endometrial adenogenesis cannot be attributed to alterations in either circulating estradiol and/or the uterine ERα system.

The ovarian factor(s) that regulates uterine growth and endometrial gland development is not known, but it could be inhibin, follistatin, or activins. Follistatin, activins, and inhibins regulate growth and differentiation in many branched epitheliomesenchymal organs via autocrine, paracrine, and perhaps, endocrine mechanisms [182-187, 201]. In general, exogenous activin inhibits gland development, whereas follistatin counteracts the inhibitory effects of activins by binding to the individual β subunits and preventing activin receptor (ActR) activation [182, 188, 189, 191, 192, 201]. Inhibin α subunit, β subunit, and follistatin are expressed in the growing and antral follicles of the neonatal ovine ovary and uterus [181, 197, 198]. Available evidence supports the hypothesis that follistatin and activins from the ovary act on the

uterus to regulate, in part, coiling and branching morphogenetic development as well as overall uterine growth. This hypothesis is supported by findings in the present study that the expression of specific components of the activin-follistatin system in the neonatal ovine uterus was affected by ovariectomy and could be correlated with reduced endometrial gland development [Chapter IV]. Indeed, marked reduction in expression of follistatin, βA subunit, ActRIA, and ActRII genes and an increase in βB subunit expression were observed in the uterus of ovariectomized ewes [Chapter IV]. It is tempting to speculate that the coordinate activities of the activin-follistatin system in the ovary and uterus may be important in prolific breeds of ewes that possess an intrinsically high ovulation rate as well as an enhanced uterine capacity to maintain large litters [207]. Future experiments should be directed toward understanding the mechanistic aspects of the novel finding that an ovarian endocrine factor includes a member of the activin-follistatin system that may act in concert with the autocrine-paracrine effects of the uterine activin-follistatin system to regulate coiling and branching morphogenesis of the endometrial glands during postnatal development of the ovine uterus.

Previous results suggest that PRL and PRLR may also play roles in endometrial adenogenesis in the neonatal ovine uterus [14]. Data presented here as well as previous data showed circulating levels of PRL are high on PND 1, peak on PND 14, and decline slightly to PND 56 [14]. These temporal changes in circulating levels of PRL parallel the ontogeny of endometrial glands in the developing intercaruncular endometrium of the uterine wall [14]. During this time, expression of short and long forms of the PRLR is restricted to the nascent endometrial glands [14]. Expression of PRLR is also

restricted to the GE in the adult ovine uterus [18]. Furthermore, intrauterine administration of placental lactogen, a PRL-like hormone that signals through PRLR [142], stimulates proliferation of endometrial glands in the adult ewe and, in particular, the coiled and branched glands in the stratum spongiosum [67]. Results presented here support the hypothesis that PRL acts directly on the endometrial GE that express the PRLR and regulates coiling and branching morphogenesis during postnatal development of the ovine uterus. Treatment of the neonatal lamb with bromocryptine induced hypoprolactinemia resulting in decreased endometrial gland number and density on PND 56 [Chapter V]. Uteri of bromocryptine treated ewes contained lower numbers of superficial ductal gland invaginations as well as coiled and branched endometrial glands in the endometrial stratum spongiosum near the myometrium [Chapter V]. Conversely, hyperprolactinemia induced by treatment with roPRL from birth increased endometrial gland number on PND 14 and density in the stratum spongiosum, but not the stratum compactum, in ewes on PND 56 [Chapter V]. Interestingly, after the budded glands elongate to a more tubular form and begin coiling and branching morphogenesis by PND 21 [14], the ductal GE loses PRLR expression, thereby preventing it from responding to PRL. These temporal and spatial changes in PRLR mRNA expression are likely to be responsible for the differential effects of hyperprolactinemia on endometrial adenogenesis on PND 14 as compared with PND 56. The increase in endometrial and myometrial thickness by roPRL treatment on PND56 may be due to epithelial-mesenchymal interactions in the developing uterus. Endometrial epithelium has been shown to affect myometrial organization and growth in the rodent uterus [215].

Similarly, ablating uterine gland development by neonatal treatment with either progestins or EV reduces endometrial and myometrial thickness [11]. These results suggest that the development of the endometrial glands is associated with endometrial and myometrial growth during as a result of epithelial-mesenchymal interactions. Additionally, PRL may be used to enhance uterine development in the neonatal ewe resulting in an increase in uterine capacity in the adult. To test this hypothesis, the effects of roPRL treatment on adult reproductive performance should be determined.

Biological responses to activation of PRLR by PRL include activation of JAK2 and STATs 1, 3, and 5 [216, 217]. Activation of the JAK2/STAT 5 cascade by PRL probably represents the hallmark of PRL signalling. PRL and STAT 5a are required for alveolar development and functional development of the mammary gland epithelium during pregnancy [219, 221, 222]. The high levels of expression of STATs 1 and 5 in the GE along with the induction of phosphorylation of these transcription factors in response to PRL treatment suggest PRL signalling via the PRLR and STAT 5 may be critical for endometrial adenogenesis in the uterus during the neonatal period [Chapter V]. Three members of the MAPK family were also phosphorylated in endometrial explants after treatment with PRL: ERK 1, ERK2, and JNK/SAPK [Chapter V]. Recently, PRL signalling in the human endometrial glands was shown to involve activation of ERK 1 and ERK 2 [229]. High levels of phosphorylated ERK 1 and ERK 2 have also been described in the nascent and proliferating endometrial glands in the neonatal ovine uterus [15]. In bovine mammary gland epithelial cells, PRL stimulation of cell proliferation involves activation of JNK/SAPK and an increase in c-Jun content

of the activator protein 1 transcriptional complex that leads to increased gene transactivation [228]. Collectively, these results indicate that PRL influences endometrial gland morphogenesis by signalling through several pathways including STATs 1 and 5, ERK 1 and 2 MAPKs, and JNK/SAPK.

The GE specific nature of PRLR expression in the uterus suggests that transcription of the PRLR gene is activated when the GE differentiates and buds from the LE. Therefore, transcription factors that regulate PRLR expression may be key regulators of GE differentiation. To date the promoter region of ovine PRLR has not been cloned and characterized. The PRLR gene possesses a complex 5' genomic structure made up of multiple promoters and non-coding first exons. These alternative first exons are differentially expressed depending on tissue type and developmental stage [149-153]. Exons 2 and 3 are highly homologous among species. The mouse, rat, and human PRLR genes range from 168 to 145 kb in length and possess four to six first exons and promoters [145, 150, 151, 154, 158, 159]. The single clone that was isolated from screening an genomic ovine library using an ovine PRLR cDNA (AF041257) as a probe contained a region homologous to human exon 3 but not exons 1 or 2 [Chapter VI]. Further analysis of the ovine PRLR cDNA used for a probe revealed that it did not contain a 5'-untranslated region homologous to that found in other species. 5'-RACE products produced from PND 28 and PND 56 uterus were 99% homologous to each other and contain regions homologous to human exon 2 [Chapter VI]. This is the first time PRLR exon 2 has been described in the sheep. A conserved exon 1, $E1_3$, and a probable steroid responsive PRLR should be detectable by 5'-RACE as it was the

method used to clone the PRLR gene in other species; however, no identifiable exon 1 was isolated [Chapter VI]. Overgo probes designed against exon 2 and a 48 nt long region 5' of exon 2 did not allow isolation of PRLR containing clones from either the genomic library or a cDNA library derived from Day 14 pregnant ovine endometrium [Chapter VI]. Analysis of the bovine genome and sequences that have not been yet been integrated revealed several contigs that contain regions of the PRLR including contigs that contain exon 2 or the 47 nt region of the 5'-RACE clones. These results indicate that as the bovine genome sequence is refined, it can be utilized to elucidate the structure of the ovine PRLR as many genes share a high degree of homology between the sheep and cattle.

The process of uterine morphogenesis is governed by a variety of hormonal, cellular, and molecular mechanisms, many of which remain to be defined. Due to their critical role in reproduction, it is important to understand the mechanisms regulating endometrial gland development. In humans, endometrial gland morphogenesis occurs with every menstrual cycle, which increases the opportunity for aberrant formation and alteration in function. The hormonal regimens used in assisted reproductive technologies may compromise the ability of the uterus to support a subsequent pregnancy. Additionally, enhancing endometrial adenogenesis in livestock species may result in better reproductive performance. Results presented here have established roles for ERα, PRL, PRLR, and ovarian factors in regulation of endometrial adenogenesis. Further, results of the present studies suggested these ovarian factors include activins, inhibins, and follistatin (Fig 7.1). Future studies should focus on elucidating the

mechanisms by which these factors, and others yet to be described act in an integrated manner to influence endometrial gland development. Experiments are being undertaken to disrupt the expression or block mRNA translation of specific genes to determine their effects in the neonatal ovine uterine gland development.

REFERENCES

1. Bazer FW. Uterine protein secretions: Relationship to development of the conceptus. J Anim Sci 1975; 41: 1376-1382.

2. Carson DD, Bagchi I, Dey SK, Enders AC, Fazleabas AT, Lessey BA, Yoshinaga K. Embryo implantation. Dev Biol 2000; 223: 217-237.

3. Gray CA, Bartol FF, Tarleton BJ, Wiley AA, Johnson GA, Bazer FW, Spencer TE. Developmental biology of uterine glands. Biol Reprod 2001; 65: 1311-1323.

4. Amoroso EC. Placentation. In: Parkes AS (ed.) Marshall's Physiology of Reproduction, vol. 2. Boston: Little Brown and Company; 1952: 127-311.

5. Bazer FW, First NL. Pregnancy and parturition. J Anim Sci 1983; 57 Suppl 2: 425-460.

6. Roberts RM, Bazer FW. The functions of uterine secretions. J Reprod Fertil 1988; 82: 875-892.

7. Simmen RC, Simmen FA. Regulation of uterine and conceptus secretory activity in the pig. J Reprod Fert Suppl 1990; 40: 279-292.

8. Martal J, Chene N, Camous S, Huynh L, Lantier F, Hermier P, L'Haridon R, Charpigny G, Charlier M, Chaouat G. Recent developments and potentialities for reducing embryo mortality in ruminants: the role of IFN-tau and other cytokines in early pregnancy. Reprod Fertil Dev 1997; 9: 355-380.

9. Burton GJ, Watson AL, Hempstock J, Skepper JN, Jauniaux E. Uterine glands provide histiotrophic nutrition for the human fetus during the first trimester of pregnancy. J Clin Endocrinol Metab 2002; 87: 2954-2959.

10. Bartol FF, Wiley AA, Coleman DA, Wolfe DF, Riddell MG. Ovine uterine morphogenesis: effects of age and progestin administration and withdrawal on neonatal endometrial development and DNA synthesis. J Anim Sci 1988; 66: 3000-3009.

11. Gray CA, Taylor KM, Bazer FW, Spencer TE. Mechanisms regulating norgestomet inhibition of endometrial gland morphogenesis in the neonatal ovine uterus. Mol Reprod Dev 2000; 57: 67-78.

12. Gray CA, Taylor KM, Ramsey WS, Hill JR, Bazer FW, Bartol FF, Spencer TE. Endometrial glands are required for preimplantation conceptus elongation and survival. Biol Reprod 2001; 64: 1608-1613.

13. Wiley AA, Bartol FF, Barron DH. Histogenesis of the ovine uterus. J Anim Sci 1987; 64: 1262-1269.

14. Taylor KM, Gray CA, Joyce MM, Stewart MD, Bazer FW, Spencer TE. Neonatal ovine uterine development involves alterations in expression of receptors for estrogen, progesterone, and prolactin. Biol Reprod 2000; 63: 1192-1204.

15. Taylor KM, Chen C, Gray CA, Bazer FW, Spencer TE. Expression of messenger ribonucleic acids for fibroblast growth factors 7 and 10, hepatocyte growth factor, and insulin-like growth factors and their receptors in the neonatal ovine uterus. Biol Reprod 2001; 64: 1236-1246.

16. Kennedy JP, Worthington CA, Cole ER. The post-natal development of the ovary and uterus of the Merino lamb. J Reprod Fertil 1974; 36: 275-282.

17. Wimsatt WA. New Histological Observations on the Placenta of the Sheep. Am J Anat 1950; 87: 391-436.

18. Stewart MD, Johnson GA, Gray CA, Burghardt RC, Schuler LA, Joyce MM, Bazer FW, Spencer TE. Prolactin receptor and uterine milk protein expression in the ovine endometrium during the estrous cycle and pregnancy. Biol Reprod 2000; 62: 1779-1789.

19. Fishman RB, Branham WS, Streck RD, Sheehan DM. Ontogeny of estrogen receptor messenger ribonucleic acid expression in the postnatal rat uterus. Biol Reprod 1996; 55: 1221-1230.

20. Korach KS, Horigome T, Tomooka Y, Yamashita S, Newbold RR, McLachlan JA. Immunodetection of estrogen receptor in epithelial and stromal tissues of neonatal mouse uterus. Proc Natl Acad Sci U S A 1988; 85: 3334-3337.

21. Yamashita S, Newbold RR, McLachlan JA, Korach KS. Developmental pattern of estrogen receptor expression in female mouse genital tracts. Endocrinology 1989; 125: 2888-2896.

22. Greco TL, Furlow JD, Duello TM, Gorski J. Immunodetection of estrogen receptors in fetal and neonatal female mouse reproductive tracts. Endocrinology 1991; 129: 1326-1332.

23. Tarleton BJ, Wiley AA, Spencer TE, Moss AG, Bartol FF. Ovary-independent estrogen receptor expression in neonatal porcine endometrium. Biol Reprod 1998; 58: 1009-1019.

24. Tarleton BJ, Wiley AA, Bartol FF. Endometrial development and adenogenesis in the neonatal pig: effects of estradiol valerate and the antiestrogen ICI 182,780. Biol Reprod 1999; 61: 253-263.

25. Smith CL. Cross-talk between peptide growth factor and estrogen receptor signaling pathways. Biol Reprod 1998; 58: 627-632.

26. Tassell R, Chamley WA, Kennedy JP. Gonadotrophin levels and ovarian development in the neonatal ewe lamb. Aust J Biol Sci 1978; 31: 267-273.

27. Foster DL, Cook B, Nalbandov AV. Regulation of luteinizing hormone (LH) in the fetal and neonatal lamb: effect of castration during the early postnatal period on levels of LHin sera and pituitaries of neonatal lambs. Biol Reprod 1978; 6: 253-257.

28. Bartol FF, Wiley AA, Goodlett DR. Ovine uterine morphogenesis: histochemical aspects of endometrial development in the fetus and neonate. J Anim Sci 1988; 66: 1303-1313.

29. Leifer RW, Foster DL, Dziuk PJ. Levels of LH in the sera and pituitaries of female lambs following ovariectomy and administration of estrogen. Endocrinology 1972; 90: 981-985.

30. Ogasawara Y, Okamoto S, Kitamura Y, Matsumoto K. Proliferative pattern of uterine cells from birth to adulthood in intact, neonatally castrated, and/or adrenalectomized mice, assayed by incorporation of [125I]iododeoxyuridine. Endocrinology 1983; 113: 582-587.

31. Bigsby RM, Cunha GR. Effects of progestins and glucocorticoids on deoxyribonucleic acid synthesis in the uterus of the neonatal mouse. Endocrinology 1985; 117: 2520-2526.

32. Branham WS, Sheehan DM. Ovarian and adrenal contributions to postnatal growth and differentiation of the rat uterus. Biol Reprod 1995; 53: 863-872.

33. Goffin V, Binart N, Touraine P, Kelly PA. Prolactin: the new biology of an old hormone. Annu Rev Physiol 2002; 64: 47-67.

34. Hooley RD, Campbell JJ, Findlay JK. The importance of prolactin for lactation in the ewe. J Endocrinol 1978; 79: 301-310.

35. Horseman ND, Zhao W, Montecino-Rodriguez E, Tanaka M, Nakashima K, Engle SJ, Smith F, Markoff E, Dorshkind K. Defective mammopoiesis, but normal hematopoiesis, in mice with a targeted disruption of the prolactin gene. EMBO J 1997; 16: 6926-6935.

36. Brisken C, Kaur S, Chavarria TE, Binart N, Sutherland RL, Weinberg RA, Kelly PA, Ormandy CJ. Prolactin controls mammary gland development via direct and indirect mechanisms. Dev Biol 1999; 210: 96-106.

37. Ebling FJ, Wood RI, Suttie JM, Adel TE, Foster DL. Prenatal photoperiod influences neonatal prolactin secretion in the sheep. Endocrinology 1989; 125: 384-391.

38. Chilton BS, Mani SK, Bullock DW. Servomechanism of prolactin and progesterone in regulating uterine gene expression. Mol Endocrinol 1988; 2: 1169-1175.

39. Young KH, Kraeling RR, Bazer FW. Effects of prolactin on conceptus survival and uterine secretory activity in pigs. J Reprod Fertil 1989; 86: 713-722.

40. Kelly MA, Rubinstein M, Asa SL, Zhang G, Saez C, Bunzow JR, Allen RG, Hnasko R, Ben-Jonathan N, Grandy DK, Low MJ. Pituitary lactotroph hyperplasia and chronic hyperprolactinemia in dopamine D2 receptor-deficient mice. Neuron 1997; 19: 103-113.

41. Bartol FF, Wiley AA, Floyd JG, Ott TL, Bazer FW, Gray CA, Spencer TE. Uterine differentiation as a foundation for subsequent fertility. J Reprod Fertil Suppl 1999; 54: 287-302.

42. Bartol FF. Uterus, nonhuman. In: Knobil E, Neill JD (eds.), Encyclopedia of Reproduction, vol. 4. San Diego: Academic Press; 1999: 950-960.

43. Grainger DA. Uterus, human. In: Knobil E, Neill JD (eds.), Encyclopedia of Reproduction, vol. 4. San Diego: Academic Press; 1999: 942-950.

44. Bagchi I, Li Q, Cheon YP. Role of steroid hormone-regulated genes in implantation. Ann NY Acad Sci 2001; 943.

45. Bhatt H, Brunet LJ, Stewart CL. Uterine expression of leukemia inhibitory factor coincides with the onset of blastocyst implantation. Proc Natl Acad Sci U S A 1991; 88: 11408-11412.

46. Yang ZM, Le SP, Chen DB, Yasukawa K, Harper MJK. Expression patterns of leukaemia inhibitory factor receptor (LIFR) and the gp130 receptor componenet in rabbit uterus during early pregnancy. J Reprod Fertil 1995; 103: 249-255.

47. Stewart CL, Kaspar P, Brunet LJ, Bhatt H, Gadi I, Kontgen F, Abbondanzo SJ. Blastocyst implantation depends on maternal expression of leukaemia inhibitory factor. Nature 1992; 359: 76-79.

48. Foster GV. Calcitonin (Thyrocalcitonin). N Engl J Med 1968; 279: 349-360.

49. Ding YQ, Zhu LJ, Bagchi MK, Bagchi I. Progesterone stimulates calcitonin gene expression in the uterus during implantation. Endocrinology 1994; 135: 2265-2274.

50. Zhu LJ, Bagchi MK, Bagchi IC. Attenuation of calcitonin gene expression in pregnant rat uterus leads to a block in embryonic implantation. Endocrinology 1998; 139: 330-339.

51. Cullinan EB, Abbondanzo SJ, Anderson PS, Pollard JW, Lessey BA, Stewart CL. Leukemia inhibitory factor (LIF) and LIF receptor expression in human endometrium suggests a potential autocrine/paracrine function in regulating embryo implantation. Proc Natl Acad Sci U S A 1996; 93: 3115-3120.

52. Senturk LM, Arici A. Leukemia inhibitory factor in human reproduction. Am J Reprod Immunol 1998; 39: 144-151.

53. Kumar A, Zhu LJ, Polihronis M, Cameron ST, Baird ST, Schatz F, Dua A, Ying YK, Bagchi MK, Bagchi I. Progesterone induces clcitonin gene expression in human endometrium withing the putative window of implantation. J Clin Endocrinol Metab 1998; 83: 4443-4450.

54. King GJ, Atkinson BA, Robertson HA. Development of the intercaruncular areas during early gestation and extablishment of the bovine placenta. J Reprod Fertil 1981; 61: 469-474.

55. Perry JS, Crombie PR. Ultrastructure of the uterine glands of the pig. J Anat 1982; 134 (Pt 2): 339-350.

56. Sinowatz F, Friess AE. Uterine glands of the pig during pregnancy. An ultrastructural and cytochemical study. Anat Embryol 1983; 166: 121-134.

57. van Niekerk CH, Allen WR. Early embryonic development in the horse. J Reprod Fertil Suppl 1975: 495-498.

58. Gerstenberg C, Allen WR. Development of the equine endometrial glands from fetal life to ovarian cycle. J Reprod Fertil Suppl 1999; 56: 317-326.

59. Samuel CA, Allen WR, Steven DH. Studies on the equine placenta. III. Ultrastructure of the uterine glands and the overlying trophoblast. J Reprod Fertil 1977; 51: 433-437.

60. Dantzer V. Scanning electron microscopy of exposed surfaces of the porcine placenta. Acta Anat (Basel) 1984; 118: 96-106.

61. Johnson GA, Burghardt RC, Bazer FW, Spencer TE. Osteopontin: roles in implantation and placentation. Biol Reprod 2003; 69: 1458-1471.

62. Johnson GA, Burghardt RC, Spencer TE, Newton GR, Ott TL, Bazer FW. Ovine osteopontin: II. Osteopontin and alpha(v)beta(3) integrin expression in the uterus and conceptus during the periimplantation period. Biol Reprod 1999; 61: 892-899.

63. Johnson GA, Burghardt RC, Joyce MM, Spencer TE, Bazer FW, Gray CA, Pfarrer C. Osteopontin is synthesized by uterine glands and a 45-kDa cleavage fragment is localized at the uterine-placental interface throughout ovine pregnancy. Biol Reprod 2003; 69: 92-98.

64. Rosen SD. Ligands for L-selectin: where and how many? Res Immunol 1993; 144: 699-703; discussion 754-662.

65. Spencer TE, Bartol FF, Bazer FW, Johnson GA, Joyce MM. Identification and characterization of glycosylation-dependent cell adhesion molecule 1-like protein expression in the ovine uterus. Biol Reprod 1999; 60: 241-250.

66. Ing NH, Francis H, McDonnell JJ, Amann JF, Roberts RM. Progesterone induction of the uterine milk proteins: major secretory proteins of sheep endometrium. Biol Reprod 1989; 41: 643-654.

67. Spencer TE, Gray A, Johnson GA, Taylor KM, Gertler A, Gootwine E, Ott TL, Bazer FW. Effects of recombinant ovine interferon tau, placental lactogen, and growth hormone on the ovine uterus. Biol Reprod 1999; 61: 1409-1418.

68. Cunha GR, Chung LW, Shannon JM, Taguchi O, Fujii H. Hormone-induced morphogenesis and growth: role of mesenchymal-epithelial interactions. Recent Prog Horm Res 1983; 39: 559-598.

69. Cunha GR. Stromal induction and specification of morphogenesis and cytodifferentiation of the epithelia of the Mullerian ducts and urogenital sinus during development of the uterus and vagina in mice. J Exp Zool 1976; 196: 361-370.

70. Kobayashi A, Behringer RR. Developmental genetics of the female reproductive tract in mammals. Nat Rev Genet 2003; 4: 969-980.

71. Cunha GR. The dual origin of vaginal epithelium. Am J Anat 1975; 143: 387-392.

72. Torrey TW, Feduccia A. The urogenital system. In: Torrey TW, Feduccia A (eds.), Morphogenesis of the Vertebrates. New York: Wiley Publishing; 1979: 365-401.

73. Capel B. The battle of the sexes. Mech Dev 2000; 92: 89-103.

74. Swain A, Lovell-Badge R. Mammalian sex determination: a molecular drama. Genes Dev 1999; 13: 755-767.

75. Jordan BK, Vilain E. Sry and the genetics of sex determination. Adv Exp Med Biol 2002; 511: 1-13; discussion 13-14.

76. Nef S, Parada LF. Hormones in male sexual development. Genes Dev 2000; 14: 3075-3086.

77. Mossman HA. Vertebrate Fetal Membranes. New Brunswick, NJ: Rutgers University Press; 1987.

78. Bartol FF, Wiley AA, Spencer TE, Vallet JL, Christenson RK. Early uterine development in pigs. J Reprod Fertil Suppl 1993; 48: 99-116.

79. Cunha GR. Epithelial-stromal interactions in development of the urogenital tract. Int Rev Cytol 1976; 47: 137-194.

80. Sassoon D. Wnt genes and endocrine disruption of the female reproductive tract: a genetic approach. Mol Cell Endocrinol 1999; 158: 1-5.

81. Mericskay M, Kitajewski J, Sassoon D. Wnt5a is required for proper epithelial-mesenchymal interactions in the uterus. Development 2004; 131: 2061-2072.

82. Cunha GR, Bigsby RM, Cooke PS, Sugimura Y. Stromal-epithelial interactions in adult organs. Cell Differ 1985; 17: 137-148.

83. Brody JR, Cunha GR. Histologic, morphometric, and immunocytochemical analysis of myometrial development in rats and mice: I. Normal development. Am J Anat 1989; 186: 1-20.

84. Branham WS, Sheehan DM, Zehr DR, Ridlon E, Nelson CJ. The postnatal ontogeny of rat uterine glands and age-related effects of 17 beta-estradiol. Endocrinology 1985; 117: 2229-2237.

85. Hu J, Gray CA, Spencer TE. Gene expression profiling of neonatal mouse uterine development. Biol Reprod 2004; 70: 1870-1876.

86. Spencer TE, Bartol FF, Wiley AA, Coleman DA, Wolfe DF. Neonatal porcine endometrial development involves coordinated changes in DNA synthesis, glycosaminoglycan distribution, and 3H-glucosamine labeling. Biol Reprod 1993; 48: 729-740.

87. Bal HS, Getty R. Postnatal growth of the swine uterus from birth to six months. Growth 1970; 34: 15-30.

88. Atkinson BA, King GJ, Amoroso EC. Development of the caruncular and intercaruncular regions in the bovine endometrium. Biol Reprod 1984; 30: 763-774.

89. Wooding FB. Current topic: the synepitheliochorial placenta of ruminants: binucleate cell fusions and hormone production. Placenta 1992; 13: 101-113.

90. Gray CA, Bazer FW, Spencer TE. Effects of neonatal progestin exposure on female reproductive tract structure and function in the adult ewe. Biol Reprod 2001; 64: 797-804.

91. Okulicz WC, Ace CI, Scarrell R. Zonal changes in proliferation in the rhesus endometrium during the late secretory phase and menses. Proc Soc Exp Biol Med 1997; 214: 132-138.

92. Padykula HA. Regeneration in the primate uterus: the role of stem cells. Ann N Y Acad Sci 1991; 622: 47-56.

93. Brenner RM, Slayden OD. Cyclic changes in the primate oviduct and endometrium. In: Knobil E, Neill JD (eds.), The Physiology of Reproduction. New York: Raven Press; 1994: 541-569.

94. Okulicz WC. Regeneration. In: Glasser SR, Aplin JD, Giudice LC, Tabibzadeh S (eds.), The Endometrium. London: Taylor and Francis Inc.; 2002: 110-120.

95. Chan RW, Schwab KE, Gargett CE. Clonogenicity of human endometrial epithelial and stromal cells. Biol Reprod 2004; 70: 1738-1750.

96. Gell JS. Mullerian anomalies. Semin Reprod Med 2003; 21: 375-388.

97. Song J. The Human Uterus: Morphogenesis and Embryological Basis for Cancer. Springfield, IL: Charles C. Thomas; 1964.

98. Valdes-Dapena MA. The development of the uterus in late fetal life, infancy, and childhood. In: Norris HJ, Hertig AT, Abell MR (eds.), The Uterus. Baltimore: Williams and Wilkins; 1973: 40-67.

99. Spencer TE, Carpenter KD, Hayashi K, Hu J. Uterine glands. In: Davies JA (ed.) Branching Morphogenesis. Georgetown, TX: Landes Biosciences; 2005.

100. Gray CA, Burghardt RC, Johnson GA, Bazer FW, Spencer TE. Evidence that absence of endometrial gland secretions in uterine gland knockout ewes compromises conceptus survival and elongation. Reproduction 2002; 124: 289-300.

101. Jost A, Vigier B, Prepin J, Perchellet JP. Studies on sex differentiation in mammals. Recent Prog Horm Res 1973; 29: 1-41.

102. Clark JH, Gorski J. Ontogeny of the estrogen receptor during early uterine development. Science 1970; 169: 76-78.

103. Dohler KD, Wuttke W. Changes with age in levels of serum gonadotropins, prolactin and gonadal steroids in prepubertal male and female rats. Endocrinology 1975; 97: 898-907.

104. Fisher CR, Graves KH, Parlow AF, Simpson ER. Characterization of mice deficient in aromatase (ArKO) because of targeted disruption of the cyp19 gene. Proc Natl Acad Sci U S A 1998; 95: 6965-6970.

105. Apter D. Serum steroids and pituitary hormones in female puberty: a partly longitudinal study. Clin Endocrinol (Oxf) 1980; 12: 107-120.

106. Lessey BA. Two pathways of progesterone action in the human endometrium: implications for implantation and contraception. Steroids 2003; 68: 809-815.

107. Hisaw FL, Hisaw FLJ. Action of estrogen and progesterone on the reproductive tract of lower primates. In: Young WC (ed.) Sex and Internal Secretions. Baltimore: Williams and Wilkins; 1961: 556-589.

108. Spencer TE, Johnson GA, Burghardt RC, Bazer FW. Progesterone and placental hormone actions on the uterus: insights from domestic animals. Biol Reprod 2004; 71(1): 2-10.

109. Dey SK, Lim H, Das SK, Reese J, Paria BC, Daikoku T, Wang H. Molecular cues to implantation. Endocr Rev 2004; 25: 341-373.

110. Lubahn DB, Moyer JS, Golding TS, Couse JF, Korach KS, Smithies O. Alteration of reproductive function but not prenatal sexual development after insertional disruption of the mouse estrogen receptor gene. Proc Natl Acad Sci USA 1993; 90: 11162-11166.

111. Krege JH, Hodgin JB, Couse JF, Enmark E, Warner M, Mahler JF, Sar M, Korach KS, Gustafsson J-A, Smithies O. Generation and reproductive phenotypes of mice lacking estrogen receptor beta. Proc Natl Acad Sci USA 1998; 95: 15677-15682.

112. Branham WS, Fishman R, Streck RD, Medlock KL, De George JJ, Sheehan DM. ICI 182,780 inhibits endogenous estrogen-dependent rat uterine growth and tamoxifen-induced developmental toxicity. Biol Reprod 1996; 54: 160-167.

113. Cooke PS, Buchanan DL, Lubahn DB, Cunha GR. Mechanism of estrogen action: lessons from the estrogen receptor-alpha knockout mouse. Biol Reprod 1998; 59: 470-475.

114. Cooke PS, Buchanan DL, Young P, Setiawan T, Brody J, Korach KS, Taylor J, Lubahn DB, Cunha GR. Stromal estrogen receptors mediate mitogenic effects of estradiol on uterine epithelium. Proc Natl Acad Sci U S A 1997; 94: 6535-6540.

115. Hall JM, Couse JF, Korach KS. The multifaceted mechanisms of estradiol and estrogen receptor signaling. J Biol Chem 2001; 276: 36869-36872.

116. Smith CL. Cross-talk between peptide growth factor and estrogen receptor signaling pathways. Biol Reprod 1998; 58: 627-632.

117. Ignar-Trowbridge DM, Pimentel M, Teng CT, Korach KS, McLachlan JA. Cross talk between peptide growth factor and estrogen receptor signaling systems. Environ Health Perspect 1995; 103 Suppl 7: 35-38.

118. Aronica SM, Katzenellenbogen BS. Stimulation of estrogen receptor-mediated transcription and alteration in the phosphorylation state of the rat uterine estrogen receptor by estrogen, cyclic adenosine monophosphate, and insulin-like growth factor-I. Mol Endocrinol 1993; 7: 743-752.

119. Cunha GR, Lung B. The importance of stroma in morphogenesis and functional activity of urogenital epithelium. In Vitro 1979; 15: 50-71.

120. Sato T, Wang G, Hardy MP, Kurita T, Cunha GR, Cooke PS. Role of systemic and local IGF-I in the effects of estrogen on growth and epithelial proliferation of mouse uterus. Endocrinology 2002; 143: 2673-2679.

121. Rubin JS, Bottaro DP, Chedid M, Miki T, Ron D, Cheon G, Taylor WG, Fortney E, Sakata H, Finch PW, et al. Keratinocyte growth factor. Cell Biol Int 1995; 19: 399-411.

122. Bellusci S, Grindley J, Emoto H, Itoh N, Hogan BL. Fibroblast growth factor 10 (FGF10) and branching morphogenesis in the embryonic mouse lung. Development 1997; 124: 4867-4878.

123. Weidner KM, Hartmann G, Sachs M, Birchmeier W. Properties and functions of scatter factor/hepatocyte growth factor and its receptor c-Met. Am J Respir Cell Mol Biol 1993; 8: 229-237.

124. Koji T, Chedid M, Rubin JS, Slayden OD, Csaky KG, Aaronson SA, Brenner RM. Progesterone-dependent expression of keratinocyte growth factor mRNA in stromal cells of the primate endometrium: keratinocyte growth factor as a progestomedin. J Cell Biol 1994; 125: 393-401.

125. Sugawara J, Fukaya T, Murakami T, Yoshida H, Yajima A. Hepatocyte growth factor stimulated proliferation, migration, and lumen formation of human endometrial epithelial cells in vitro. Biol Reprod 1997; 57: 936-942.

126. Giudice LC. Growth factors and growth modulators in human uterine endometrium: their potential relevance to reproductive medicine. Fertil Steril 1994; 61: 1-17.

127. Nayak NR, Giudice LC. Comparative biology of the IGF system in endometrium, decidua, and placenta, and clinical implications for foetal growth and implantation disorders. Placenta 2003; 24: 281-296.

128. Baker J, Hardy MP, Zhou J, Bondy C, Lupu F, Bellve AR, Efstratiadis A. Effects of an Igf1 gene null mutation on mouse reproduction. Mol Endocrinol 1996; 10: 903-918.

129. Giudice LC, Saleh W. Growth factors in reproduction. Trends Endocrinol Metab 1995; 6: 60-69.

130. Yeh J, Danehy FT, Osathanondh R, Villa-Komaroff L. mRNAs for insulin-like growth factor-II (IGF-II) and variant IGF-II are co-expressed in human fetal ovary and uterus. Mol Cell Endocrinol 1991; 80: 75-82.

131. Thiet MP, Osathanondh R, Yeh J. Localization and timing of appearance of insulin, insulin-like growth factor-I, and their receptors in the human fetal mullerian tract. Am J Obstet Gynecol 1994; 170: 152-156.

132. Gu Y, Branham WS, Sheehan DM, Webb PJ, Moland CL, Streck RD. Tissue-specific expression of messenger ribonucleic acids for insulin- like growth factors and insulin-like growth factor-binding proteins during perinatal development of the rat uterus. Biol Reprod 1999; 60: 1172-1182.

133. Sharpe PM, Ferguson MW. Mesenchymal influences on epithelial differentiation in developing systems. J Cell Sci Suppl 1988; 10: 195-230.

134. Cunha GR, Young P, Brody JR. Role of uterine epithelium in the development of myometrial smooth muscle cells. Biol Reprod 1989; 40: 861-871.

135. Kurita T, Cooke PS, Cunha GR. Epithelial-stromal tissue interaction in paramesonephric (Mullerian) epithelial differentiation. Dev Biol 2001; 240: 194-211.

136. Padykula HA, Coles LG, Okulicz WC, Rapaport SI, McCracken JA, King NW, Jr., Longcope C, Kaiserman-Abramof IR. The basalis of the primate endometrium: a bifunctional germinal compartment. Biol Reprod 1989; 40: 681-690.

137. Padykula HA, Coles LG, McCracken JA, King NW, Jr., Longcope C, Kaiserman-Abramof IR. A zonal pattern of cell proliferation and differentiation in the rhesus endometrium during the estrogen surge. Biol Reprod 1984; 31: 1103-1118.

138. Curry TE, Jr., Osteen KG. Cyclic changes in the matrix metalloproteinase system in the ovary and uterus. Biol Reprod 2001; 64: 1285-1296.

139. Nothnick WB. Disruption of the tissue inhibitor of metalloproteinase-1 gene in reproductive-age female mice is associated with estrous cycle stage-specific increases in stromelysin messenger RNA expression and activity. Biol Reprod 2001; 65: 1780-1788.

140. Hu J, Zhang X, Nothnick WB, Spencer TE. Matrix metalloproteinases and their tissue inhibitors in the developing neonatal mouse uterus. Biol Reprod 2004; 71: 1598-1604.

141. Horseman ND, Yu-Lee LY. Transcriptional regulation by the helix bundle peptide hormones: growth hormone, prolactin, and hematopoietic cytokines. Endocr Rev 1994; 15: 627-649.

142. Herman A, Bignon C, Daniel N, Grosclaude J, Gertler A, Djiane J. Functional heterodimerization of prolactin and growth hormone receptors by ovine placental lactogen. J Biol Chem 2000; 275: 6295-6301.

143. Hu ZZ, Meng J, Dufau ML. Isolation and characterization of two novel forms of the human prolactin receptor generated by alternative splicing of a newly identified exon 11. J Biol Chem 2001; 276: 41086-41094.

144. Kelly PA, Djiane J, Postel-Vinay MC, Edery M. The prolactin/growth hormone receptor super family. Endocr Rev 1991; 3: 235-251.

145. Ormandy CJ, Binart N, Helloco C, Kelly PA. Mouse prolactin receptor gene: genomic organization reveals alternative promoter usage and generation of isoforms via alternative 3'-exon splicing. DNA Cell Biol 1998; 17: 761-770.

146. Boutin JM, Edery M, Shirota M, Jolicoeur C, Lesueur L, Ali S, Gould D, Djiane J, Kelly PA. Identification of a cDNA encoding a long form of prolactin receptor in human hepatoma and breast cancer cells. Mol Endocrinol 1989; 3: 1455-1461.

147. Davis JA, Linzer DI. Expression of multiple forms of the prolactin receptor in mouse liver. Mol Endocrinol 1989; 3: 674-680.

148. Bole-Feysot C, Goffin V, Edery M, Binart N, Kelly PA. Prolactin (PRL) and its receptor: actions, signal transduction pathways and phenotypes observed in PRL receptor knockout mice. Endocr Rev 1998; 19: 225-268.

149. Schuler LA, Nagel RJ, Gao J, Horseman ND, Kessler MA. Prolactin receptor heterogeneity in bovine fetal and maternal tissues. Endocrinology 1997; 138: 3187-3194.

150. Tanaka M, Hayashida Y, Iguchi T, Nakao K, Suzuki M, Nakai N, Nakashima K. Identification of a novel first exon of prolactin receptor gene expression in the rat brain. Endocrinology 2002; 143: 2080-2084.

151. Hu ZZ, Zhuang L, Dufau ML. Multiple and tissue-specific promoter control of gonadal and non-gonadal prolactin receptor gene expression. J Biol Chem 1996; 271: 10242-10246.

152. Hu ZZ, Zhuang L, Meng J, Dufau ML. Transcriptional regulation of the generic promoter III of the rat prolactin receptor gene by C/EBPβ and Sp1. J Biol Chem 1998; 273: 26225-26235.

153. Moldrup A, Ormandy C, Nagano M, Murthy K, Banville D, Tronche F, Kelly PA. Differential promoter usage in prolactin receptor gene expression: hepatocyte nuclear factor 4 binds to and activates the promoter preferentially active in the liver. Mol Endocrinol 2005; 10: 661-671.

154. Hu ZZ, Zhuang L, Guan X, Meng J, Dufau ML. Steroidogenic factor-1 is an essential transcriptional activator for gonad-specific expression of promoter I of the rat prolactin receptor gene. J Biol Chem 1997; 272: 14263-14271.

155. Tanaka M, Yamamoto I, Hayahida Y, Nakao N, Ohkubo T, Wakita M, Nakashima K. Two novel first exons in the prolactin receptor gene are transcribed in a tissue-specific and sexual maturation-dependent manner to encode multiple 5'-truncated transcripts in the testis of the chicken. Biochim Biophys Acta 2000; 1491: 279-284.

156. Hu ZZ, Dufau ML. Multiple and differential regulation of ovarian prolactin receptor messenger RNAs and their expression. Biochem Biophys Res Commun 1991; 181: 219-225.

157. Barker CS, Bear SE, Keler T, Copeland NG, Gilbert DJ, Jenkins NA, Yeung RS, Tsichlis PN. Activation of the prolactin receptor gene by promoter insertion in a Moloney murine leukemia virus-induced rat thymoma. J Virol 1992; 66: 6763-6768.

158. Hu ZZ, Zhuang L, Meng J, Tsai-Morris CH, Dufau ML. Complex 5' genomic structure of the human prolactin receptor: multiple alternative exons 1 and promoter utilization. Endocrinology 2002; 143: 2139-2142.

159. Hu ZZ, Zhuang L, Meng J, Leondires MP, Dufau ML. The human prolactin receptor gene structure and alternative promoter utilization: the generic promoter hPIII and a novel human promoter hP_N. J Clin Endocrinol Metab 1999; 84: 1153-1156.

160. Tremblay A, Tremblay GB, Labrie C, Labrie F, Giguere V. EM-800, a novel antiestrogen, acts as a pure antagonist of the transcriptional functions of estrogen receptors alpha and beta. Endocrinology 1998; 139: 111-118.

161. Martel C, Labrie C, Belanger A, Gauthier S, Merand Y, Li X, Provencher L, Candas B, Labrie F. Comparison of the effects of the new orally active antiestrogen EM-800 with ICI 182 780 and toremifene on estrogen-sensitive parameters in the ovariectomized mouse. Endocrinology 1998; 139: 2486-2492.

162. Spencer TE, Wiley AA, Bartol FF. Neonatal age and period of estrogen exposure affect porcine uterine growth, morphogenesis, and protein synthesis. Biology of Reproduction 1993; 48: 741-751.

163. Albrecht ED, Aberdeen GW, Pepe GJ. The role of estrogen in the maintenance of primate pregnancy. Am J Obstet Gynecol 2000; 182: 432-438.

164. Spencer TE, Stagg AG, Joyce MM, Jenster G, Wood CG, Bazer FW, Wiley AA, Bartol FF. Discovery and characterization of endometrial epithelial messenger ribonucleic acids using the ovine uterine gland knockout model. Endocrinology 1999; 140: 4070-4080.

165. Spencer TE, Bazer FW. Temporal and spatial alterations in uterine estrogen receptor and progesterone receptor gene expression during the estrous cycle and early pregnancy in the ewe. Biol Reprod 1995; 53: 1527-1543.

166. Scott P, Kessler MA, Schuler LA. Molecular cloning of the bovine prolactin receptor and distribution of prolactin and growth hormone receptor transcripts in fetal and utero- placental tissues. Mol Cell Endocrinol 1992; 89: 47-58.

167. SAS. SAS User's Guide: Statistics version 6. Cary, NC: Statistical Analysis System Institute; 1990.

168. Waseem NH, Lane DP. Monoclonal antibody analysis of the proliferating cell nuclear antigen (PCNA). Structural conservation and the detection of a nucleolar form. J Cell Sci 1990; 96 (Pt 1): 121-129.

169. Zachos NC, Billiar RB, Albrecht ED, Pepe GJ. Developmental regulation of baboon fetal ovarian maturation by estrogen. Biol Reprod 2002; 67: 1148-1156.

170. Mitwally MF, Casper RF. Use of an aromatase inhibitor for induction of ovulation in patients with an inadequate response to clomiphene citrate. Fertil Steril 2001; 75: 305-309.

171. Ignar-Trowbridge DM, Pimentel M, Parker MG, McLachlan JA, Korach KS. Peptide growth factor cross-talk with the estrogen receptor requires the A/B domain and occurs independently of protein kinase C or estradiol. Endocrinology 1996; 137: 1735-1744.

172. Branham WS, Sheehan DM, Zehr DR, Medlock KL, Nelson CJ, Ridlon E. Inhibition of rat uterine gland genesis by tamoxifen. Endocrinology 1985; 117: 2238-2248.

173. Bazer FW, Spencer TE. Biology of progesterone action during pregnancy recognition and maintenance of pregnancy. Front Biosci 2002; 7: d1879-d1898.

174. Nogawa H, Morita K, Cardoso WV. Bud formation precedes the appearance of differential cell proliferation during branching morphogenesis of mouse lung epithelium in vitro. Dev Dyn 1998; 213: 228-235.

175. Mollard R, Dziadek M. A correlation between epithelial proliferation rates, basement membrane component localization patterns, and morphogenetic potential in the embryonic mouse lung. Am J Respir Cell Mol Biol 1998; 19: 71-82.

176. Spencer TE, Wiley AA, Bartol FF. Lectin binding sites as markers of neonatal porcine uterine development. J Histochem Cytochem 1992; 40: 1937-1942.

177. Werb Z, Chin JR. Extracellular matrix remodeling during morphogenesis. Ann N Y Acad Sci 1998; 857: 110-118.

178. Lelievre S, Weaver VM, Bissell MJ. Extracellular matrix signaling from the cellular membrane skeleton to the nuclear skeleton: a model of gene regulation. Recent Prog Horm Res 1996; 51: 417-432.

179. Kleinberg DL, Feldman M, Ruan W. IGF-I: an essential factor in terminal end bud formation and ductal morphogenesis. J Mammary Gland Biol Neoplasia 2000; 5: 7-17.

180. Liefer RW, Foster DL, Dziuk PJ. Levels of LH in the sera and pituitaries of female lambs following ovariectomy and administration of estrogen. Endocrinology 1972; 90: 981-985.

181. Hayashi K, Carpenter KD, Gray CA, Spencer TE. The activin-follistatin system in the neonatal ovine uterus. Biol Reprod 2003; 69: 843-850.

182. Cancilla B, Jarred RA, Wang H, Mellor SL, Cunha GR, Risbridger GP. Regulation of prostate branching morphogenesis by activin A and follistatin. Dev Biol 2001; 237: 145-158.

183. Liu QY, Niranjan B, Gomes P, Gomm JJ, Davies D, Coombes RC, Buluwela L. Inhibitory effects of activin on the growth and morpholgenesis of primary and transformed mammary epithelial cells. Cancer Res 1996; 56: 1155-1163.

184. Maldonado TS, Kadison AS, Crisera CA, Grau JB, Alkasab SL, Longaker MT, Gittes GK. Ontogeny of activin B and follistatin in developing embryonic mouse pancreas: implications for lineage selection. J Gastrointest Surg 2000; 4: 269-275.

185. Miralles F, Czernichow P, Scharfmann R. Follistatin regulates the relative proportions of endocrine versus exocrine tissue during pancreatic development. Development 1998; 125: 1017-1024.

186. Ritvos O, Tuuri T, Eramaa M, Sainio K, Hilden K, Saxen L, Gilbert SF. Activin disrupts epithelial branching morphogenesis in developing glandular organs of the mouse. Mech Dev 1995; 50: 229-245.

187. Tuuri T, Eramaa M, Hilden K, Ritvos O. The tissue distribution of activin beta A- and beta B-subunit and follistatin messenger ribonucleic acids suggests multiple sites of action for the activin-follistatin system during human development. J Clin Endocrinol Metab 1994; 78: 1521-1524.

188. Welt C, Sidis Y, Keutmann H, Schneyer A. Activins, inhibins, and follistatins: from endocrinology to signaling. A paradigm for the new millennium. Exp Biol Med (Maywood) 2002; 227: 724-752.

189. Ethier JF, Findlay JK. Roles of activin and its signal transduction mechanisms in reproductive tissues. Reproduction 2001; 121: 667-675.

190. Ball EM, Risbridger GP. Activins as regulators of branching morphogenesis. Dev Biol 2001; 238: 1-12.

191. Iemura S, Yamamoto TS, Takagi C, Uchiyama H, Natsume T, Shimasaki S, Sugino H, Ueno N. Direct binding of follistatin to a complex of bone-morphogenetic protein and its receptor inhibits ventral and epidermal cell fates in early Xenopus embryo. Proc Natl Acad Sci U S A 1998; 95: 9337-9342.

192. Xu J, McKeehan K, Matsuzaki K, McKeehan WL. Inhibin antagonizes inhibition of liver cell growth by activin by a dominant-negative mechanism. J Biol Chem 1995; 270: 6308-6313.

193. Phillips DJ, de Kretser DM. Follistatin: a multifunctional regulatory protein. Front Neuroendocrinol 1998; 19: 287-322.

194. Nakamura T, Takio K, Eto Y, Shibai H, Titani K, Sugino H. Activin-binding protein from rat ovary is follistatin. Science 1990; 247: 836-838.

195. De Winter JP, ten Dijke P, de Vries CJ, van Achterberg TA, Sugino H, de Waele P, Huylebroeck D, Verschueren K, J. vdE-vRA. Follistatin neutralizes activin bioactivity by inhibition of activin binding to its type II receptors. Mol Cell Endocrinol 1996; 116: 105-114.

196. McFarlane JR, Xia Y, O'Shea T, Hayward S, O'Connor AE, de Kretser DM. Follistatin concentrations in maternal and fetal fluids during oestrous cycle, gestation and parturition in Merino sheep. Reproduction 2002; 124: 259-265.

197. Braw-Tal R. Expression of mRNA for follistatin and inhibin/activin subunits during follicular growth and atresia. J Mol Endocrinol 1994; 13: 253-264.

198. Braw-Tal R, Yossefi S, Zenou A, Bor A. Differential expression pattern of inhibin alpha and betaA subunits in the ovaries of postnatal and prepubertal lambs. Reprod Fertil Dev 1997; 9: 825-832.

199. Braw-Tal R, Bor A, Gootwine E. Plasma immunoreactive inhibin and FSH in prepubertal Assaf and Booroola-Assaf ewe lambs. Anim Endocrinol 1993; 10.

200. Foster DL, Lemons JA, Jaffe RB, Niswender GD. Sequential patterns of circulating luteinizing hormone and follicle-stimulating hormone in female sheep from early postnatal life through the first estrous cycles. Endocrinology 1975; 97: 985-994.

201. Jones RL, Salamonsen LA, Findlay JK. Potential roles for endometrial inhibins, activins and follistatin during human embryo implantation and early pregnancy. Trends Endocrinol Metab 2002; 13: 144-150.

202. Vanttinen T, Kuulasmaa T, Liu J, Voutilainen R. Expression of activin/inhibin receptor and binding protein genes and regulation of activin/inhibin peptide secretion in human adrenocortical cells. J Clin Endocrinol Metab 2002; 87: 4257-4263.

203. Eramaa M, Hilden K, Tuuri T, Ritvos O. Regulation of inhibin/activin subunit messenger ribonucleic acids (mRNAs) by activin A and expression of activin receptor mRNAs in cultured human granulosa-luteal cells. Endocrinology 1995; 136: 4382-4389.

204. Di Simone N, Hall HA, Welt C, Schneyer AL. Activin regulates betaA-subunit and activin receptor messenger ribonucleic acid and cellular proliferation in activin-responsive testicular tumor cells. Endocrinology 1998; 139: 1147-1155.

205. Dalkin AC, Haisenleder DJ, Yasin M, Gilrain JT, Marshall JC. Pituitary activin receptor subtypes and follistatin gene expression in female rats: differential regulation by activin and follistatin. Endocrinology 1996; 137: 548-554.

206. Buzzard JJ, Farnworth PG, De Kretser DM, O'Connor AE, Wreford NG, Morrison JR. Proliferative phase sertoli cells display a developmentally regulated response to activin in vitro. Endocrinology 2003; 144: 474-483.

207. Fahmy MH. Prolific Sheep. Wallingford, Oxon, U. K.: CAB International; 1996.

208. Yu-Lee L. Stimulation of interferon regulatory factor-1 by prolactin. Lupus 2001; 10: 691-699.

209. Freeman ME, Kanyicska B, Lerant A, Nagy G. Prolactin: structure, function, and regulation of secretion. Physiol Rev 2000; 80: 1523-1631.

210. Leibovich H, Raver N, Herman A, Gregoraszczuk EL, Gootwine E, Gertler A. Large-scale preparation of recombinant ovine prolactin and determination of its in vitro and in vivo activity. Protein Expr Purif 2001; 22: 489-496.

211. Choi Y, Johnson GA, Burghardt RC, Berghman LR, Joyce MM, Taylor KM, Stewart MD, Bazer FW, Spencer TE. Interferon regulatory factor-two restricts expression of interferon- stimulated genes to the endometrial stroma and glandular epithelium of the ovine uterus. Biol Reprod 2001; 65: 1038-1049.

212. Kann G, Denamur R. Possible role of prolactin during the oestrous cycle and gestation in the ewe. J Reprod Fertil 1974; 39: 473-483.

213. Bernichtein S, Kinet S, Jeay S, Llovera M, Madern D, Martial JA, Kelly PA, Goffin V. S179D-human PRL, a pseudophosphorylated human PRL analog, is an agonist and not an antagonist. Endocrinology 2001; 142: 3950-3963.

214. Ormandy CJ, Camus A, Barra J, Damotte D, Lucas B, Buteau H, Edery M, Brousse N, Babinet C, Binart N, Kelly PA. Null mutation of the prolactin receptor gene produces multiple reproductive defects in the mouse. Genes Dev 1997; 11: 167-178.

215. Cunha GR, Battle E, Young P, Brody J, Donjacour A, Hayashi N, Kinbara H. Role of epithelial-mesenchymal interactions in the differentiation and spatial organization of visceral smooth muscle. Epithelial Cell Biol 1992; 1: 76-83.

216. Jabbour HN, Critchley HO, Boddy SC. Expression of functional prolactin receptors in nonpregnant human endometrium: janus kinase-2, signal transducer and activator of transcription-1 (STAT1), and STAT5 proteins are phosphorylated after stimulation with prolactin. J Clin Endocrinol Metab 1998; 83: 2545-2553.

217. DaSilva L, Rui H, Erwin RA, Howard OM, Kirken RA, Malabarba MG, Hackett RH, Larner AC, Farrar WL. Prolactin recruits STAT1, STAT3 and STAT5 independent of conserved receptor tyrosines TYR402, TYR479, TYR515 and TYR580. Mol Cell Endocrinol 1996; 117: 131-140.

218. Wakao H, Gouilleux F, Groner B. Mammary gland factor (MGF) is a novel member of the cytokine regulated transcription factor gene family and confers the prolactin response. EMBO J 1994; 13: 2182-2191.

219. Watson CJ. Stat transcription factors in mammary gland development and tumorigenesis. J Mammary Gland Biol Neoplasia 2001; 6: 115-127.

220. Liu X, Robinson GW, Wagner KU, Garrett L, Wynshaw-Boris A, Hennighausen L. Stat5a is mandatory for adult mammary gland development and lactogenesis. Genes Dev 1997; 11: 179-186.

221. Hennighausen L, Robinson GW, Wagner KU, Liu X. Developing a mammary gland is a stat affair. J Mammary Gland Biol Neoplasia 1997; 2: 365-372.

222. Stevens AM, Wang YF, Sieger KA, Lu HF, Yu-Lee LY. Biphasic transcriptional regulation of the interferon regulatory factor- 1 gene by prolactin: involvement of gamma-interferon-activated sequence and Stat-related proteins. Mol Endocrinol 1995; 9: 513-525.

223. Dalrymple A, Jabbour HN. Localization and signaling of the prolactin receptor in the uterus of the common marmoset monkey. J Clin Endocrinol Metab 2000; 85: 1711-1718.

224. Marshall CJ. Specificity of receptor tyrosine kinase signaling: transient versus sustained extracellular signal-regulated kinase activation. Cell 1995; 80: 179-185.

225. Hunter T. Protein kinases and phosphatases: the yin and yang of protein phosphorylation and signaling. Cell 1995; 80: 225-236.

226. Galcheva-Gargova Z, Derijard B, Wu IH, Davis RJ. An osmosensing signal transduction pathway in mammalian cells. Science 1994; 265: 806-808.

227. Schwertfeger KL, Hunter S, Heasley LE, Levresse V, Leon RP, DeGregori J, Anderson SM. Prolactin stimulates activation of c-jun N-terminal kinase (JNK). Mol Endocrinol 2000; 14: 1592-1602.

228. Olazabal I, Munoz J, Ogueta S, Obregon E, Garcia-Ruiz JP. Prolactin (PRL)-PRL receptor system increases cell proliferation involving JNK (c-Jun amino terminal kinase) and AP-1 activation: inhibition by glucocorticoids. Mol Endocrinol 2000; 14: 564-575.

229. Gubbay O, Critchley HO, Bowen JM, King A, Jabbour HN. Prolactin induces ERK phosphorylation in epithelial and CD56(+) natural killer cells of the human endometrium. J Clin Endocrinol Metab 2002; 87: 2329-2335.

230. Bignon C, Binart N, Ormandy C, Schuler LA, Kelly PA, Djiane J. Long and short forms of the ovine prolactin receptor: cDNA cloning and genomic analysis reveal that the two forms arise by different alternative splicing mechanisms in ruminants and in rodents. J Mol Endocrinol 1997; 19: 109-120.

231. Sambrook J, Fritsch EF, Maniatis T. Molecular Cloning: A Laboratory Manual. Cold Spring Harbor, NY: Cold Spring Harbor Laboratory Press; 1989.

232. Hayashi K, Carpenter KD, Spencer TE. Neonatal estrogen exposure disrupts uterine development in the postnatal sheep. Endocrinology 2004; 145: 3247-3257.

233. Delbe J, Blat C, Desauty G, Harel L. Presence of IDF45 (mlGFBP-3) binding sites on chick embryo fibroblasts. Biochem Biophys Res Commun 1991; 179: 495-501.

234. Valentinis B, Bhala A, DeAngelis T, Baserga R, Cohen P. The human insulin-like growth factor (IGF) binding protein-3 inhibits the growth of fibroblasts with a targeted disruption of the IGF-I receptor gene. Mol Endocrinol 1995; 9: 361-367.

VITA

Karen Denise Carpenter was raised on a family farm in Flat Rock, Indiana, south of Indianapolis. She showed purebred Limousins with her family for fourteen years and served a two year term on the North American Limousin Junior Association Board of Directors. She received a Bachelor of Science in Animal Science from Texas A&M University in December 1996. Karen then held various full time positions in the College of Veterinary Medicine before returning to school in September of 2000. She received her Ph.D. in August 2005. Karen was the recipient of the Dr. A. M. "Tony" Sorenson, Jr. Achievement Award in 2005. She also received the Level I Recognition Award from the Texas Branch of the American Association for Laboratory Animal Science in 1998. Her professional activities include being a trainee member of the Society for the Study of Reproduction (SSR) from 2001 to 2005 and serving on the SSR Trainee Affairs Committee from 2004 to 2005. She also served as the Graduate Student Representative to the Executive Committee of the Interdisciplinary Faculty of Reproductive Biology of Texas A&M University from 2004 to 2005. In November of 2005, Karen assumed a post-doctoral position with Dr. Kenneth Korach at the National Institute of Environmental Health Sciences in Research Triangle Park, North Carolina. Karen may be reached at 226 W. Flat Rock Road, Flat Rock, Indiana 47234. Her email address is kcarpenter@neo.tamu.edu.